THESIS ON NATURAL AND EXACT SCIENCES B153

Investigation of Properties and Reaction Mechanisms of Redox-Active Proteins by ESI MS

JULIA SMIRNOVA

TUT PRESS

TALLINN UNIVERSITY OF TECHNOLOGY
Faculty of Science
Department of Gene Technology

Dissertation was accepted for the defense of the degree of Doctor of Philosophy in Gene Technology on May 09, 2013.

Supervisors:

Professor Peep Palumaa, PhD, Department of Gene Technology, Tallinn University of Technology, Estonia

Professor Wojciech Bal, DSc, PhD, Department of Biophysics, Institute of Biochemistry and Biophysics, Polish Academy of Sciences, Poland

Opponents:

Professor Lloyd Ruddock, PhD, Biocenter Oulu and Department of Biochemistry, University of Oulu, Finland

Professor Ursel Soomets, PhD, Department of Biochemistry, University of Tartu, Estonia

Defense of the thesis: June 25, 2013, Tallinn University of Technology

Declaration:
I hereby declare that this doctoral thesis, my original investigation and achievement, submitted for the doctoral degree at Tallinn University of Technology has not been submitted for any academic degree.

This dissertation was supported by European Social Fund.

ISSN 1406-4723
ISBN 978-9949-23-491-2 (publication)
ISBN 978-9949-23-492-9 (PDF)

LOODUS- JA TÄPPISTEADUSED B153

Redoks-aktiivsete valkude omaduste ja reaktsioonimehhanismide uurimine ESI-MS abil

JULIA SMIRNOVA

TTÜ
KIRJASTUS

CONTENTS

INTRODUCTION

Oxygen forms roughly 21% of the air we breathe and is necessary to sustain life on Earth. Many organisms are forced to live in an oxygen rich environment. Heterotrophic cells use most of the oxygen they uptake for energy production in mitochondria, however, superoxide ($\cdot O_2^-$) is also metabolized there, where it transforms into a cascade of reactive oxygen species (ROS). ROS act on most biological pathways by either stimulating or inhibiting them. Under physiological conditions, ROS, together with reactive nitrogen species (RNS) generated from nitric oxide (NO) and superoxide, are essential second messengers in several redox pathways that are required for our cells to operate from the moment when our first two cells merge until death. Specific protein targets sense local changes in redox conditions and convert them into signals which are transduced by signaling pathways. However, during aging or under diseased states, ROS and RNS are often present in higher concentrations because of both elevated production and failure of defense mechanisms which continuously operate to counterbalance ROS production. This imbalance is termed oxidative stress, and recently, together with co-existing nitrosative stress, the term has been broadened to redox-stress. Oxidative stress may be considered from the point of view of the cell, as well as the entire human body, however, one result is always the same – oxidation by free radicals can damage every macromolecule within the cell, and in particular is harmful for proteins.

Proteins are susceptible to oxidation in different ways. Cysteine is an important determinant of protein oxidation due to its high reactivity with ROS and RNS – upon oxidation two adjacent Cys thiols can form a disulfide bridge which is accompanied by changes in protein conformation or release of coordinated metals, if present. Disulfide bridges are reversible modifications of Cys, and thus can be reduced back to thiols to restore proteins into their original conformation and function. Because of this they often function as redox switches which can be used as a means of cellular regulation or redox signaling. It is commonly believed that ROS are harmful reactants that react with every molecule in their vicinity. However, for years scientists have suggested that not all oxidative processes lead to oxidative stress, and that some ROS may actually have signaling functions through reversible modifications of specific protein thiols at specific points in the cell cycle. Indeed, while several ROS are extremely reactive (especially the hydroxyl radical) and are capable of oxidizing all types of macromolecules, including proteins, the functions of others - H_2O_2 and NO, - have been suggested to act as secondary messengers when present at physiological concentrations.

One of the first mechanisms of redox signaling by ROS was discovered to operate in *Escherichia coli* and involves transcriptional factor OxyR, which effectively senses even low concentrations of intracellular H_2O_2 and elicits the transcription of antioxidant genes through the formation of an un-favored

disulfide bond. Today, an increasing number of other proteins containing redox-sensitive thiol groups have been shown to be involved in redox signaling. These proteins include signal transduction pathway proteins, such as phosphatases and mitogen-activated protein kinases, embryogenesis regulating proteins, many transcription factors, proteins involved in histone acetylation, deacetylation or methylation, and proteins involved in cellular metal homeostasis and storage, such as metallothioneins.

Redox processes within and outside cells depend to a large extent on their immediate chemical environment which differs between organelles and location. For example, the cytoplasm, mitochondrial inner membrane space, and extracellular matrix all support different chemical environments. The redox potential of all cellular environments depends on the content of both reduced and oxidized species and is commonly defined by the ratio of GSH to GSSG because of their relatively high concentrations. The environmental redox potential, E_h, of the cytoplasm lies between -200 and -240 mV, and fluctuates depending on the type of cell, phase in the cell cycle, and the operation of other cellular events such as apoptosis. Moreover, the redox potential differs between organelles and the extracellular environment. The extracellular redox potential is more oxidizing than most intracellular environments. However, redox potentials became more oxidizing with age or during the course of many diseases. Disorders such as neurodegenerative diseases, acute or chronic inflammatory reactions, or cancer, are often characterized by high levels of oxidative species and associated with impaired antioxidant defense. Neurons appear to be particularly vulnerable to attack by ROS because of their low GSH content, large amounts of polyunsaturated fatty acids in their membranes, and intense aerobic metabolism. Considering all of these facts, the redox potential is an important determinant of cellular homeostasis.

Oxidative processes are fundamental for most living organisms, and thus it is necessary for biologists to characterize them. This task requires measuring and characterization of oxidative modifications and reactions of proteins both *in vivo* and *in vitro*. Scientific technologies are increasingly more sensitive and accurate and thus provide opportunities to resolve complex biological questions that could not be previously addressed. Much effort has been directed to investigate the behaviour of proteins under oxidative conditions *in vivo*; however, even more information has been obtained from *in vitro* investigations under simplified environmental conditions. It is currently possible to study the reaction mechanisms of many proteins with oxidizing species such as H_2O_2 or NO, by modifying Cys and measuring the various species using HPLC, or is it possible to follow the release of metals spectrophotometrically. However, one method is specifically useful for these tasks − ESI-MS, which often provides unique information about redox reactions of proteins. This technique is fast and sensitive, allowing direct measurement of the various species from the liquid phase. In particular, it allows one to follow the release of metals and to see

labile non-covalent modifications that are often required to clarify the oxidation mechanisms between proteins and oxidizing species and determine the redox potential of individual proteins.

In the work presented in this dissertation, ESI-MS was applied to study different oxidation processes, and in particular, reactions of a small XPA zinc finger with H_2O_2 and GSNO, a biological NO carrier, and determination of redox potential of extracellular human hormone IGF-1. Zinc fingers are important in the regulation of various redox reactions because their functions are redox-dependent through reversible or irreversible modification of Zn(II)-binding sites upon action of oxidative or nitrosative stimuli. Indeed, both H_2O_2 and GSNO were found to cause Zn(II) release from XPAzf and both reaction mechanisms are discussed in presented herein. The biological implications and importance of the redox modifications of XPAzf are also discussed. In addition, ESI MS was applied to measure the redox potential of extracellular human hormone IGF-1, which contains three disulfide bonds important for binding to its receptor. The redox potential of hIGF-1 was found to be low enough to guarantee its native oxidative folding inside both the ER and the extracellular environment. In order to characterize hIGF-1 we also performed Zn(II)- and Cu(I)-binding experiments. These findings provide a detailed understanding of the redox behaviour of two different proteins and also reaffirm ESI-MS as a useful method to study the redox properties of proteins.

ABBREVATIONS

ALS	acid-labile subunit
AP-1	transcription factor activator protein 1
ASK1	apoptosis signal-regulating kinase 1
BME	β- mercaptoethanol, 2-mercaptoethanol
BMEox	oxidized form of β- mercaptoethanol
CySS	cystine
DTT	dithiothreitol
EGFR	epidermal growth factor receptor
ER	endoplasmatic reticulum
ERCC1	excision repair cross-complementing rodent repair deficiency, complementation group 1
ERK	extracellular signal-regulated kinase
EXAFS	extended X-ray absorption fine structure
GFP	green fluorescent protein
GH	growth hormone
GPx	glutathione peroxidase
GR	glutathione reductase
Grx	glutaredoxine
GSH	glutathione
GSNO	S-nitrosoglutathione, NO derivative of GSH
GSNOR	S-nitrosoglutathione reductase
GSSG	glutathione disulfide
GST	glutathione S-transferase
IGF-1	insulin-like growth factor 1
IGFBP	IGF binding proteins 1-6
IGFR	IGF binding receptor
IMS	mitochondrial intermembrane space
JNK	c-Jun N-terminal kinase
Keap1	Kelch-like ECH-associated protein 1
MAPK	mitogen-activated protein kinase
MMTS	methyl methanethiosulfonate
MT	metallothionein
MTF-1	metal-responsive transcription factor-1
NER	nucleotide excision repair complex
NF-κB	nuclear factor kappa-light-chain-enhancer of activated B cells
NMR	nuclear magnetic resonance
NOS	nitric oxide synthase
Nrf2	nuclear factor (erythroid-derived 2)-like 2
Orp1	oxidant receptor peroxidase 1, also known as Gpx3 in yeast
OxyR	hydrogen peroxide inducible DNA-binding transcriptional factor
PAR	4-(2-Pyridylazo)-resorcinol
Prx	peroxiredoxin

PTK	protein tyrosine kinase
PTP	protein tyrosine phosphatases
RNS	reactive nitrogen species
ROS	reactive oxygen species
RPA	replication protein A
RSNO	S-nitrosylated organic molecule (R), ex. protein, where NO is attached to the Cys thiol (S)
SLC30	solute carrier family 30 member 8, ZNT8
Srx	sulfiredoxin
TFIIH	transcription factor II H
TNF	tumor necrosis factor
Trx	thioredoxin
TrxR	thioredoxin reductase
$Trx(SH)_2$	reduced thioredoxin
TrxSS	oxidized thioredoxin
Trx-80	truncated form of Trx
TXNIP	thioredoxin interacting protein
VSMC	vascular smooth muscle cell
XPA	xeroderma pigmentosum, complementation group A
XPAzf	zinc-finger motif of xeroderma pigmentosum, complementation group A
Yap1	yes-associated protein 1
YFP	yellow fluorescent protein
ZIP	zinc importer
ZNT	zinc transporter

ORIGINAL PUBLICATIONS

The present dissertation is based on the following publications, which will be referred to in the text by their Roman numbers.

I Smirnova, J., Zhukova, L., Witkiewicz-Kucharczyk, A., Kopera, E., Oledzki, J., Wyslouch-Cieszynska, A., Palumaa, P., Hartwig, A., Bal, W. "Quantitative electrospray ionization mass spectrometry of zinc finger oxidation: the reaction of XPA zinc finger with H(2)O(2)" (2007) Anal Biochem.; 369(2):226-31

II Smirnova, J., Zhukova, L., Witkiewicz-Kucharczyk, A., Kopera, E., Oledzki, J., Wyslouch-Cieszynska, A., Palumaa, P., Hartwig, A., Bal, W. "Reaction of the XPA zinc finger with S-nitrosoglutathione" (2008) Chem Res Toxicol.; 21(2):386-92

III Smirnova, J., Muhhina, J., Tõugu, V., Palumaa, P. "Redox and Metal Ion Binding Properties of Human Insulin-like Growth Factor 1 Determined by Electrospray Ionization Mass Spectrometry" (2012) Biochemistry; 51(29):5851-9

Author's contribution

Publication I: The author participated in planning and performed the experimental work, analyzed the data, and participated in manuscript preparation.
Publication II: The author participated in planning and performed the experimental work, analyzed the data, and participated in manuscript preparation.
Publication III: The author participated in planning and in experimental work, analyzed the data, and participated in manuscript preparation.

1. REVIEW OF THE LITERATURE

1.1 Redox signaling and biological redox switches

In recent years, oxidative stress has become a major topic in all areas of life science and medicine. The number of publications on PubMed (http://www.ncbi.nlm.nih.gov/pubmed) containing term "oxidative stress" increased dramatically from the early 1970's with only a few to over 90 000 peer-reviewed articles in 2011 (Jimenez-Del-Rio and Velez-Pardo 2012). Oxidative stress has been defined as a state with elevated concentrations of reactive oxygen species (ROS) and/or reactive nitrogen species (RNS) that overwhelm the antioxidant defense systems of the cell (Halliwell and Whiteman 2004). However, since the identification of signaling processes that depend on changes in local redox conditions, the term "oxidative stress" has been redefined to a "disruption of redox and control" (Jones 2006). As a consequence of our growing knowledge regarding ROS and RNS, several of these molecules have been identified as playing a signaling role, such as hydrogen peroxide (H_2O_2) and nitric oxide (NO). This means that at low concentrations they may act as messengers, by activating or deactivating proteins, which participate in redox signaling pathways (Finkel 2000; Sen 2000; Rhee, Chang et al. 2003; Cadenas 2004; Forman, Fukuto et al. 2004; DeYulia, Carcamo et al. 2005; Rhee 2006; Stone and Yang 2006; Forman 2007; Zhang and Gutterman 2007; Rigoulet, Yoboue et al. 2011). Redox signaling could be viewed then as the process wherein signal is delivered by specific ROS and RNS through the modification of specific protein targets (Santos, Anilkumar et al. 2011; Bindoli and Rigobello 2012). Signal sensing and transduction through oxidation/reduction reactions rely largely on the redox chemistry of sulphur, which is a constituent of "reactive" thiols within certain proteins, and in particular, peroxiredoxins (Prxs) (Brigelius-Flohe and Flohe 2011). Regulatory disulfide bonds are formed inside the cell in spite of the reducing conditions that prevail in the cytosol (Jensen, Hansen et al. 2009). These bonds could be classified as the redox switches (Shelton and Mieyal 2008), which must be protected from enzymatic reduction by kinetic barriers and thus are able to exist long enough to elicit the signal.

The formation of a disulfide bond between two Cys residues or between a Cys residue and a small thiol containing molecule (for example, glutathione (GSH)) may have a significant impact on the structure and function of the protein (Choi, Kim et al. 2001). The regulation of cellular function by direct alteration of protein activity through thiol-switching has been widely reported (Toledano, Delaunay et al. 2004; Ilbert, Horst et al. 2007; Paulsen and Carroll 2010).

However, the most prominent cellular redox sensors are thiol peroxidases, which do not initially sense changes in the redox environment by thiol-disulfide exchange reactions, but rather form sulfenic acid or S-nitrosylated derivatives (depending on the oxidant) (Linke and Jakob 2003; Gallogly and Mieyal 2007). The next step in the transmission of a redox signal to other proteins occurs via thiol-disulfide exchange reactions (Forman, Maiorino et al. 2010; Brigelius-Flohe and Flohe 2011). A well known example of such a sensing mechanism originates from yeast and is represented by glutathione peroxidase (GPx)-type peroxidase Orp1, which senses H_2O_2 and transfers an oxidative signal to the activator protein 1 (AP-1) like transcription factor Yap1 (Fourquet, Huang et al. 2008). Analogous sensing of H_2O_2 and other peroxides by peroxidases has not yet been reported in mammals, although similar mechanisms, driven by 2-Cys Prxs have been reported that involve indirect ways of sensing and transducing oxidative signals (Brigelius-Flohe and Flohe 2011).

Thiolates are also able to bind transition metal ions such as Zn(II), Cu(I), Fe(II). These metal-thiolate motifs also function as redox switches (Outten and Theil 2009). In addition to the modulatory role of metal ions on the oxidation of Cys residues, such as defense from oxidation, the release of metal ions from a variety of metal-containing redox switches during redox signaling and oxidative stress is an inseparable part of redox signaling. It is known that redox signaling and oxidative stress lead to a release of substantial amounts of Zn(II) ions from metallothioneins (MTs) and zinc finger proteins (Kroncke and Klotz 2009) and the biological consequences of this metal release are being intensively investigated. A similar release of metal ions might also occur in the case of iron or copper proteins with potentially devastating consequences because these free redox-active metal ions can, in the presence of oxygen metabolites, initiate the production of highly reactive ROS and cause oxidative stress (Comporti, Signorini et al. 2002; Gaetke and Chow 2003; Uriu-Adams and Keen 2005).

A thiol group is also present in the structure of the GSH/GSSG cellular redox buffer system which largely defines the cellular redox environment, and to a lesser degree the extracellular redox environment. This pair, together with other redox pairs, determines the redox state of the intracellular/extracellular milieu and various cellular compartments (Schafer and Buettner 2001). Several signaling mechanisms are known to respond to changes in the thiol/disulfide redox state, involving transcription factors AP-1, NF-κB, Nrf2 and p53, bacterial OxyR, protein tyrosine phosphatases (PTPs), Src family kinases, JNK and p38 MAPK signaling pathways, insulin receptor kinase, and perhaps others (Valko, Leibfritz et al. 2007; Trachootham, Lu et al. 2008; Brigelius-Flohe and Flohe 2011; Bindoli and Rigobello 2012).

1.1.1 Thiol-based redox switches

Cys is considered to be the most chemically reactive natural amino acid (Hansen, Roth et al. 2009). Oxidation of Cys thiols is a complex process (Jacob, Knight et al. 2006) which leads to different oxidation states of sulfur (Figure 1). The first step in the oxidation of thiols is the formation of sulfenic acid (SOH), which is commonly considered to be a transient intermediate formed during the oxidation of thiols to disulfides (SS) or sulfinic acids (SO_2H) (Bindoli and Rigobello 2012). Next, in participation with another thiol in its vicinity, a disulfide bond could be formed, which in cells exists in proteins, in oxidized glutathione (GSSG), or in mixed disulfides between protein and low molecular weight thiols − mainly GSH (SSG) (Figure 1). Another oxidation product of Cys thiols caused by RNS is the nitrosylated thiol or nitrosothiol (SNO) (Bindoli and Rigobello 2012) (Figure 1). All of these reactive thiol derivative groups are reversible and can be efficiently reduced back through reactions catalyzed by thioredoxins (Trxs), glutaredoxins (Grxs), and thiol peroxidases (Filomeni, Rotilio et al. 2002; Bindoli and Rigobello 2012).

Sulfenic acids within the biological systems are formed by the reaction of thiols with peroxides, from sulfenyl halides, and from nitrosothiols (Bindoli and Rigobello 2012). They are quite unstable and react readily with accessible thiols to form disulfide bonds, releasing one molecule of water (Claiborne, Yeh et al. 1999; Bindoli and Rigobello 2012). The high reactivity of sulfenic acid is partly explained by its both nucleophilic and electrophilic properties (Allison 1976), and by their ability to self-condensate, forming thiolsulfinates (Davis, Jenkins et al. 1986). However, in some cases sulfenic acids could be stabilized within active sites of particular proteins (Claiborne, Miller et al. 1993; Goto, Holler et al. 1997). The stabilization of sulfenic acid includes several aspects, with the most important being the absence of thiol groups in close proximity to a sulfenic acid residue (Claiborne, Miller et al. 1993; Yeh, Claiborne et al. 1996). Disulfide formation in the catalytic cycle of Prxs (Rhee and Woo 2011) or with GSH (Forman, Fukuto et al. 2004), probably are the most important reactions of sulfenic acids in proteins. Besides disulfide formation, sulfenic acids can also undergo other reactions, such as reaction with a protein backbone to form a sulfenyl amide, which is proposed to serve as protection from over-oxidation (Salmeen, Andersen et al. 2003; van Montfort, Congreve et al. 2003); a self-condensation reaction to form thiolsulfinates (Claiborne, Miller et al. 1993; Hogg 2010); and further oxidation to sulfinic and sulfonic (SO_3H) acids (Bindoli and Rigobello 2012).

A disulfide bond is relatively resistant to oxidation (E_{ox} ~ 0.8 V in water at pH 7 or 1.2 V in an aprotic solvent) (Bontempelli, Magno et al. 1973; Howie, Houts et al. 1977) and therefore it could be concluded that the formation of disulfides that competes with the formation of a sulfinic acid prevents further oxidation of Cys thiols (Forman, Maiorino et al. 2010). Thiol context-specific pK_a values

determine their relative ease of deprotonation and subsequent ease of oxidation, being the important determinant of proteins oxidation by ROS (Harris and Hansen 2012). Additional factors that affect the rate of thiol-disulfide exchange and stability are the local electrostatic environment, molecular strain, and entropy (Jensen, Hansen et al. 2009; Harris and Hansen 2012). Even though a thiol-disulfide exchange reaction is thermodynamically favourable, it will only take place if the activation energy to form the transition state complex can be overcome, which requires the action of enzymes (e.g. oxidoreductases) which lowers the activation energy barrier (Jensen, Hansen et al. 2009).

Based on the relative stability of the SS bond, the disulfide proteome is divided into two sub-proteomes: a structural group and a redox-sensitive group (Wouters, Fan et al. 2010). The redox-sensitive group consists of less stable disulfides and is often associated with regions of strain in protein structures. Some characterized redox-active disulfides are the helical CXXC motif, often associated with Trx-fold proteins, and forbidden disulfides, a group of metastable disulfides that disobey elucidated rules of protein stereochemistry (Wouters, Fan et al. 2010). The ultimate parameter in determining whether disulfide bonds are structural or redox-sensitive is their redox potential. Disulfide redox potentials measured for thiol-disulfide oxidoreductases range from -95 to -330 mV (Lin and Kim 1989; Krause and Holmgren 1991; Wunderlich, Jaenicke et al. 1993; Huber-Wunderlich and Glockshuber 1998), while for structural disulfides, the redox potential can be as low as -470 mV (Gilbert 1990).

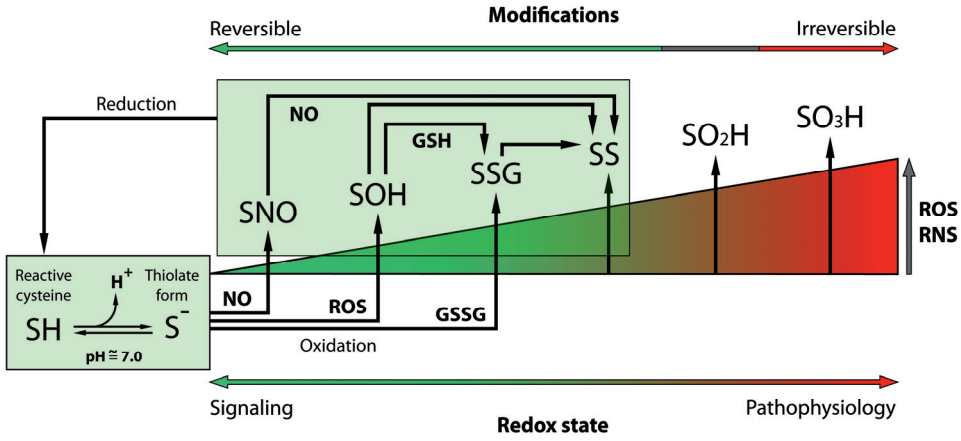

Figure 1: Major routes of cellular thiols modifications caused by ROS and RNS in dependence with redox state: signaling VS pathology. SNO – nitrosothiol; SOH – sulfenic acid; SSG – S-glutathionylated thiol; SS – disulfide; SO_2H – sulfinic acid; SO_3H – sulfonic acid.

Higher oxidation states of thiols, such as sulfinic and sulfonic acids, are generally considered to be irreversible (Rhee and Woo 2011) with an exception being Prxs, which have been demonstrated to undergo reversible sulfinylation (Yang, Kang et al. 2002; Filomeni, Rotilio et al. 2005) by ATP-dependent enzyme sulfiredoxin (Srx) (Biteau, Labarre et al. 2003; Jeong, Park et al. 2006; Rhee and Woo 2011). This feature of Prxs allows for the accumulation of H_2O_2 in order to propagate its signal (Wood, Poole et al. 2003; Rhee and Woo 2011). Formation of sulfonic acid is irreversible and accumulation of irreversibly oxidized proteins is an important hallmark of biological aging and pathological situations which are associated with redox stress (Stadtman and Berlett 1998; Giustarini, Rossi et al. 2004; Stadtman 2004).

Protein S-glutathionylation is a process by which protein thiols form mixed disulfides with a low-molecular-mass thiol GSH (Shenton and Grant 2003; Dalle-Donne, Rossi et al. 2009). One possible mechanism whereby S-glutathionylation can occur is a reaction between sulfenic acid and GSH. Reversible formation of this GSH-mixed protein disulfide bond is catalyzed by Grx (Beer, Taylor et al. 2004; Berndt, Lillig et al. 2007), whereas the reduction of protein-GSH mixed disulfides with the help of Grx is favoured to the formation of mixed disulfides, which could take place under conditions of increased GSSG content (Ruoppolo, Lundstrom-Ljung et al. 1997; Lillig, Berndt et al. 2008). S-glutathionylation was proposed to serve as a regulatory process or as an adaptive cellular response protecting critical regulatory molecules from permanent (irreversible) loss of function through the formation of higher oxidation states of thiols, or as a consequence of redox stress (Dalle-Donne, Colombo et al. 2011). It has been suggested that 1% of all proteins are S-glutathionylated in resting cells (Biswas, Chida et al. 2006). Alterations in S-glutathionylation levels occur under disease conditions such as diabetes, various cardiovascular pathologies, lung disease, and neurodegenerative diseases (Mieyal, Gallogly et al. 2008). Studies with leucocytes (Chai, Ashraf et al. 1994) and monocytes (Ravichandran, Seres et al. 1994) have revealed that S-glutathionylation of proteins occurs within minutes after a burst in generation of oxidative metabolites. Several proteins have been identified to undergo S-glutathionylation under oxidative stress conditions, including cyclophilin A, Prx5 and Trx (Fratelli, Demol et al. 2003). The latter is of specific importance because its reversible S-glutathionylation at Cys72 provides a possible link between the GSH and Trx systems (Casagrande, Bonetto et al. 2002).

A well-studied example of a thiol-dependent redox switch was obtained by studying bacteria. Redox regulation of prokaryotic transcription factor OxyR depends on the chemical status of specific Cys residues and is sensitive to low amounts of intracellular H_2O_2, SH-reactive compounds (i.e. diamide), and RNS (Georgiou 2002; Paget and Buttner 2003; Lee, Lee et al. 2004). Upon exposure to H_2O_2, the activation of OxyR involves the formation of sulfenic acid at Cys199 (Aslund, Zheng et al. 1999), followed by the formation of a specific

disulfide bond between Cys199 and Cys208, which are separated by 17 Å in the reduced and inactive form of the protein (Zheng, Aslund et al. 1998). Disulfide bond formation is unfavourable and is associated with large structural changes within the regulatory domain (Choi, Kim et al. 2001). The net outcome of this reaction is a change in DNA binding specificity, which occurs in a tetrameric protein, and the recruitment of RNA polymerase (Zheng, Aslund et al. 1998). This disulfide bond is reduced by Grx1 with further deactivation of OxyR (Zheng, Aslund et al. 1998).

The regulation of redox-mediated mechanisms through the regulation of protein function which accounts for the modification of thiols could be achieved on several levels. Expression of proteins is controlled on transcriptional level by a number of redox-regulated transcriptional factors (NF-κB, AP-1, Nrf2, p53) (Brigelius-Flohe and Flohe 2011). Oxidative modifications of thiols are involved in redox-regulation on a posttranslational level, whereas the function of a particular protein could be influenced by direct modification of Cys thiols by ROS/RNS (Trachootham, Lu et al. 2008). Proteins that are stabilized by contact with others could be regulated through redox-modifications of interacting partners (examples includes ASK1-Trx, JNK-GST, p53-JNK, Nrf2-Keap1) (Cross and Templeton 2006). Regulation of protein posttranslational modifications, especially that of phosphorylation, could also be mediated by redox-modifications of phosphotyrosine kinase (PTK) and PTPs (Chiarugi 2005; Heneberg and Draber 2005; Brigelius-Flohe and Flohe 2011). In addition, degradation of proteins is also redox-regulated (Trachootham, Lu et al. 2008).

1.1.2 Zinc fingers as biological redox switches

Zinc is the second most abundant essential transition metal present in living organisms next to iron (Kroncke and Klotz 2009). Zinc is present as Zn(II) ion and does not change its oxidation state in biological systems. In proteins, Zn(II) could be coordinated by Cys, His, Asp, and Glu to form two types of zinc-binding sites: catalytic and structural (Vallee and Auld 1990; Vallee 1991). Tridentate catalytic zinc sites are enzymatically active sites that contain mainly His, Asp, and Glu, with His being the most frequent ligand found. Cys residues are exclusive zinc ligands at structural sites, where Zn(II) ions are coordinated tetrahedrally by 4 Cys ligands or by Cys/His ligands in zinc fingers. It was long believed that Zn(II) in structural sites is inaccessible to solvents, by a critically controlled local protein structure, folding, and conformation (Vallee and Auld 1990; Vallee 1991).

The term ‘zinc finger’ is generally used to describe tetrahedral zinc-binding sites with at least two Cys thiolates involved in metal binding. The remaining two ligands are two Cys, one Cys and one His or two His (Laity, Lee et al. 2001). Cys_4 and Cys_2His_2 are the most common types of zinc fingers (Andreini, Banci et al. 2006). In the so-called classic zinc finger, Zn(II) is coordinated by

two Cys and two His, which creates an independent structural domain consisting of a two-stranded antiparallel β-sheet and a short α-helix (Kroncke and Klotz 2009). Zinc finger domains comprise one of the most abundant families of protein motifs in the eukaryotic genome and up to 3% of the human proteome contains one or more zinc finger domains (Maret 2003). The functions of zinc finger proteins include the binding and recognition of nucleic acids and the formation of multiprotein complexes (Mackay and Crossley 1998; Laity, Lee et al. 2001).

Zn(II) binding to proteins such as zinc fingers and MTs allows Zn(II) to be both tightly bound and yet available (Maret 2004). Zn(II)-stabilized structures of zinc fingers can be disrupted by oxidative modification of Zn(II)-binding Cys with formation of sulfenic acid or disulfide, by chelation of Zn(II), or under conditions of Zn(II) deficiency (Korichneva 2006; Maret 2006; D'Autreaux and Toledano 2007; Brigelius-Flohe and Flohe 2011). These structures release Zn(II) upon thiol oxidation and could result in a loss of zinc finger function and also secondary effects such as intracellular signaling by Zn(II) (Kroncke and Klotz 2009). This process is reversible depending on the respective redox conditions and this enables zinc fingers to operate as efficient redox switches resulting in alterations of various cellular processes such as signal transduction, regulation of apoptosis, differentiation and proliferation, and also the general metabolism of the cell (Kroncke and Klotz 2009). Several examples in the literature demonstrate that oxidative or nitrosative stress causes a loss of DNA-binding activity of zinc finger transcription factors (Brigelius-Flohe and Flohe 2011). However, the examples of direct oxidation of transcriptional factor through disulfide formation have only been described in bacteria and yeast (Brigelius-Flohe and Flohe 2011). In eukaryotes, transcription factors are commonly present in the cytosol in the form of multiprotein complexes from which they must be released in order to activate genes in the nucleus (Brigelius-Flohe and Flohe 2011). Activation of the transcriptional factor requires modification of one or more components of the complex to enable release of the factor and its transport to nucleus. In most cases, a redox modification of the zinc finger containing component of the complex is essential and is followed by ubiquitination and proteasomal degradation of the same or another component (Hilt and Wolf 1996; Brigelius-Flohe and Flohe 2011). A well studied example representing the system described above is the Keap1/Nrf2 system (Brigelius-Flohe and Flohe 2011). NF-κB is a mammalian transcriptional factor, which was suggested to be directly activated by oxidative stimuli (Schreck, Rieber et al. 1991). However, it has become clear that the NF-κB system is primarily activated by cytokines and non-oxidant foreign stressors via TNF, Toll-like and other receptors (Brigelius-Flohe and Flohe 2011).

1.1.3 Cellular Zn(II) homeostasis and role of Zn(II) in redox signaling

Zn(II) is an important structural constituent within many proteins, including enzymes and transcription factors, and is essential for their biological activity (Vallee and Falchuk 1993; Prasad 1995). Moreover, Zn(II) acts as a neurotransmitter upon synaptic release in neurons (Colvin, Fontaine et al. 2003; Frederickson, Koh et al. 2005) and has a variety of effects on the immune and nervous systems that are concentration dependent (Rink and Gabriel 2000; Frederickson, Koh et al. 2005). However, under physiological conditions the concentration of free (also referred to as "labile", "rapidly exchangeable", "easily available", "loosely bound") Zn(II) in cells is in the pico- to low-nanomolar range due to an excess of complexing ligands (Palmiter and Findley 1995; Krezel and Maret 2006). Free Zn(II) concentrations are expressed as zinc potentials, pZn = -log[Zn(II)], in analogy to pH (Maret 2009). Such a low intracellular concentration of free Zn(II) is believed to be tightly controlled by the cell via zinc importers (ZIPs/SLA39s; (Eide 2004)) and exporters (zinc transporters/SLC30s; (Palmiter and Huang 2004)) and is thought to be in equilibrium with many intracellular Zn(II)-binding proteins, in particular with MTs and zinc fingers (Vallee 1995; Krezel, Hao et al. 2007). In addition, zinc-sensing molecules such as metal response element–binding transcription factor-1 (MTF-1) respond to free Zn(II) levels by regulating gene expression to maintain zinc homeostasis (Andrews 2001). Moreover, the dominant Zn(II)-binding ligand within the cell is probably GSH, which is present in millimolar concentrations (Diaz-Cruz, Mendieta et al. 1998; Kroncke and Klotz 2009).

The availability of zinc is determined by the cellular Zn(II) buffering capacity. Eukaryotic cells have a relatively high Zn(II) buffering capacity due to a large number of weak coordination sites. However, Zn(II) buffering capacity under physiological pZn is rather modest. Buffering is determined by Zn(II) proteins and other ligands that have the potential to bind Zn(II) tightly, however, have unoccupied sites under normal conditions (Krezel and Maret 2006). About one third of these ligands have been estimated to be thiols (Krezel, Hao et al. 2007) and thus the Zn(II) buffering capacity is redox sensitive. Shifting the redox balance to a more oxidative increases the availability of free Zn(II), mainly due to its release from Cys residues, and thus affects the cellular Zn(II) homeostasis (for review, see (Kroncke 2007) and (Maret 2006)). Application of several oxidants as well as ·NO to cells has repeatedly been demonstrated to lead to an increase in the level of intracellular free Zn(II) (Turan, Fliss et al. 1997; Korichneva, Hoyos et al. 2002; Spahl, Berendji-Grun et al. 2003; Kroncke 2007; Bernal, Leelavanichkul et al. 2008; Pirev, Calles et al. 2008). Released Zn(II) may act as a messenger in a fundamental molecular pathway where a redox signal is converted into a Zn(II) signal (Maret 2009):

Redox signal → Proteins with zinc/thiolate coordination → Zn(II) → Target(s).

In summary, re-distribution and control of the concentration of the Zn(II) ion is not trivial because Zn(II) must be mobilized from its tight binding sites in a controlled way so that it may act specifically and with minimal interference with the actions of other metal ions. MT is proposed to participate in this process by serving as a reservoir of cellular Zn(II); about 10% of zinc in a hepatocyte is bound to MT (Maret 2009). MTs also function as intracellular redox sensors (Jiang, Maret et al. 1998; Maret 2004; Maret 2006; Krezel, Hao et al. 2007) because of their high sensitivity to Cys modifications (Fabisiak, Borisenko et al. 2002).

1.1.4 Role of S-nitrosylation in redox signaling and stress

S-nitrosylation is the covalent attachment of a NO group to the thiol group of Cys via the formation of nitrosothiols. As such, it provides a mechanism for redox-based physiological regulation through dynamic, post-translational modifications of Cys containing proteins (Hess, Matsumoto et al. 2005; Forman, Fukuto et al. 2008; Sengupta and Holmgren 2012).

Nitric monoxide (NO) is a pluripotent regulatory molecule, which is involved in cellular signaling pathways (Stamler, Singel et al. 1992; Becker, Savvides et al. 1998). Excessive or uncontrolled nitrosylation, however, can lead to the so called "nitrosative stress" – a condition characterized by an accumulation of protein SNOs and a loss of cellular function (Chung, Thomas et al. 2004; Liu, Yan et al. 2004; Massy, Fumeron et al. 2004; Yao, Gu et al. 2004; Hess, Matsumoto et al. 2005). However, the half-life of the NO free radical molecule *in vivo* is short (0.1 s), and the major cellular NO carrier is GSH, which forms GSNO upon reaction with NO (Becker, Gui et al. 1995; Piantadosi 2012).

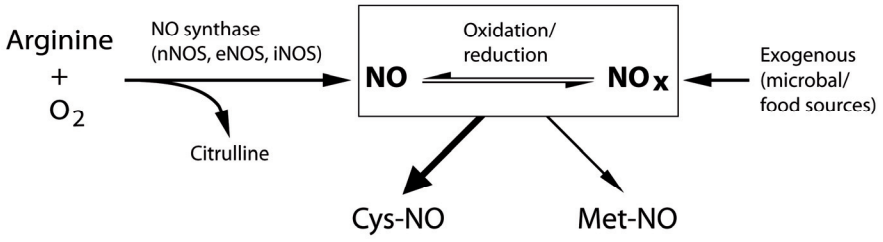

Figure 2: Cellular sources and targets of nitric oxide. Cys-NO denotes for thiol containing proteins or low molecular weight substances (based on (Hess, Matsumoto et al. 2005)).

In most cell types NO is generated from Arg and O_2 by NO synthases (NOSs) and potentially, by the reduction of NOx species, which are derived from

exogenous (NO_2 - from food or from bacterial flora) and endogenous sources (NO oxidation products, including N_2O_3) (Hess, Matsumoto et al. 2005) (Figure 2). Separate genes code for different NOSs: eNOS stands for endothelial NOS or NOS3, nNOS stands for neuronal NOS or NOS1, and iNOS stands for inducible/Ca(II) - independent NOS or NOS2. All NOSs are expressed constitutively and might be induced. Besides cellular thiols, NO is also able to bind to metal ions. For example NO binds to the haem Fe(II) of guanylate cyclase and NO might be exchanged between transition metals and thiols (Hess, Matsumoto et al. 2005).

A major route of NO action and function is signaling through the formation of S-nitrosothiols. S-nitrosothiols have been detected in many biological systems and in many cells (Stamler, Jaraki et al. 1992; Jaffrey, Erdjument-Bromage et al. 2001; Gow, Chen et al. 2002; Bryan, Rassaf et al. 2004; Ckless, Reynaert et al. 2004; Zhang and Hogg 2004; Sengupta and Holmgren 2012). In enzymes, S-nitrosylation can either lead to activation or inhibition of activity (Sengupta and Holmgren 2012; Nakamura and Lipton 2013). The concentrations of S-nitrosylated proteins have been shown to increase in response to inflammatory stimuli (Jourd'heuil, Gray et al. 2000; Crawford, Chacko et al. 2004). A proteomic study of S-nitrosylation of the Rat Cardiac Proteins was performed *in vitro*, in which protein S-nitrosylation was induced using GSNO and two-dimensional gel electroforesis (2-DE) was employed to separate proteins (Shi, Feng et al. 2008). A total of 10 S-nitrosylated proteins were identified by MALDI-TOF-MS/MS including triosephosphate isomerase, glyceraldehyde-3-phosphate dehydrogenase, creatine kinase, enolase 1, destrin, actin, myosin, albumin, Hsp27 and adenylate kinase 1 (AK1) (Shi, Feng et al. 2008).

S-nitrosothiols can be generated indirectly by nitrogen dioxide (NO_2), which is produced by an interaction of NO with oxygen (Forman, Fukuto et al. 2008). In this case, S-nitrosothiols are formed with thiyl radical as an intermediate product (Broniowska and Hogg 2012). Nitrogen dioxide can further react with NO, producing N_2O_3, which can also react with thiol groups by forming S-nitrosothiol (Forman, Fukuto et al. 2008). Another way of forming S-nitrosothiols is by a transnitrosylation reaction either within proteins or between proteins and low molecular weight thiols, such as GSNO (Piantadosi 2012; Sengupta and Holmgren 2012; Nakamura and Lipton 2013). In particular, protein-protein transnitrosylation is of interest because it was suggested to give rise to transnitrosylation cascades, which are important for the regulation of cellular signaling functions (Nakamura and Lipton 2013).

NO can modify Cys thiols and transition metal centers in a broad range of proteins (Stamler, Lamas et al. 2001). Endogenous protein S-nitrosylation is very specific and the majority of these proteins are regulated by S-nitrosylation at a critical Cys residue (or only a few) (Campbell, Stamler et al. 1996; Stamler, Lamas et al. 2001; Boehning and Snyder 2003; Matsumoto, Comatas et al.

2003; Matsushita, Morrell et al. 2003; Hess, Matsumoto et al. 2005). This specificity is influenced by several parameters: thiol pK_a (nucleophilicity) (Stamler, Jia et al. 1997); the hydrophobic microenvironment (Hess, Matsumoto et al. 2001); the presence of allosteric regulators (for example, Ca(II) or Mg(II)) that can modulate thiol accessibility or reactivity (Eu, Sun et al. 2000; Lai, Hausladen et al. 2001). Potential S-nitrosylation sites can be predicted by the presence of "acid-base" motifs, where charged side groups are provided by acidic (Asp, Glu) and basic (Arg, Lys, His) residues in proximity with the target thiol (Stamler, Toone et al. 1997; Perez-Mato, Castro et al. 1999; Hess, Matsumoto et al. 2001). The same NO-related posttranslational modifications that operate as specific signals in mammalian cells can be used to fight invasion by microbes and cancer cells. This latter effect can be achieved because S-nitrosylation can disrupt the function of critical proteins in rapidly proliferating cells, thus causing nitrosative stress (Stamler, Lamas et al. 2001).

The functional behaviour of various proteins is regulated via S-nitrosylation by several mechanisms that control both the addition of the NO group to a Cys thiol and its removal. Physiological RSNO denitrosylation is promoted significantly by reduced GSH and Trx systems (Sengupta and Holmgren 2012). GSNO is reduced by GSNO reductase (GSNOR) to NH_3 and GSSG with recruiting reducing equivalents from NADH (Liu, Hausladen et al. 2001). The following reduction of GSSG by glutathione reductase (GR) sets up a cyclic process (Piantadosi 2012). GSNOR acts as modulator of the cellular S-nitrosylation status, which is based on an equilibrium between GSNO and S-nitrosylated proteins (Sengupta and Holmgren 2012). Denitrosylation of a wide range of proteins could be induced by the Trx system, including caspase-3 (Benhar, Forrester et al. 2008; Sengupta and Holmgren 2012). Both Trx and superoxide dismutase (SOD) can liberate NO from GSNO *in vivo* (Nikitovic and Holmgren 1996; Romeo, Capobianco et al. 2003). However, under specific conditions, oxidized Trx could become nitrosylated and transnitrosylate specific proteins (Sengupta and Holmgren 2012).

1.2 Redox messengers

Life in an oxygen-rich environment that affects living organisms and one of the consequences is the formation of ROS and RNS that are produced from metabolic events, including respiration, fatty acid oxidation, and various environmental processes (Georgiou 2002). As mentioned above, ROS and RNS may function as double-edged swords playing dual roles as both deleterious and beneficial species depending on their concentration (Valko, Leibfritz et al. 2007) (Figure 3).

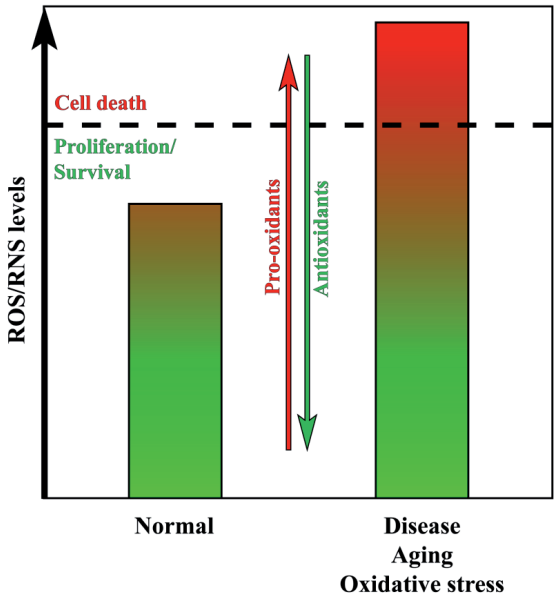

Figure 3: In healthy individuals, basal ROS are maintained at low levels by controlling the balance between ROS/RNS generation (pro-oxidants) and elimination (antioxidants). Under normal conditions, cells can tolerate a certain level of ROS stress by using their "reserve" antioxidant capacity to prevent cells from reaching the cell death threshold (horizontal dotted line in the figure), however under conditions of elevated ROS and increased oxidative stress the antioxidant capacity of the cells is overwhelmed and cells are triggered to apoptosis or necrosis (based on (Trachootham, Alexandre et al. 2009))

Production of signaling ROS and RNS is not limited to a single source or pathway. Mitochondria, endoplasmatic reticulum (ER), NADPH oxidase in the plasma membrane, peroxisomes, along with other systems, produce ROS within cells (Bindoli and Rigobello 2012; Brown and Borutaite 2012). Recently, the role of mitochondria in ROS production was analyzed and it was concluded that mitochondria are not the major sources of ROS: mitochondria produce and metabolize H_2O_2, and the net mitochondrial production of these species is involved in redox signaling (Brand 2010; Brown and Borutaite 2012). However, intensive production of ROS during prolonged periods is able to induce apoptosis and autophagy (Finkel 2012). ROS thus provide crosstalk links between organelles and other sources of oxidizing species (Daiber 2010). Of particular importance is the redox communication between mitochondria and NADPH oxidase in which ROS production by either source stimulates reciprocal production of oxidants (Zinkevich and Gutterman 2011). NADPH oxidase plays a critical role in signaling because of its ability to modulate the ROS release form various sources within the cell, and has been defined as the "master oxidase" (McNally, Davis et al. 2003).

In comparison with other ROS, H_2O_2 fits best to the role of secondary messenger because of its high abundance and due to enzymatic production and degradation (Forman, Maiorino et al. 2010). Enzymatic formation of NO and its diverse biological functions (Stamler, Singel et al. 1992) supports the idea that latter may also act as secondary messenger, giving rise to several reactive derivatives or through formation of GSNO (Stamler, Singel et al. 1992). Despite the fact that high levels of GSNO might be implicated in irreversible effects of nitrosative stress (Kim, Merchant et al. 2002), at lower concentrations, GSNO is also involved in signaling by transferring the NO group to the redox-active Cys thiols which regulates the function of various redox active proteins (Zaman, Palmer et al. 2004).

1.2.1 H_2O_2 as a redox messenger

The history of H_2O_2 as a redox messenger began when it was found that exogenously added H_2O_2 could mimic growth factor activity and that some growth factors stimulate endogenous production of H_2O_2 within the cells (Czech 1976; Mukherjee, Lane et al. 1978; Mukherjee and Mukherjee 1982). Since then, hormones, growth factors, neurotransmitters, and cytokines have been shown to induce transient increases of hydrogen peroxide in mammalian cells (Meier, Radeke et al. 1989; Sundaresan, Yu et al. 1995; Bae, Kang et al. 1997; Mahadev, Wu et al. 2001; Roy, Khanna et al. 2008), thus supporting its action as a secondary messenger within the cell.

H_2O_2 is the most abundant ROS (Giorgio, Trinei et al. 2007; Halliwell and Gutteridge 2007). Its concentrations in tissues and fluids in the human body is in the range of 10^{-7} M and may vary widely (Halliwell, Clement et al. 2000) depending on the intracellular iron content and/or the presence of enzymes such as Prxs, catalases, GPs and systems associated with Trx (Chance, Sies et al. 1979; Eshghi, Lourdault et al. 2012; He, Banach-Latapy et al. 2012). Concentrations in the hundreds of micromolar have also been reported, and consumption of common beverages (e.g. instant coffee) and smoking may result in levels of >500 μM (Halliwell, Clement et al. 2000; Sticozzi, Belmonte et al. 2012). Loss of H_2O_2 regulation is believed to play a central role in disease and aging (Rojkind, Dominguez-Rosales et al. 2002). At potentially toxic levels, H_2O_2 results in oxidative damage to proteins, lipids, and nucleic acids. H_2O_2 could mediate its toxicity through oxidative modification of Zn(II)-containing proteins. Indeed, it was shown, that alterations in Zn(II) homeostasis induce pulmonary artery endothelial cells (PAECs) death caused by oxidative stress from exposure to H_2O_2 (Wiseman, Wells et al. 2007).

There are many determinants of the specificity of hydrogen peroxide as a secondary messenger. First, H_2O_2 is relatively stable and can cross biological membranes (Rhee 1999; Bienert, Schjoerring et al. 2006; Giorgio, Trinei et al. 2007), thus having an ability to translocate easily from one compartment to

another by mechanisms facilitated by specific aquaporins (Bienert, Moller et al. 2007). Second, it is produced and degraded enzymatically (Figure 4). Third, it is chemically specific for oxidation of "sensor" thiols through the formation of sulfenic acid (Kettenhofen and Wood 2010).

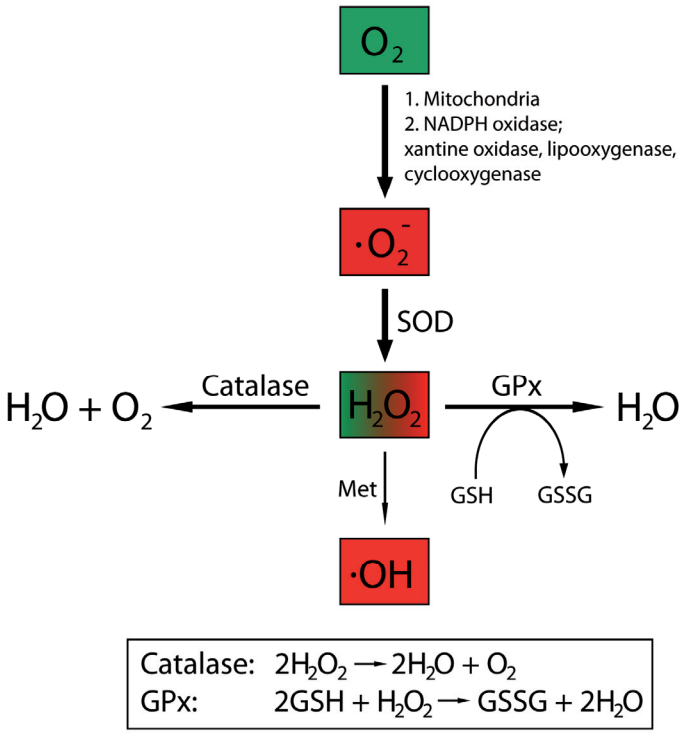

Figure 4: Metabolism of H_2O_2. SOD is the major enzyme for dismutation of superoxide anion and production of H_2O_2. The latter could be decomposed enzymatically by catalases and GPs, and in the presence of redox-active metals, an extremely reactive ·OH radical can be generated. In addition, H_2O_2 is implicated in mediating several signaling mechanisms, by oxidizing Cys thiols in particular proteins. ROS that do not contribute to signaling directly are denoted by red rectangles in the figure; H_2O_2 could have deleterious effects if present at elevated concentrations and is therefore placed into a partially red rectangle.

H_2O_2 could be produced both nonenzymatically and enzymatically, with a rate constants much higher for the SODs (10^9 M^{-1} s^{-1}) than for nonenzymatical reactions (10^5 M^{-1} s^{-1}) (Forman and Fridovich 1973). In biological systems, H_2O_2 is produced enzymatically mainly in mitochondria from superoxide (Hawkins, Madesh et al. 2007; Forman, Maiorino et al. 2010) (Figure 4) through dismutation of the superoxide anion by SOD according to the following net reaction:

$$2 \cdot O_2^- + 2H^+ \overset{SOD}{\rightarrow} O_2 + H_2O_2 \quad (1)$$

H_2O_2 is also a product of oxygen consumption in the peroxisomes. However, peroxisomes contain catalases, which decompose H_2O_2 and may help to prevent accumulation of H_2O_2. Upon damage of peroxisomes or downregulation of catalase, H_2O_2 releases into the cytosol and promotes oxidative stress (Valko, Leibfritz et al. 2007).

H_2O_2 is a strong oxidant (E^0 = 1.776 V for its reduction to water) (Forman, Maiorino et al. 2010). In biological systems H_2O_2 is reduced in two ways: by one-electron reduction, that produces ·OH which is an extremely strong oxidant that reacts with practically all biological molecules and therefore cannot play any specific role in signaling (Figure 4); and by a two-electron nucleophilic substitution reaction that had been suggested for the oxidation of thiols (RS^-) (Forman, Maiorino et al. 2010):

$$H_2O_2 + RS^- \rightarrow OH^- + RSOH \quad (2)$$

However, to proceed at a biologically relevant rate, this reaction requires the presence of a proton, at sufficient proximity to allow the hydroxyl ion to leave as water. Reaction (3) would proceed then at a much faster rate:

$$H^+ + H_2O_2 + RS^- \rightarrow H_2O + RSOH \quad (3)$$

This reaction would not occur in solution, because the thiolate would be protonated, however, Prxs and GPxs, catalyse this reaction by favouring both the dissociation of thiol and the protonation of the leaving group (Forman, Maiorino et al. 2010; Rhee and Woo 2011). In addition, the oxygen-oxygen bond of the peroxide molecule must be polarized to favour nucleophilic attack (Toppo, Flohe et al. 2009; Flohe, Toppo et al. 2011). In proteins, the thiolate form could be stabilized through electrostatic interactions with polar or positively charged amino acids, which lowers the pK_a of the Cys residue from the typical ~8.5 to as low as 3.5 (Salsbury, Knutson et al. 2008; Paulsen and Carroll 2010). In both selenium and non-selenium GPxs, the thiolate at the active site is surrounded by specific amino acid residues Asn, Gln, and Trp that are essential for stabilization of the transition state (Stone 2004; Flohe, Toppo et al. 2011). The catalytic site in Prx is composed of Cys (pK_a = 4.5 – 5.9 (Nelson, Parsonage et al. 2008; Hugo, Turell et al. 2009)), Thr, or Ser and Arg (Hall, Parsonage et al. 2010; Flohe, Toppo et al. 2011). By creating point mutations, two highly conserved Arg residues in human Prx2 and Prx3 had been shown to be critical for the peroxidase activity of these enzymes (Nagy, Karton et al. 2011).

Sulfenic acid, formed as a product in this reaction, could react with a range of oxidants or with another Cys in the same protein, a neighbouring protein, or GSH (Paulsen and Carroll 2010). Disulfide formation could be followed by a cascade of thiol-disulfide exchange reactions (Forman, Maiorino et al. 2010). If oxidative stress occurs, higher non-reversible oxidation states could also be formed that render the protein non-functional (Paulsen and Carroll 2010).

1.2.2 Role of GSNO in redox regulation

NO derivative nitrosothiols, and in particular S-nitrosylated GSH (GSNO), are believed to be major signaling molecules involved in the actions of NO, including apoptosis, oxidative stress and immune responses (Stamler, Lamas et al. 2001; Piantadosi 2012). GSNO formation was first demonstrated in Escherichia coli in 1996 by Hausladen et al. (Hausladen, Privalle et al. 1996). Recently, ferric cytochrome c was found to catalyze the formation of GSNO in the presence of NO and GSH (Broniowska, Keszler et al. 2012). GSNO levels are found to be affected in disease, which reflects the importance of GSNO in redox signaling (Ju, Chen et al. 2005; Khan, Sekhon et al. 2005; Schonhoff, Matsuoka et al. 2006).

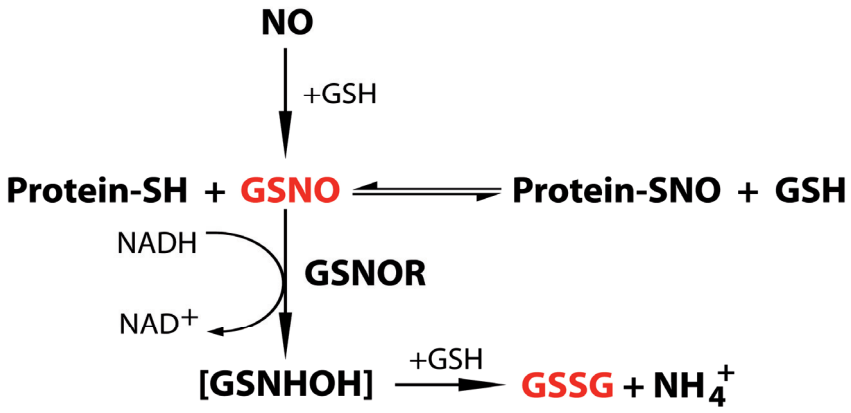

Figure 5: Metabolism of GSNO. In biological systems, GSNO is in equilibrium with protein S-nitrosothiols. GSNO metabolised to GSSG and ammonia by GSNOR, with intermediate product GSH N-hydroxysulfenamide (GSNHOH) (according to (Foster, Hess et al. 2009)).

GSNO is also believed to be a primary low molecular weight non-protein SNO in cells and in extracellular fluids (Gaston, Reilly et al. 1993); micromolar amounts of GSNO were detected in the brain (Kluge, Gutteck-Amsler et al. 1997) and liver (Steffen, Sarkela et al. 2001) of healthy rats. GSNO is not directly transported into cells, and transfer of their S-nitroso group to the interior of the cell is mediated by Cys through the formation of CysNO, which is then taken up by the cells via the amino acid transport system L (Zhang and

Hogg 2005). Once inside the cell, CysNO readily transfers its nitroso group to other cellular thiols, including proteins and GSH. In addition to CysNO, NO and, more possibly, NO/oxygen reaction products might diffuse into cells and directly S-nitrosylate intracellular targets (Zhang and Hogg 2005).

Once formed, GSNO could be metabolized to GSSG by the enzyme GSNOR (Figure 5) (Liu, Hausladen et al. 2001). This process is important for maintenance of the equilibrium between S-nitrosylated proteins and GSNO.

GSNO may participate in protein S-nitrosylation in two different ways: first, through a thiol-to-thiol transnitrosation process, which is reversible (Foster, McMahon et al. 2003), or, second, functioning as a source of free-radical NO that is generated by release of the latter from GSNO. NO release from GSNO is observed in the presence of endogenous cellular reductants and transition metals (Stubauer, Giuffre et al. 1999; Romeo, Capobianco et al. 2003; Sun, Xu et al. 2003), whereas cleavage of GSNO may be catalysed by several enzymes (Hou, Guo et al. 1996; Nikitovic and Holmgren 1996; Trujillo, Alvarez et al. 1998; Jourd'heuil, Laroux et al. 1999; Romeo, Capobianco et al. 2003; Staab, Alander et al. 2008). In addition, formation a protein-GSH mixed disulfide was proposed as the net outcome of the reaction of protein with GSNO (Wong, Hyun et al. 1998; Brigelius-Flohe and Flohe 2011).

In summary, GSNO may be able to mediate or modulate signaling pathways participating in the transnitrosylation of proteins and also act as a store or buffer of NO within the cell. Moreover, anti-inflammatory and ameliorative roles have been demonstrated for low-molecular-weight SNOs, including GSNO, and those findings suggest that GSNO might serve as a potential therapeutic agent in diseases or in disease models (Khan, Sekhon et al. 2005; Foster, Hess et al. 2009; Khan, Im et al. 2009; Nath, Morinaga et al. 2010).

1.3 Investigation of the redox properties of proteins

Cys modifications by ROS were first discovered in diseases accompanied by oxidative stress, including type II diabetes, cancer, neurodegenerative diseases, and cardiovascular disease, and are also associated with aging (Harman 1956). Reductive pathways, which reverse the effects of ROS on Cys, were discovered in plants: the activity of chloroplast enzymes was shown to be differentially regulated by a disulfide-mediated redox mechanism in response to light (Buchanan 1980). A significant number of cell proteins have been found to be redox-regulated on a proteome-wide scale using gel electrophoresis or chromatographic methods coupled with mass spectrometry (Stroher and Dietz 2006). The proteins identified comprise a portion of the so called redox proteome, which includes proteins that undergo thiol-disulfide transitions and are direct targets of redox metabolism. Moreover, proteins with iron-sulfur

clusters, including heme, purine, and flavin cofactors, are among others involved in sensing and transmitting redox information to downstream signaling elements (Stroher and Dietz 2006). On the inventory step of redox proteomics, bioinformatics techniques are applied to search for redox active thiol containing proteins on the proteome wide scale. In general, the redox active proteins identified to date include several dithiols/disulfide exchanging families of proteins such as Trxs, Grxs, and Prxs, enzymes, and transcriptional factors among other, however, the actual number of redox-active proteins remains unknown (Stroher and Dietz 2006; Butterfield and Dalle-Donne 2012). Besides identification, studies at the proteome level are useful to study the redox properties and behaviour of particular proteins *in vivo* and *in vitro*.

1.3.1 Determination of the reactivity of proteins against oxidants *in vitro*

Investigation of reaction mechanisms and pathways is the subject of *in vivo* or *in vitro* studies. *In vivo* studies typically comprise treatment of bacteria, yeast or cells with different exogenous oxidative agents or by inducing endogenous oxidative stress while following the creation of Cys modifications (Katakai, Liu et al. 2001; Lee, Lee et al. 2004; Maret 2011). Despite the importance of *in vivo* studies, *in vitro* investigations are often easier to perform, follow, and interpret, and resulting in accurate data that may allow for the prediction of protein function from the context of redox regulation within biological systems.

Oxidation of Cys and zinc release under redox stress conditions *in vitro* has been investigated intensively in recent years. Reactions of metal-containing proteins with oxidants *in vitro* are usually followed by spectrophotometry, chromatography, mass-spectrometry (MS) and/or structural analysis. Release of metal ions, and in particular Zn(II), from metal-protein complexes during the course of oxidation reactions is often followed spectrophotometrically using a metal indicator, such as PAR or Zincon (McCall and Fierke 2000; Blessing, Kraus et al. 2004; Sabel, Neureuther et al. 2010). In conjunction with Cys derivatisation, followed by MS, liquid chromatography has evolved into a particularly powerful tool to detect and characterize oxidized products (Meza, Scott et al. 2003). Structural studies include NMR and crystallography (Baldwin and Benz 2002; Jung, Yee et al. 2005; Sainsbury, Ren et al. 2010).

1.4 Redox potential

Redox potential (ORP, pE, Eh) determines the tendency of a chemical species to acquire electrons and thereby be reduced. Any redox reaction consists of two half-reactions: oxidation and reduction that are always coupled because “free” electrons cannot exist in solution. In an oxidation reaction a substance looses or donates electrons, while in a reduction reaction a substance gains or accepts

electrons. The coupling between two half-reactions is achieved by electrons which are either generated (oxidation) or consumed (reduction) (Snoeyink 1980). By definition, electrons tend to flow from the conjugated redox pair of lower reduction potential to a pair with a higher reduction potential. The Nernst equation relates the redox potential of a half reaction to the standard redox potential and the present concentrations of the electron donor and acceptor (Eq. 2a). The standard reduction potential ($E^{0\prime}$) is measured under standard conditions: 25°C, a 1 M concentration for each substance that is participating in the reaction, partial pressure of 1 atm for each gas that is participating in the reaction at pH 7. The change in redox potential ($\Delta E'$) associated with the reaction is defined in Equation 3 (Jensen, Hansen et al. 2009).

The redox equilibrium between protein-GSH and GSSG is described in (Eq. 1 a-c).

$$P_{SH}^{SH} + GSSG \rightleftharpoons P_{S}^{S}] + 2GSH \qquad \text{(eq. 1a)}$$

Half reaction 1: $$P_{SH}^{SH} \rightleftharpoons P_{S}^{S}] + 2e^{-} + 2H^{+} \qquad \text{(eq. 1b)}$$

Half reaction 2: $$GSSG + 2e^{-} + 2H^{+} \rightleftharpoons 2GSH \qquad \text{(eq. 1c)}$$

Nernst equation:

$$E' = E^{\circ\prime} + \frac{RT}{nF} ln \frac{[electron\ acceptor]}{[electron\ donor]} \qquad \text{(eq. 2a)}$$

where n is the number of electrons transferred, F is the Faraday constant (9.65×10^4 C mol^{-1}), E' is the redox potential (V) at pH 7, and $E^{0\prime}$ is the standard redox potential (V) (Jensen, Hansen et al. 2009).

Half reaction 1: $$E_1' = E_{P_{SH}^{SH}/P_{S}^{S}]}^{0\prime} + \frac{RT}{nF} ln \frac{[P_{S}^{S}]]}{[P_{SH}^{SH}]} \qquad \text{(eq. 2b)}$$

Half reaction 2: $$E_2' = E_{GSH/GSSG}^{0\prime} + \frac{RT}{nF} ln \frac{[GSSG]}{[GSH]^2} \qquad \text{(eq. 2c)}$$

$$\Delta E' = E_{acceptor}' - E_{donor}' = E_2' - E_1' \qquad \text{(eq. 3)}$$

The redox potential is proportional to the Gibbs free energy of reaction (Eq. 4). From this, a relation between the equilibrium constant of the reaction and the standard redox potential may be derived (Eq. 5 and 6). $\Delta E^{0\prime}$ and $\Delta G^{0\prime}$ are

constants of the reaction that predict which way a reaction will proceed when the concentrations of all involved species are at the non-physiological concentration of 1M.

$$\Delta G' = -nF\Delta E' \quad \text{(eq. 4)}$$

$$\Delta G^{0'} = -nF\Delta E^{0'} \quad \text{(eq. 5)}$$

$$RT\ lnK_{eq} = -nF\Delta E^{0'} \quad \text{(eq. 6)}$$

From this, the standard redox potential of a conjugated redox pair in equilibrium with another conjugated redox pair of known standard redox potential can be calculated (Eq. 7).

$$E^{0'}_{P^{SH}_{SH}/P^{S}_{S}]} = E^{0'}_{GSH/GSSG} + \frac{RT}{nF} lnK_{ox} \quad \text{(eq. 7)}$$

However, major cellular redox pairs (Trx(SH)2/TrxSS, GSH/GSSG, Cys/CySS) are not at equilibrium with each other and their concentrations, which determine E_h values, vary in different compartments or organelles. As a consequence, biological E_h values are operational: they are a function of the extraction, fractionation, and assay methods (Kemp, Go et al. 2008). Two major systematic errors often occur: incorrect estimate of the pH, which gives an error of ~5.9 mV per 0.1 pH units and incorrect estimate of the concentration of redox couples, which gives 30 mV for a 10-fold error in concentration estimates for GSH and Cys couples (Clarke 1960). Inefficient trapping of the redox couples could additionally result in increased variability. When these systematic errors were combined to determine the cytoplasmic E_h values in HT29 cells, the error was estimated to be as high as 10 mV (Kirlin, Cai et al. 1999; Jones, Go et al. 2004).

1.4.1 Intracellular redox potential

Two major redox systems determine the redox environment within biological systems: the GSH and Trx redox systems. GSH/GSSG, Trx(SH)2/TrxSS, and Cys/CySS are major redox pairs and referred to as redox control nodes.

The GSH redox system, which compromises one of the two major redox systems that control the cellular thiol redox balance, regulates levels of hydrogen peroxide within cells, and consists of the species NADPH, GR, and GSH (Bindoli and Rigobello 2012). GSH concentration is 100- to 1000- fold higher than the reduced forms of the other couples. Therefore, the GSH/GSSG redox pair usually determines the steady-state value of the intracellular redox potential (Filomeni, Rotilio et al. 2002). GSH and GSSG concentrations

fluctuate as GSH homeostasis is maintained through a delicate balance between synthesis, uptake, usage, breakdown, and excretion depending on the type of cell, phase in the cell cycle, and external environment. Variations in this ratio influence the signaling pathways that regulate proliferation, apoptosis, gene expression, and autophagy (Biswas and Rahman 2009). Because the GSH level has been established to be in the low millimolar (0.5-10 mM) range (Kosower and Kosower 1978; Ostergaard, Tachibana et al. 2004), the GSSG level falls into the low micromolar range (Ostergaard, Tachibana et al. 2004). The ratio of GSH to GSSG is expressed as the redox potential of the GSH/GSSG redox couple ($E_{GSH/GSSG}$), and this is generally tightly regulated to maintain cellular redox homeostasis (Schafer and Buettner 2001).

The cytosolic redox state, characterized by redox potential, under normal conditions is maintained in a very narrow range by a pool of low-molecular weight thiols and controlled by enzymes. The cytosol has been found to be highly reducing with redox potentials between -230 and -260 mV (Kemp, Go et al. 2008). To determine the GSH/GSSG intracellular redox potential *in vivo*, compartment-specific ratios and absolute concentrations of GSH and GSSG have to be determined in each compartment. However, accurate determination of both of these quantities remains technically challenging *in vivo*. Genetically encoded yellow fluorescent protein (YFP)- and green fluorescent protein (GFP)-based redox probes (Dooley, Dore et al. 2004; Ostergaard, Tachibana et al. 2004; Gutscher, Pauleau et al. 2008) have enabled scientists to measure and report sub-cellular compartment specific $E_{GSH/GSSG}$ values from a variety of model organisms (Ostergaard, Tachibana et al. 2004; Gutscher, Pauleau et al. 2008; Meyer and Dick 2010; Albrecht, Barata et al. 2011; Morgan, Sobotta et al. 2011; Dardalhon, Kumar et al. 2012). The reported values are close to -320 mV, which corresponds to a GSH:GSSG ratio of 50000:1, assuming a 10 mM total cytosolic GSH pool (Ostergaard, Tachibana et al. 2004). This ratio is several orders of magnitude greater than previously believed (Morgan, Ezerina et al. 2012).

The reducing power of GSH allows one to maintain ROS and glutathionylated proteins at low levels under normal conditions (Heeren, Jarolim et al. 2004; Ostergaard, Tachibana et al. 2004; Lopez-Mirabal and Winther 2008). However, very small changes in the redox potential affect critical biochemical steps: a 30 mV change means a 10-fold change in the ratio between reducing and oxidizing species (Schafer and Buettner 2001). Thus, in apoptosis a change of 72 mV occurs, thus shifting to more oxidizing conditions for the intracellular GSH/GSSG couple (Cai and Jones 1998); the difference between proliferating and confluent fibroplasts is 34 mV (Hutter, Till et al. 1997); a small difference of 15 mV abolishes the binding of redox-sensitive transcription factors to DNA (Clive and Greene 1996).

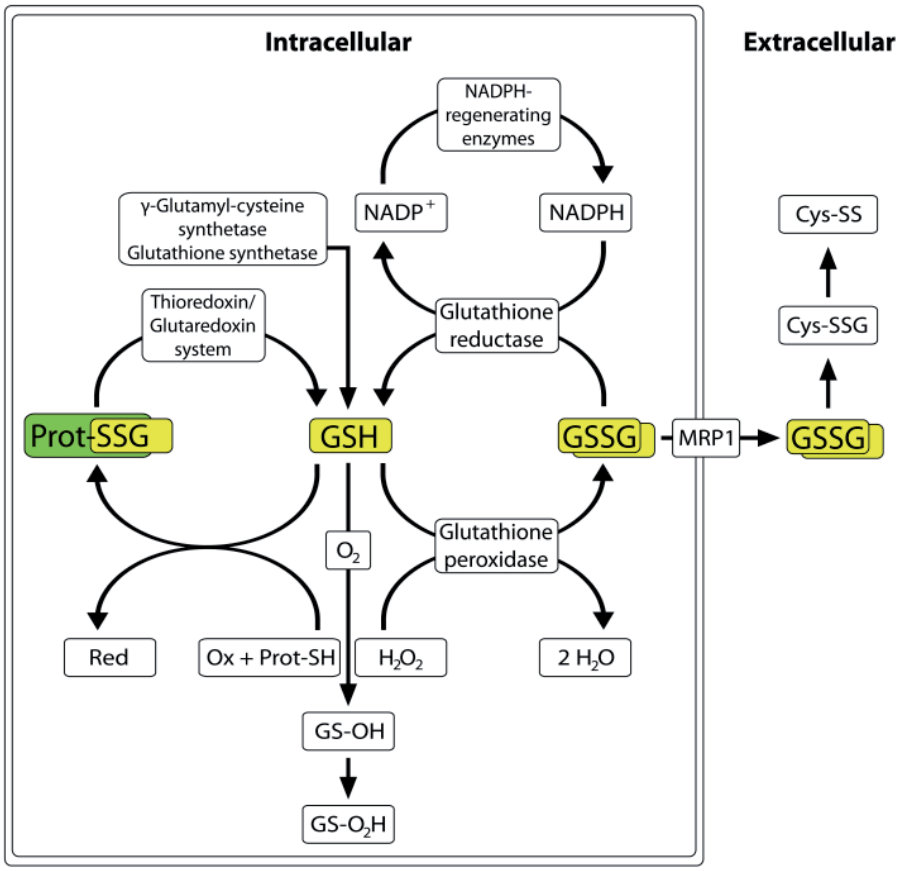

Figure 6: GSH/GSSG redox cycle. Prot-SSG stands for S-glutathionylated protein; GS-OH – sulfenic acid derivative of GSH; GS-O_2H – sulfinic acid derivative of GSH; MRP1 – multidrug resistant protein 1; Cys-SSG – glutathionylated derivative of Cys; Cys-SS – 2 Cys molecules bound by disulfide.

GSH is synthesized in the cytosol in two steps catalyzed by γ-glutamyl-Cys ligase and GSH synthase (Figure 6); both require ATP. In Saccharomyces cerevisiae, the γ-glutamyl-Cys ligase activity is the rate limiting in GSH synthesis (Ohtake and Yabuuchi 1991), which is up-regulated during oxidative stress (Stephen and Jamieson 1997; Dormer, Westwater et al. 2002) and during exposure to heavy metals (Westwater, McLaren et al. 2002).

After being synthesized, GSH, together with GSSG, participates in redox regulation both by creating a specific redox environment, and by providing reducing equivalents for a range of enzymes, including GPx (Figure 6), glutation S-transferase (GST), and Grx (Dickinson and Forman 2002; Lillig, Berndt et al. 2008).

To maintain a reducing environment, cells must maintain GSSG at very low levels. This is achieved by either de novo synthesizing GSH or by modulating

GSSG levels using two competing mechanisms: reduction of GSSG by GR in the presence of NADPH (Filomeni, Rotilio et al. 2002) and GSSG export from the cell via multidrug resistance protein 1 (MRP1, ABCC-1) (Mueller, Widder et al. 2005; Ballatori, Krance et al. 2009) (Figure 6). Recent studies in yeast show, that GSSG levels are strictly controlled in the cytosol under conditions of severe stress and the GSSG portion that is not immediately reduced is transported into the vacuole by the Ycf1, a yeast homolog of MRP1 (Morgan, Ezerina et al. 2012). Grx2 was also found to function in the yeast cytosol as a backup system for GSSG reduction (Morgan, Ezerina et al. 2012). Despite these active control mechanisms, the GSH/GSSG ratio is altered during oxidative stress, which may lead to a disruption in redox homeostasis (Backos, Franklin et al. 2012).

In parallel with the GSH redox system, the Trx system is another major determinant of the cellular thiol redox balance (Bindoli and Rigobello 2012), despite having lower cellular concentrations in the micromolar range (Holmgren and Luthman 1978; Gromer, Urig et al. 2004). Both of these redox couples, GSH/GSSG and Trx(SH)2/TrxSS, are not in equilibrium with each other (Hansen, Zhang et al. 2006; Go and Jones 2008), and both fulfil distinct key roles in cellular redox metabolism (Trotter and Grant 2003; Hansen, Zhang et al. 2006; Patwari and Lee 2007; Go and Jones 2008; Bindoli and Rigobello 2012; Mahmood, Abderrazak et al. 2012). However, evidence for possible crosstalk between these two systems is provided by several observations. Under conditions where one of the two pathways is compromised, the other one provides a compensatory mechanisms for cell maintenance (Casagrande, Bonetto et al. 2002; Conrad, Jakupoglu et al. 2004; Conrad 2009; Mandal, Schneider et al. 2010; Scarbrough, Mapuskar et al. 2012). The Trx system consists of Trx (Trx1 or Trx2), truncated Trx (Trx-80), tioredoxin reductase (TrxR), NADPH, and the Trx-interacting protein (TXNIP) (Mahmood, Abderrazak et al. 2012). Trx isoforms and homologs from all organisms contain a highly conserved –C-X-Y-C- active site, where X and Y are often, but not necessarily, hydrophobic amino acids. This active site is essential for the protein to function as disulfide oxidoreductase (Holmgren 1989). Specific protein targets for reduction by Trx proteins include ribonucleotide reductase (Zahedi Avval and Holmgren 2009), methionine sulfoxide reductases (Sagher, Brunell et al. 2006; Tarrago, Laugier et al. 2009), and several transcription factors including p53, NF-κB, glycocorticoid receptor and AP-1 (Bindoli and Rigobello 2012; Mahmood, Abderrazak et al. 2012). Furthermore, Trx is integral for the reduction of Prxs (Chae, Kang et al. 1999; Nordberg and Arner 2001; Lillig and Holmgren 2007), which play a primary role in redox signaling as sensors of peroxides for other proteins in addition to their function as peroxidases (Brigelius-Flohe and Flohe 2011; Rhee and Woo 2011). Other functions of Trx include direct reduction of some ROS and refolding of various oxidized proteins (Filomeni, Rotilio et al. 2002). A lack of cytosolic Trx may indirectly affect the mechanisms necessary for ROS scavenging and/or redox regulation by the GSH

system (Lopez-Mirabal and Winther 2008). In addition to Trx, Grx also catalyzes reactivation of various oxidized and glutathionylated proteins with strong preference for glutathionylated substrates (Jung and Thomas 1996) (Thomas, Poland et al. 1995; Jung and Thomas 1996; Filomeni, Rotilio et al. 2002).

The Cys/CySS redox pair is also present in the cytosol. Its steady-state redox potential is equal to -145 mV in HT29 cells and is more oxidized (around 90 mV) relative to the $E_{GSH/GSSG}$ and $E_{Trx(SH)2/TrxSS}$ (Jones, Go et al. 2004). In similarity to conditions in the extracellular milieu, the cellular Cys/CySS redox pair operates independently of the GSH/GSSG redox pair (Jones, Go et al. 2004). This suggests that the Cys/CySS redox couple within cells acts as an oxidant during redox switching by oxidizing proteins without directly involving more potent oxidants (Jones, Go et al. 2004).

The total cellular redox potential is a very complex parameter to quantify because it is determined by multiple redox systems including those mentioned above together with hundreds of different protein thiol/disulfide couples which are not necessarily in thermodynamic equilibrium with each other and operate through major redox control nodes. Even if it were possible to obtain this data it would still be difficult to obtain a reliable estimation of the cellular redox potential. Moreover, under physiological conditions, transition metal ions such as Zn(II), Fe(II), and Cu(I) are present, which could modulate thiol-disulfide redox equilibria (Palumaa 2009; Zovo and Palumaa 2009). Zn(II) ions and other soft metal ions have a high affinity towards thiolates, whereas two spatially close thiolates in biological redox switches can create a Zn(II) binding site of substantial affinity. Zn(II) complexes, if formed, protect SH-groups from oxidation and shift the standard redox potentials of proteins to more negative values (Zovo and Palumaa 2009). These principles may apply to other transition metal-binding proteins a variety of other redox switches, and also to GSH (Kemp, Go et al. 2008; Lopez-Mirabal and Winther 2008).

1.4.2 Extracellular redox potential

The dominant low-molecular weight thiol/disulfide couple in the mammalian blood plasma is Cys and its disulfide, cystine (CySS) (Jones, Mody et al. 2002; Go and Jones 2008). This pool is one of the central redox control nodes in the extracellular compartment, and plays a major role in redox communication between cells and tissues, as described in (Jones, Go et al. 2004). In culture media, cells regulate the extracellular redox potential to values similar to the plasma Cys/CySS (Go and Jones 2005; Jiang, Moriarty-Craige et al. 2005). The mean plasma Cys/CySS redox value ($E_{Cys/CySS}$) is approximately -80 mV and is thus about 60 mV more oxidized than the cytoplasmic redox value for Cys/CySS.

The GSH/GSSG redox couple also operates within blood plasma. The mean plasma $E_{GSH/GSSG}$ value is -138 mV in young healthy adults (Jones, Carlson et al. 2000), which is 90 mV more oxidized than the cytoplasmic pool (Go and Jones 2008). Importantly, the plasma GSH/GSSG redox couple is not in equilibrium with the plasma Cys/CySS pool. Both pools change, but with different characteristics, in particular, after meals becoming more reducing (Blanco, Ziegler et al. 2007), or in association with age becoming more oxidizing (Samiec, Drews-Botsch et al. 1998; Hildebrandt, Kinscherf et al. 2002; Jones, Mody et al. 2002). In addition, the thiol/disulfide redox state in plasma is oxidized with oxidative stress-involving conditions such as chemotherapy (Jonas, Puckett et al. 2000), diabetes (Samiec, Drews-Botsch et al. 1998), cardiovascular disease (Ashfaq, Abramson et al. 2006), smoking (Moriarty, Shah et al. 2003), and alcohol abuse (Brown, Ping et al. 2007). The plasma redox potential value correlates with plasma protein S-glutathionylation (Piemonte, Pastore et al. 2001; Pastore, Tozzi et al. 2003).

Another redox-active plasma component is albumin, which contains redox-active Cys. The S-cysteinylated form of albumin normally forms about half of the albumin pool. The content of this disulfide correlates with the plasma Cys/CySS redox potential (Jones, Mody et al. 2002). Albumin thiol has been suggested to function also as a carrier of NO and play a role in detoxification (Ng and Kubes 2003; Tellez-Sanz, Cesareo et al. 2006).

The Trx1 represents a Trx system in plasma (Mahmood, Abderrazak et al. 2012) and provides important protective functions in extracellular compartments (Sahaf and Rosen 2000; Nakamura, De Rosa et al. 2001; Nakamura, Herzenberg et al. 2001; Mahmood, Abderrazak et al. 2012) . Trx1 also serves as a biomarker for a wide variety of diseases (Hoshino, Shioji et al. 2007). There are two forms of Trx1 found in the extracellular compartments: intact Trx1 (12 kDa) and a truncated form containing only N-terminal 1-80 residues (Trx-80, 10 kDa) (Mahmood, Abderrazak et al. 2012). Intact Trx1 exists predominantly in an oxidized form (Billiet, Furman et al. 2005; Hoshino, Shioji et al. 2007) while truncated Trx-1 can be secreted by cells (Silberstein, McDonough et al. 1993). Secretion occurs predominantly under conditions associated with oxidative stress, apoptosis, and inflammation (Billiet, Furman et al. 2005; Hoshino, Shioji et al. 2007). Consistently, plasma Trx-1 concentrations are raised in patients with several cardiovascular risk factors (Miwa, Kishimoto et al. 2005) and with acute lung injury (Callister, Burke-Gaffney et al. 2006). The truncated form of Trx is proposed to function with both cytokine-like and chemokine-like activities (Gon, Sasada et al. 2001; Hagg, Englund et al. 2006; Mahmood, Abderrazak et al. 2012).

In order to understand the mechanisms and functional consequences of redox changes in the extracellular compartment, attempts have been made to adjust the Cys/CySS redox state in cell culture (Go and Jones 2005). These studies show

accelerated cell proliferation at reduced E_h values in human gut epithelial (Caco-2) cells and normal human retinal pigment epithelial (hRPE) cells (Jonas, Gu et al. 2003; Jiang, Moriarty-Craige et al. 2005). However, the oxidized E_h values stimulated fibroplast proliferation in a lung fibroplast model relevant to pulmonary fibrosis (Ramirez, Ramadan et al. 2007). These results suggest that extracellular Cys/CySS redox-dependent cell proliferation is cell type specific and mediated by intracellular kinase (e.g. p44/p42 MAPK) activation (Go and Jones 2008). Such cell type specificity is derived from differential cell response to physiologic conditions. For example, fibroblasts respond to proliferate in order to repair tissue caused by immune cell-induced oxidative conditions, while reducing conditions are most stimulatory to other cells (Go and Jones 2008). In contrast to greater proliferation under reducing extracellular conditions, hRPE cells were more prone to oxidant-induced apoptosis under more oxidizing extracellular conditions with E_h > -55 mV (Jiang, Moriarty-Craige et al. 2005). Other studies show that ROS production increases in cells exposed to a more oxidizing E_h value (Go and Jones 2005). Thus, this data suggest that factors which control the balance of plasma or extracellular Cys/CySS influence cellular functions, with a general trend that a more reduced state stimulates cell proliferation while a more oxidized state sensitizes cells to oxidative stress and other stress responses (Go and Jones 2008).

1.4.3 Redox compartmentalization

Redox conditions differ from one cellular compartment to another: the mitochondria, cytosol, and nucleus are considered to be reducing environments, while the ER and Golgi apparatus are considered to be more oxidizing (Go and Jones 2008; Kemp, Go et al. 2008; Malinouski, Zhou et al. 2011).

Mitochondria are considered to be the most redox-active compartments of the eukaryotic cell (Jocelyn 1972) and function as the energy stations of the cell through the generation of ATP through the oxidation of various metabolic substrates (e.g. pyruvate and fatty acids). Different steady-state $E_{GSH/GSSG}$ values in mitochondria have been reported: -280 mV (Cai and Jones 1998; Rebrin and Sohal 2004), -300 mV, and -330 mV (Kemp, Go et al. 2008). Moreover, fluctuations in redox state are observed within mitochondria: the redox environment of mitochondrial intermembrane space (IMS) is maintained separately from the matrix and cell cytosol, and is considerably more oxidizing compared to the other two compartments: -255 mV (pH 7.0) in the IMS versus -286 mV (pH 7.0) in the cytosol and -296 mV in the mitochondrial matrix (Hu, Dong et al. 2008). The key determinant of the GSH/GSSG ratio in mitochondria is GSH transport (Chen, Putt et al. 2000; Lash 2006) because GSH is not synthesized in mitochondria, but is synthesized in the cytoplasm and subsequently transported into mitochondria (Griffith and Meister 1985; Kurosawa, Hayashi et al. 1990). Recent studies show that GSH depletion has a profound effect on the stability of the mitochondrial genome in Saccharomyces

cerevisiae, emphasizing the importance of GSH availability during growth (Dardalhon, Kumar et al. 2012 14310). Mitochondria contain several GSH-dependent enzymes, including GPx1 and GPx4, GR, and Grx2 (Nomura, Imai et al. 1999; Lundberg, Johansson et al. 2001), which are all essential to protect mitochondria against oxidative stress. The Trx system within mitochondria includes mitochondria specific Trx2, TrxR2, and mitochondrial Prxs3 and Prxs5 (Spyrou, Enmark et al. 1997; Miranda-Vizuete, Damdimopoulos et al. 1999; Go and Jones 2008). Based on redox values obtained using a redox western blot method and a redox-sensitive GFP method (Halvey, Watson et al. 2005; Hansen, Zhang et al. 2006), mitochondria are considered to house the most reducing environment in the cell (Hansen, Go et al. 2006). The E_h value of the Trx2 redox pair (-330 mV at pH 7.6) corresponds to a more reducing environment compared to the E_h values of the Trx1 redox pair in the cytoplasm (-280 mV at pH 7.0) and nucleus (-300 mV at pH 7.0) (Kemp, Go et al. 2008).

It is critical to maintain the nucleus under reducing conditions because it contains proteins with Cys residues that are necessary for genome control and protection from ROS and RNS. These proteins include enzymes, transport machinery, structural proteins, and transcription factors (Go and Jones 2008). Regulation of transcriptional activity through critical Cys residues within zinc fingers and the DNA binding domain is among the most important aspects of nuclear redox control. Several transcriptional factors, including AP-1, NF-κB, Nrf2, p53, and the glucocorticoid receptor (Bodwell, Holbrook et al. 1984; Abate, Patel et al. 1990; Hainaut and Milner 1993; Galter, Mihm et al. 1994; Allen and Tresini 2000; Bloom, Dhakshinamoorthy et al. 2002), have been shown to be regulated by both the GSH and Trx1 redox mechanisms. Recently, targeting rxYFP to the nucleus helped to establish that the nuclear GSH/GSSG redox environment is highly reducing, with values similar to that found in the cytosol: -290 mV (Dardalhon, Kumar et al. 2012). GSH and GSSG may be exchanged between the cytosol and nucleus; however, GSH depletion does not profoundly affect nuclear genome stability (Dardalhon, Kumar et al. 2012).

Peroxisomes utilize H_2O_2 as an oxidative agent (Fagarasanu, Fagarasanu et al. 2007) and they contain ROS- and RNS- generating enzymes, being additional source of ROS and RNS in the cell (Loughran, Stolz et al. 2005; Schrader and Fahimi 2006; Wanders and Waterham 2006). Large amounts of peroxide are metabolized by catalase in the peroxisomes (Jones, Eklow et al. 1981) and peroxisomes are considered to house an oxidizing redox environment. Similar to peroxisomes, the secretory pathway is characterized by oxidizing conditions ($E_{GHS/GSSG}$ is from -172 to -188 mV) (Hwang, Sinskey et al. 1992). ER contains an oxidase system for introducing disulfides into proteins destined for export (Gross, Sevier et al. 2006). GSH in ER serves as glutathionylating agent, forming mixed disulfides with proteins that function to modulate the activity of redox-active proteins and protect against hyper oxidizing conditions (Cuozzo and Kaiser 1999). Lastly, lysosomes have been suggested to have an oxidizing

environment and, moreover, are deficient in mechanisms to reduce disulfides to thiols (Cherqui, Kalatzis et al. 2001; Kemp, Go et al. 2008).

The variability in redox characteristics between different organelles within the cell and a lack of the equilibrium between thiol/disulfide control systems within each compartment provides evidence regarding the complexity of the redox balance within biological systems (Go and Jones 2008). Different redox characteristics appear to have evolved in conjunction with the specific functions of each organelle. In the cytoplasm, there are only a few enzymes identified that generate ROS as part of normal metabolic function (D'Autreaux and Toledano 2007). The first role of the cytoplasm is to provide a buffer zone between mitochondria, ER, and nuclei, so that each organelle is protected against aberrant ROS production by the others. The second role is to allow for a very low background of ROS and RNS so that these can be used as sensitive and specific signaling molecules dependent upon NADPH oxidases and NOS (D'Autreaux and Toledano 2007). Finally, extracellular compartments serve as protective barriers against external oxidants, they act as a medium for communication between cells, and they provide appropriate conditions for receptors and transporters to function in the plasma membrane. Techniques to measure the redox state within extracellular compartments are emerging as useful tools to assess disease risk and to monitor the progress of diseases and their response to interventions (Go and Jones 2008).

1.4.4 Determination of protein's redox potential *in vitro*

The midpoint redox potential E_m determines the environmental redox potential value at which reduced and oxidized forms of protein are present in equimolar concentrations. Determining the E_m of a particular protein in a given environment relies on the detection of the equilibrium between oxidized and reduced forms of a particular protein at different environmental redox potential values created by the combined action of various redox buffer systems (Dutton 1978; Zovo and Palumaa 2009). Redox buffers such as DTT/oxidized DTT and GSH/GSSG are used routinely, and the redox potentials for different component ratios can be calculated using the Nernst equation (Dutton 1978).

The content of reduced and oxidized proteins are usually measured using a variety of spectroscopic and bioanalytical methods, from the mixture of protein redox forms or after trapping and separation of different redox states (Dutton 1978; Bjornberg, Ostergaard et al. 2006; Piotukh, Kosslick et al. 2007; Marri, Trost et al. 2008). Metal ions, if present in complex with Cys thiols, can exclude or complicate the application of many techniques because the metal ions affect the spectroscopic properties of proteins and interfere with chemical modifications of Cys. Moreover, using GSH/GSSG redox buffers that mimic cellular redox conditions, GSH adducts could occur under mildly oxidizing

conditions, which could have a biological role in protein redox regulation (Fratelli, Demol et al. 2002; Dalle-Donne, Rossi et al. 2007). MS, and in particular ESI-MS, allows for the identification of protein-metal complexes that coexist with different redox forms of proteins. Importantly, the accuracy of a high resolution MS instruments is sufficiently high to directly monitor disulfide bond formation, which enables one to determine redox equilibria without chemical modification of Cys, thus avoiding this source of error (Zovo and Palumaa 2009).

1.5 Characterization of selected proteins

1.5.1 Cys_4 Zn-fnger domain of XPA

Xeroderma pigmentosum, complementation group A (XPA) is an essential member of a nucleotide excision repair (NER) multiprotein complex (Tanaka, Miura et al. 1990). It interacts with damaged DNA and other proteins to chemically remove structurally distinct DNA lesions from the eukaryotic genome (Tanaka and Wood 1994). A loss of XPA function leads to xeroderma pigmentosum type A, a severe autosomal recessive disease characterized by UV hypersensitivity, enhanced skin cancer risk and neurological abnormalities (Cleaver and States 1997). In humans, the XPA gene product (hXPA) is a 31-kDa protein comprised of 273 amino acid residues (Tanaka, Miura et al. 1990). XPA plays a central role in NER: it recognizes and/or verifies damaged DNA (Sugasawa, Ng et al. 1998) and recruits other NER complex proteins (including ERCC1 (Li, Elledge et al. 1994), TFIIH (Park, Mu et al. 1995), and RPA (Matsuda, Saijo et al. 1995)) to aid in the repair process.

XPA contains a single Cys_4 type zinc finger domain (XPAzf), which is essential for XPA function. The activity of XPA is inhibited by several metal ions other than Zn(II) (Asmuss, Mullenders et al. 2000; Asmuss, Mullenders et al. 2000). The structure of XPA was solved using NMR and EXAFS (Buchko, Ni et al. 1998; Buchko, Iakoucheva et al. 1999) and the NMR structure of the XPA minimal DNA-binding domain (XPA-MBD) consists of well-defined secondary structure elements interspaced with disordered loops organized into two non-interactive sub-domains: a zinc-binding core (D101-K137) and a loop-rich domain (L138-F219). The zinc-binding core contains an antiparallel β-sheet (Y102-C105 and K110-M113) and an α-helix (C126-K137) separated by a poorly defined turn (Buchko, Ni et al. 1998). Further EXAFS studies on a lyophilized sample of hXPA-MBD show that the latter contains a zinc-binding motif and that the metal ion is coordinated to four Cys residues (Hess, Buchko et al. 1998).

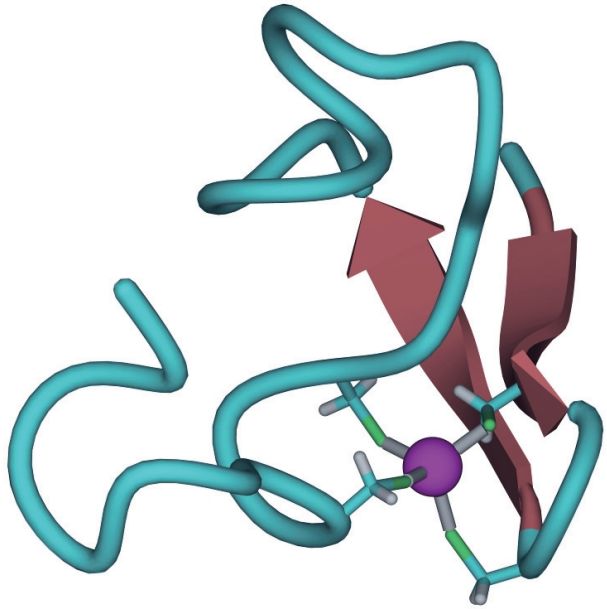

Figure 7: Zinc finger domain of XPA (PDB 1D4U). Figure was created by using the program YASARA.

XPAzf and its complex with Zn(II) (ZnXPAzf) (Figure 7) are suitable and models to study the molecular mechanisms behind the damage of Cys_4 type zinc fingers by metals and oxidants (Bal, Schwerdtle et al. 2003; Schwerdtle, Walter et al. 2003; Blessing, Kraus et al. 2004; Kopera, Schwerdtle et al. 2004).

1.5.2 Human IGF-1

Insulin-like growth factor 1 (somatomedin C, IGF-1) is a polypeptide hormone consisting of a single polypeptide chain of 70 amino acid residues (MW=7649 Da) cross-linked by three disulfide bridges. IGF-1 displays an obvious homology to insulin (Lund 1994; De Wolf, Gill et al. 1996) and is mainly secreted by the liver, although most other peripheral tissues also synthesize it in low concentrations. IGF-1 secretion is regulated by growth hormone (GH) (Jones and Clemmons 1995). IFG-1 expression has been shown to be essential for brain development and both IGF-1 and its receptor (IGFR) are expressed in the central nervous system (Popken, Dechert-Zeger et al. 2005; Russo, Gluckman et al. 2005).

IGF-1 exerts its action through its receptor and is inhibited or regulated by IGF binding proteins – IGFBP(1-6)s (Baxter 2000). The concentration of IGF-1 in the bloodstream is very high (150-400 ng/ml in plasma), and only a small fraction of the peptide (less than 1%) is found in its unbound physiologically

active form (Clemmons 2007). A major portion of the circulating IGF-1 pool is present as 150 kDa ternary complexes consisting of IGF-1, IGFBP-3 (the predominant IGFBP in serum) or IGFBP-5, and ALS (acid-labile subunit, a 85 kD glycoprotein) (Rechler 1993; Baxter 2000), which restricts IGFs to the circulation system and prolongs their half-lives, thus allowing them to be stored at high concentration in plasma (Zapf, Hauri et al. 1995). Plasma also contains ~50 kDa molecular mass complexes made up of IGFBP 1-6 and IGF-1 in much lower concentrations, which are able to cross vascular endothelium (Jones and Clemmons 1995; Stewart and Rotwein 1996).

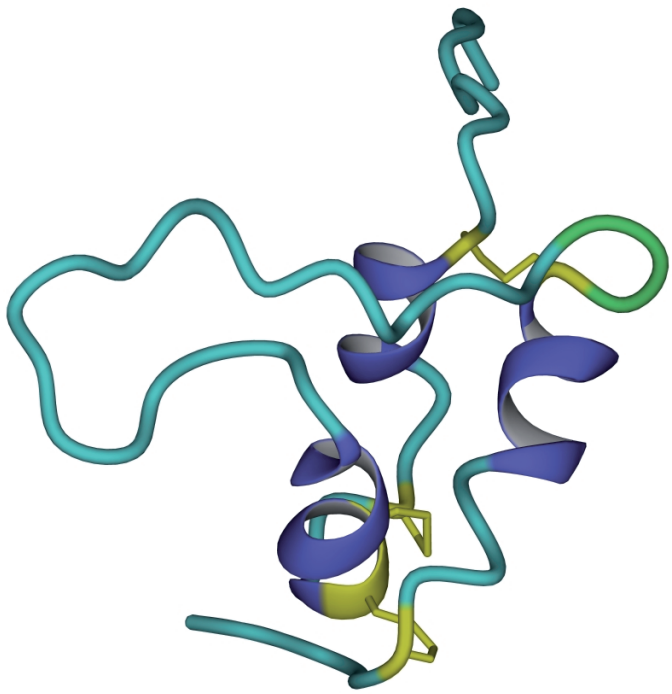

Figure 8: Human IGF-1 (PDB 1BQT). Disulfides are shown in yellow. Figure was created by using the program YASARA.

Alterations in IGF-1 levels and/or IGF-1 induced signaling networks have been associated with multiple pathological conditions. For example, a connection of IGF-1 to the brain amyloid pathogenesis of AD has been identified (Carro, Trejo et al. 2002; Jarvis, Assis-Nascimento et al. 2007; Jacobsen, Adlerz et al. 2010). IGF-1 was shown to decrease amyloid beta levels (Carro, Trejo et al. 2002; Jacobsen, Adlerz et al. 2010). Recent studies demonstrate the importance of IGF-1 in the elimination of other oxidized proteins in the brain (Li and Ren 2007; Crowe, Sell et al. 2009). IGFs are modulated and affected by multiple factors such as IGFBPs (Baxter 2000), ROS (Delafontaine and Ku 1997; Juarez, Manuia et al. 2008), and RNS (Ceacareanu, Ceacareanu et al. 2006). ROS-induced oxidative stress has been shown to enhance the action of IGF-1,

especially in vascular smooth muscle cells (VSMCs), through upregulation of IGF-1 and IGFR expression (Delafontaine and Ku 1997; Du, Peng et al. 1999; Delafontaine, Song et al. 2004; Ma, Zhang et al. 2006). On the other hand, ROS and RNS play a certain role in transducing downstream effects of IGF-1 (Cruzado, Risler et al. 2005; Meng, Shi et al. 2007).

Although many observations demonstrate that IGF-1 plays a role in redox pathways, the functioning of putative redox switches of IGF-1 and the metal-binding properties of the protein are still largely unknown. However, these aspects are of significant importance for the biological function of IGF-1, which rely on the presence of three native disulfide bridges in IGF-1 (Narhi, Hua et al. 1993) (Figure 8). IGFBPs may function to form and maintain correct (native) disulfides of IGF-1 *in vivo* (Hober, Hansson et al. 1994).

2. AIMS OF THE STUDY

The general aim of this study was to investigate and compare the redox properties of various redox active proteins *in vitro* using ESI-MS. For this purpose, the following studies were pursued:

1) To study the reaction of the XPAzf with H_2O_2
2) To study the reaction of the XPAzf with GSNO
3) To measure the redox potential and metal-binding properties of extracellular hormone hIGF-1

3. MATERIALS AND METHODS

All procedures were performed according to the standard protocols or according to the manufacturer's instructions. Some experiments were performed with slight modification using the following methods (detailed descriptions are provided in the publications reproduced at the end of this dissertation):

Paper I

- Zn(II) release followed spectrophotometrically using PAR
- Kinetic studies using HPLC
- Cys derivatisation using MMTS
- Kinetic studies using ESI-MS

Paper II

- Synthesis of GSNO
- Zn(II) release followed spectrophotometrically using PAR
- Kinetic studies using ESI-MS

Paper III

- Kinetic studies and determination of redox potential using ESI-MS
- Identification of reaction intermediates using HPLC
- Metal-binding studies using ESI-MS

4. RESULTS

Publication I

- XPAzf reacted with H_2O_2 with concomitant release of Zn(II).
- Reaction rates, followed by several techniques, including spectrophotometrical assay with PAR, HPLC and ESI-MS, were in a good agreement with each other.
- ESI-MS can be applied as a quantitative tool to study zinc finger oxidation at a neutral pH and, in conjunction with derivatisation procedures, it can provide information about the reaction mechanism.
- The initial reaction product of the XPAzf with H_2O_2 is the zinc finger with one intramolecular disulfide bond forming between Cys5 and Cys8.
- A lack of Zn(II)-containing disulfides, confirmed by ESI-MS, shows, that the formation of a single disulfide bond is sufficient for the release of Zn(II) and, therefore, at least three thiolate ligands are required for Zn(II) binding in Cys_4-type zinc fingers.

Publication II

- The stability of GSNO and its reactivity towards XPAzf were examined. XPAzf reacted with GSNO with concomitant release of Zn(II).
- A reaction mechanism was proposed on the basis of this ESI-MS and Zn(II)-release assay by PAR.
- In addition to XPAzf, the fate of GSNO was studied from the low molecular portion of the m/z spectrum and the tentative equilibrium between GSSG, GSNO, and GSH was reached at 40% of the apparent initial GSNO level.
- Initially, the reaction of XPAzf with GSNO proceeded rapidly (around 10-fold faster compared with with H_2O_2), however, at longer incubation times it slowed down significantly.
- In addition to internal disulfides, S-nitrosylated and S-glutathionylated products of the reaction were identified by ESI-MS.
- S-nitrosylation occurred largely within the first 2 hours of the reaction, however, at later times the occurrence of S-nitrosylated products began to decay, which was accompanied by an accumulation of disulfide products with $XPAzf(SS)_2$ being the major product.
- A ZnXPAzf[GSNO] peak appeared immediately in the spectra and was present at all time points studied. GSNO has been suggested to be bound to the Zn(II) ion of the 3S coordination isomer of the XPAzf via

a Glu residue. The apparent equilibrium constant of corresponding reaction was found to be 1540 ± 47 M^{-1}.

- A ttransnitrosylation reaction proceeded next by attack of the available thiolate by SNO moiety of GSNO; this step is reversible.
- An attack of second GSNO molecule is required for Zn(II) release, yielding XPAzf$(NO)_2$ as a product and was found to be strongly susceptible to oxidation, thus producing the internal disulfide.
- In the third phase, SNO groups in the peptide were converted into kinetically stable intramolecular and GSH-mixed disulfides.

Publication III

- The midpoint redox potential E_m of IGF-1 was determined to be equal to -332 mV, which is sufficiently low compared to both the redox potentials of the secretory pathway and the extracellular environment to guarantee that IGF-1 remains in its native folding which is required for IGFR binding.
- BME/BMEox was used as a substitution for the commonly used GSH/GSSG redox buffer because the $E^{0\prime}$ of BME/BMEox is close to the $E^{0\prime}$ of GSH/GSSG, and BME does not disturb ESI-MS measurements.
- Cu(I) binding to fully reduced IGF-1 was threefold weaker compared to copper chaperone Cox17.

5. DISCUSSION

Direct application of ESI-MS in conjunction with HPLC to study the kinetic mechanism of zinc finger oxidation yielded much richer information than other experimental methods used currently [Publication I]. Besides Zn(II) complexes, ESI-MS can simultaneously detect other species, including labile intermediates, present in the sample. Moreover, this method requires very small amount of substance. The synthetic 37-residue peptide (101-137 amino acids of XPA) containing Cys_4 zinc finger motif – XPAzf, has been used as a model for studies of the molecular mechanism of XPA damage by oxidants [Publication I; Publication II].

Among ROS, H_2O_2 best fulfils the requirements of being a secondary messenger within the cell. In Publication I, we used the reaction of H_2O_2 oxidation of ZnXPAzf to determine whether ESI-MS is suitable to study the kinetics of ZF oxidative reactions. In parallel, Zn(II) release was followed spectrophotometrically using PAR as a Zn(II) dye and the decay of a XPAzf peak (formed by acidic dissociation of ZnXPAzf) was monitored by HPLC. Quantitative analysis of HPLC data was performed by integrating three principal peaks (XPAzf, XPAzf(-SS-), and XPAzf(-SS-)$_2$, Figure 1 in [Publication I]) and the oxidation of ZnXPAzf to disulfides progressed linearly (Figure 2 in [Publication I]). As with the HPLC results, ZnXPAzf initial decomposition followed using PAR was linear (Figure 3 in [Publication I]). ESI-MS allowed for the simultaneous monitoring of ZnXPAzf and its oxidation products (Figure 5 in [Publication I]) and the ZnXPAzf complex decay was again found to be linear. The general conclusion of this study, based on the agreement of reaction rates from PAR, HPLC, and ESI-MS experiments presented in Table 1 in [Publication I], is that ESI-MS is a suitable tool to study the kinetics of ZnXPAzf oxidation. ESI-MS also showed no intramolecular disulfides in the Zn(II) containing peptide, which demonstrates that the formation of a single disulfide was sufficient for Zn(II) release, meaning that at least three thiolate ligands are required to complex a Zn(II) ion. The exact position of the initial disulfide Cys5-Cys8 was obtained using a derivatisation procedure with MMTS followed by ESI-MS/MS sequencing.

ESI-MS was used to further study a XPAzf reaction with the nitrosative species GSNO. GSNO has been proposed as a mean of storage and redistribution of NO through transnitrosation reactions. It is possible that GSNO exerts its cellular effects via interactions with ZF transcription factors. PAR and ESI-MS studies of the reaction of ZnXPAzf with GSNO were performed [Publication II]. The stability of GSNO in a 10 mM ammonium acetate buffer was determined and the time span for each experiment was estimated to be between 5-6 hours. Zn(II) release from ZnXPAzf was studied by ESI-MS under conditions which allow for the detection of non-covalent species such as S-nitrosothiols. Time-

dependent changes in the fractional content of individual species are presented in Figure 2, [Publication II]. Decay of a ZnXPAzf peak proceeded exponentially and an apparent equilibrium of the reaction of ZnXPAzf with 10-fold molar excess of GSNO was reached at around 25% of the starting ZnXPAzf concentration. Additionally, GSNO decomposition was monitored in the 600-700 m/z region of the spectrum and the signal of $(GSNO)_2H^+$ decayed exponentially (Figure 4 in [Publication II]). Several peaks were identified from the complex spectra of the reaction of ZnXPAzf with GSNO, and are presented in Table 1, [Publication II]. In addition to internal disulfides, the S-nitrosylated and S-glutathionylated derivatives of XPAzf were identified in the ESI-MS spectra. The reaction of XPAzf with GSNO proceeded rapidly in the first 2 hours of incubation. An initial linear reaction rate was estimated ca. $2 \pm 0.5 \times 10^{-9}$ M s^{-1} from both PAR assay and ESI-MS and this rate is 10-fold higher than the one measured previously for 100 μM H_2O_2. However, at longer incubation times, the reaction slowed down significantly. An equilibrium condition of approximately 80% Zn(II) release was suggested with respect to the starting ZnXPAzf complex. By investigating the complex ESI-MS spectra, several conclusions were drawn regarding the mechanism of XPAzf oxidation by GSNO. First, a peak corresponding to ZnXPAzf[GSNO] appeared immediately and nitrosylated products were detected in ESI-MS spectra at all time points, while non-nitrosylated mixed GSH disulfides were formed at longer incubation times. This shows that disulfide formation follows, rather than parallels transnitrosylation. The mechanism proceeds in three phases. The first phase is the binding of GSNO and the initial transnitrosylation processes (Scheme 1, [Publication II]), which is rapid but reversible. At initial stages in the reaction, GSNO can bind to the Zn(II) ion of the ZnXPAzf using the amine and carboxylate groups of its Glu residue. The apparent equilibrium constant of the corresponding reaction,

$$ZnXPAzf + GSNO \overset{K}{\leftrightarrow} ZnXPAzf[GSNO],$$

was estimated to be 1540 ± 47 M^{-1}, which is in good agreement with the conditional stability constant for the $Zn(GSNO)^-$ complex at pH 7.4; thus supporting the proposed mechanism. The SNO moiety of GSNO then attacks the available thiolate in a reversible reaction. GSH is a product of this reaction and may remain bounded to the ZnXPAzf, thus forming ZnXPAzf(NO)[GSH].

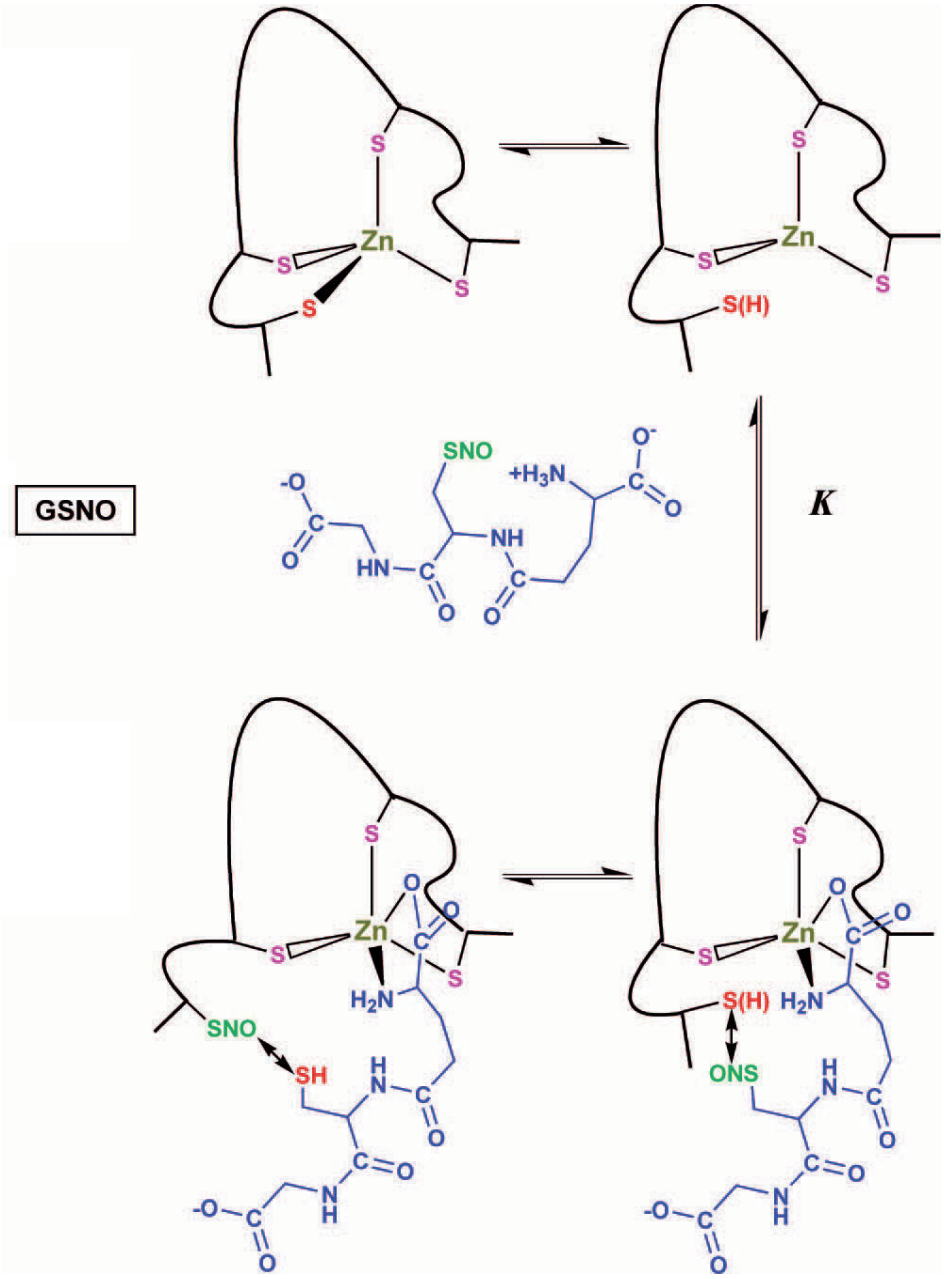

Scheme 1. Reversible Steps of the Reaction Mechanism of ZnXPAzf with GSNO. [Publication II]. The choice of the S-nitrosylation position is arbitrary.

An attack of a second GSNO molecule is required for Zn(II) release and the formation of the intermediate product XPAzf$(NO)_2$, which is very susceptible to oxidation upon which it yields an intramolecular disulfide. The formation and accumulation of nitrosylated XPAzf derivatives constitute the second reaction

phase, which occurs largely within the first 2 hours of the incubation until a decrease in apparent GSNO concentration to 40% of its initial level. In the third phase of the reaction, SNO groups in the peptide were converted into kinetically stable disulfides, whereas both intermolecular and mixed disulfides with GSH were formed. In these studies, a GSNO concentration of 100 μM was used, which may represent intermediate cellular GSNO levels that correspond with mild nitrosative stress.

Our results suggest, that at similar cellular conditions, Zn(II) is expected be lost from the zinc finger and the latter will be subsequently oxidized; on the other hand, the proposed mechanism allows one to suggest that under low, micromolar GSNO exposures, this zinc finger can be nitrosylated reversibly without Zn(II) release, which could occur under normal physiological conditions in many tissues. Also, the transnitrosylation of zinc finger is controlled by presence of GSH and thus this reaction is dependent on the local GSH/GSNO ratio.

For studies of the dependence of protein folding with regards to its redox properties, human hormone IGF-1 was investigated using ESI-MS [Publication III]. IGF-1 is a polypeptide hormone composed of a single polypeptide chain consisting of 70 amino acid residues (MW=7649 Da). There are three intramolecular disulfide bridges in the IGF-1 molecule (De Wolf, Gill et al. 1996) which are all required for IGF-1 binding to its receptor. Before its release into blood, IGF-1 should pass oxidative folding in the ER; both of these environments are characterized by oxidative redox potentials.

ESI-MS studies help one to understand the interplay between different redox states of hIGF-1. Data obtained from titration curves, together with the absence of intermediate disulfide species assessed using HPLC, suggest that hIGF-1 exists mainly in two forms: fully oxidized and fully reduced. We measured the midpoint redox potential of hIGF-1 using a previously established method (Zovo and Palumaa 2009). Different redox forms of hIGF-1 were equilibrated with two redox buffers: DTT/DTTox and BME/BMEox. BME/BMEox was used instead of the GSH/GSSG redox pair because of their similar $E^{0\prime}$ and because non-ionic BME is compatible with ESI-MS measurements.

The midpoint redox potential of the hIGF-1_{3S-S} → hIGF-1_{0S-S} reaction was determined by fitting the fractional content of hIGF-1_{0S-S} to the equation

$$y = (A_1 - A_2)/[1 + e^{(x-x_0)/dx}] + A_2 \qquad (6)$$

where y is the fractional content of hIGF-1_{0S-S}, x is the environmental redox potential (E_h), A_1 and A_2 are constants, and x_0 is the midpoint redox potential (E_m). Data were fit using an A_1 of 0 (initial fractional content of hIGF-1_{0S-S}) and

an A_2 of 1 (final fractional content of IGF-1_{0S-S}) with Origin 6.1 (Originlab Corp.). The E_m of hIGF-1 was found to be -332 mV (at pH 7.5 and 40°C).

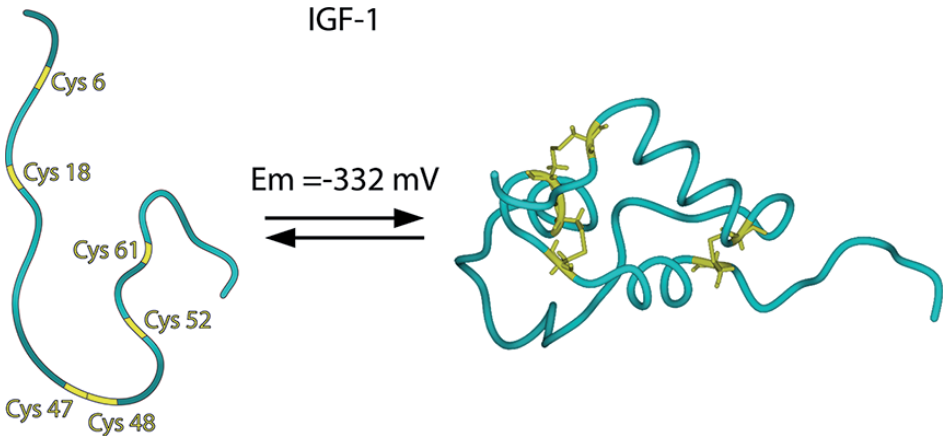

Insert in Publication III: Oxidative folding of hIGF-1.

This redox value ensures that hIGF-1 is oxidized and all three disulfides are formed *in vivo*, which is important for binding to its receptor. In addition, the presence of thiol groups in fully reduced hIGF-1 suggests that it may potentially bind zinc and copper ions. Our results clearly demonstrate that fully reduced hIGF-1 does not bind Zn(II) ions, however, the protein can bind four Cu(I) ions in a highly co-operative manner and most probably into a tetracopper-hexathiolate cluster. The Cu(I) binding affinity ($K_d = 3.00 \pm 0.86 \times 10^{-18}$ M) of fully reduced hIGF-1 is 3-fold lower than that of Cox17, which has the lowest affinity among the cellular copper chaperones. Fully reduced hIGF-1 is a good model for metal-binding studies.

CONCLUSIONS

- ESI-MS experiments together with a zinc release assay and HPLC analysis demonstrated that the reaction of Cys_4-type zinc finger XPAzf with H_2O_2 leads initially to the formation of a single disulfide bond with concomitant release of Zn(II) that is followed by the formation of the second disulfide bond.

- ESI-MS results clarified the reaction mechanism of XPAzf with GSNO and indicated that at low levels GSNO may bind reversibly to Cys_4-type zinc finger XPAzf followed by S-nitrosylation without concomitant Zn(II) release. At higher GSNO concentrations the S-nitrosylated groups of XPAzf are converted into kinetically stable disulfides and this conversion is accompanied with release of Zn(II).

- The redox potential of hormone hIGF-1 determined by ESI-MS indicates that hIGF-1 is completely oxidized within the ER and in plasma. Fully reduced hIGF-1, which serves as a model peptide for metal-binding studies, can bind preferably four Cu(I) ions into a tetracopper-hexathiolate cluster.

REFERENCES

Abate, C., L. Patel, et al. (1990). "Redox regulation of fos and jun DNA-binding activity in vitro." Science 249(4973): 1157-1161.

Albrecht, S. C., A. G. Barata, et al. (2011). "In vivo mapping of hydrogen peroxide and oxidized glutathione reveals chemical and regional specificity of redox homeostasis." Cell Metab 14(6): 819-829.

Allen, R. G. and M. Tresini (2000). "Oxidative stress and gene regulation." Free Radic Biol Med 28(3): 463-499.

Allison, W. S. (1976). "Formation and reactions of sulfenic acids in proteins." Accounts of Chemical Research 9(8): 293-299.

Andreini, C., L. Banci, et al. (2006). "Counting the zinc-proteins encoded in the human genome." J Proteome Res 5(1): 196-201.

Andrews, G. K. (2001). "Cellular zinc sensors: MTF-1 regulation of gene expression." Biometals 14(3-4): 223-237.

Ashfaq, S., J. L. Abramson, et al. (2006). "The relationship between plasma levels of oxidized and reduced thiols and early atherosclerosis in healthy adults." J Am Coll Cardiol 47(5): 1005-1011.

Aslund, F., M. Zheng, et al. (1999). "Regulation of the OxyR transcription factor by hydrogen peroxide and the cellular thiol-disulfide status." Proc Natl Acad Sci U S A 96(11): 6161-6165.

Asmuss, M., L. H. Mullenders, et al. (2000). "Differential effects of toxic metal compounds on the activities of Fpg and XPA, two zinc finger proteins involved in DNA repair." Carcinogenesis 21(11): 2097-2104.

Asmuss, M., L. H. Mullenders, et al. (2000). "Interference by toxic metal compounds with isolated zinc finger DNA repair proteins." Toxicol Lett 112-113: 227-231.

Backos, D. S., C. C. Franklin, et al. (2012). "The role of glutathione in brain tumor drug resistance." Biochem Pharmacol 83(8): 1005-1012.

Bae, Y. S., S. W. Kang, et al. (1997). "Epidermal growth factor (EGF)-induced generation of hydrogen peroxide. Role in EGF receptor-mediated tyrosine phosphorylation." J Biol Chem 272(1): 217-221.

Bal, W., T. Schwerdtle, et al. (2003). "Mechanism of nickel assault on the zinc finger of DNA repair protein XPA." Chem Res Toxicol 16(2): 242-248.

Baldwin, M. A. and C. C. Benz (2002). "Redox control of zinc finger proteins." Methods Enzymol 353: 54-69.

Ballatori, N., S. M. Krance, et al. (2009). "Plasma membrane glutathione transporters and their roles in cell physiology and pathophysiology." Mol Aspects Med 30(1-2): 13-28.

Baxter, R. C. (2000). "Insulin-like growth factor (IGF)-binding proteins: interactions with IGFs and intrinsic bioactivities." Am J Physiol Endocrinol Metab 278(6): E967-976.
Becker, K., M. Gui, et al. (1995). "Inhibition of human glutathione reductase by S-nitrosoglutathione." Eur J Biochem 234(2): 472-478.
Becker, K., S. N. Savvides, et al. (1998). "Enzyme inactivation through sulfhydryl oxidation by physiologic NO-carriers." Nat Struct Biol 5(4): 267-271.
Beer, S. M., E. R. Taylor, et al. (2004). "Glutaredoxin 2 catalyzes the reversible oxidation and glutathionylation of mitochondrial membrane thiol proteins: implications for mitochondrial redox regulation and antioxidant DEFENSE." J Biol Chem 279(46): 47939-47951.
Benhar, M., M. T. Forrester, et al. (2008). "Regulated protein denitrosylation by cytosolic and mitochondrial thioredoxins." Science 320(5879): 1050-1054.
Bernal, P. J., K. Leelavanichkul, et al. (2008). "Nitric-oxide-mediated zinc release contributes to hypoxic regulation of pulmonary vascular tone." Circ Res 102(12): 1575-1583.
Berndt, C., C. H. Lillig, et al. (2007). "Thiol-based mechanisms of the thioredoxin and glutaredoxin systems: implications for diseases in the cardiovascular system." Am J Physiol Heart Circ Physiol 292(3): H1227-1236.
Bienert, G. P., A. L. Moller, et al. (2007). "Specific aquaporins facilitate the diffusion of hydrogen peroxide across membranes." J Biol Chem 282(2): 1183-1192.
Bienert, G. P., J. K. Schjoerring, et al. (2006). "Membrane transport of hydrogen peroxide." Biochim Biophys Acta 1758(8): 994-1003.
Billiet, L., C. Furman, et al. (2005). "Extracellular human thioredoxin-1 inhibits lipopolysaccharide-induced interleukin-1beta expression in human monocyte-derived macrophages." J Biol Chem 280(48): 40310-40318.
Bindoli, A. and M. P. Rigobello (2012). "Principles in Redox Signaling: From Chemistry to Functional Significance." Antioxid Redox Signal.
Biswas, S., A. S. Chida, et al. (2006). "Redox modifications of protein-thiols: emerging roles in cell signaling." Biochem Pharmacol 71(5): 551-564.
Biswas, S. K. and I. Rahman (2009). "Environmental toxicity, redox signaling and lung inflammation: the role of glutathione." Mol Aspects Med 30(1-2): 60-76.
Biteau, B., J. Labarre, et al. (2003). "ATP-dependent reduction of cysteine-sulphinic acid by S. cerevisiae sulphiredoxin." Nature 425(6961): 980-984.

Bjornberg, O., H. Ostergaard, et al. (2006). "Measuring intracellular redox conditions using GFP-based sensors." Antioxid Redox Signal 8(3-4): 354-361.

Blanco, R. A., T. R. Ziegler, et al. (2007). "Diurnal variation in glutathione and cysteine redox states in human plasma." Am J Clin Nutr 86(4): 1016-1023.

Blessing, H., S. Kraus, et al. (2004). "Interaction of selenium compounds with zinc finger proteins involved in DNA repair." Eur J Biochem 271(15): 3190-3199.

Bloom, D., S. Dhakshinamoorthy, et al. (2002). "Site-directed mutagenesis of cysteine to serine in the DNA binding region of Nrf2 decreases its capacity to upregulate antioxidant response element-mediated expression and antioxidant induction of NAD(P)H:quinone oxidoreductase1 gene." Oncogene 21(14): 2191-2200.

Bodwell, J. E., N. J. Holbrook, et al. (1984). "Evidence for distinct sulfhydryl groups associated with steroid- and DNA-binding domains of rat thymus glucocorticoid receptors." Biochemistry 23(18): 4237-4242.

Boehning, D. and S. H. Snyder (2003). "Novel neural modulators." Annu Rev Neurosci 26: 105-131.

Bontempelli, G., F. Magno, et al. (1973). "Electrochemical oxidation of phenyldisulfide in acetonitrile medium." Journal of Electroanalytical Chemistry and Interfacial Electrochemistry 42(1): 57-67.

Brand, M. D. (2010). "The sites and topology of mitochondrial superoxide production." Exp Gerontol 45(7-8): 466-472.

Brigelius-Flohe, R. and L. Flohe (2011). "Basic principles and emerging concepts in the redox control of transcription factors." Antioxid Redox Signal 15(8): 2335-2381.

Broniowska, K. A. and N. Hogg (2012). "The chemical biology of S-nitrosothiols." Antioxid Redox Signal 17(7): 969-980.

Broniowska, K. A., A. Keszler, et al. (2012). "Cytochrome c-mediated formation of S-nitrosothiol in cells." Biochem J 442(1): 191-197.

Brown, G. C. and V. Borutaite (2012). "There is no evidence that mitochondria are the main source of reactive oxygen species in mammalian cells." Mitochondrion 12(1): 1-4.

Brown, L. A., X. D. Ping, et al. (2007). "Glutathione availability modulates alveolar macrophage function in the chronic ethanol-fed rat." Am J Physiol Lung Cell Mol Physiol 292(4): L824-832.

Bryan, N. S., T. Rassaf, et al. (2004). "Cellular targets and mechanisms of nitros(yl)ation: an insight into their nature and kinetics in vivo." Proc Natl Acad Sci U S A 101(12): 4308-4313.

Buchanan, B. B. (1980). "Role of Light in the Regulation of Chloroplast Enzymes." Annual Review of Plant Physiology and Plant Molecular Biology 31: 341-374.

Buchko, G. W., L. M. Iakoucheva, et al. (1999). "Extended X-ray absorption fine structure evidence for a single metal binding domain in Xenopus laevis nucleotide excision repair protein XPA." Biochem Biophys Res Commun 254(1): 109-113.

Buchko, G. W., S. Ni, et al. (1998). "Structural features of the minimal DNA binding domain (M98-F219) of human nucleotide excision repair protein XPA." Nucleic Acids Res 26(11): 2779-2788.

Butterfield, D. A. and I. Dalle-Donne (2012). "Redox proteomics." Antioxid Redox Signal 17(11): 1487-1489.

Cadenas, E. (2004). "Mitochondrial free radical production and cell signaling." Mol Aspects Med 25(1-2): 17-26.

Cai, J. and D. P. Jones (1998). "Superoxide in apoptosis. Mitochondrial generation triggered by cytochrome c loss." J Biol Chem 273(19): 11401-11404.

Callister, M. E., A. Burke-Gaffney, et al. (2006). "Extracellular thioredoxin levels are increased in patients with acute lung injury." Thorax 61(6): 521-527.

Campbell, D. L., J. S. Stamler, et al. (1996). "Redox modulation of L-type calcium channels in ferret ventricular myocytes. Dual mechanism regulation by nitric oxide and S-nitrosothiols." J Gen Physiol 108(4): 277-293.

Carro, E., J. L. Trejo, et al. (2002). "Serum insulin-like growth factor I regulates brain amyloid-beta levels." Nat Med 8(12): 1390-1397.

Casagrande, S., V. Bonetto, et al. (2002). "Glutathionylation of human thioredoxin: a possible crosstalk between the glutathione and thioredoxin systems." Proc Natl Acad Sci U S A 99(15): 9745-9749.

Ceacareanu, A. C., B. Ceacareanu, et al. (2006). "Nitric oxide attenuates IGF-I-induced aortic smooth muscle cell motility by decreasing Rac1 activity: essential role of PTP-PEST and p130cas." Am J Physiol Cell Physiol 290(4): C1263-1270.

Chae, H. Z., S. W. Kang, et al. (1999). "Isoforms of mammalian peroxiredoxin that reduce peroxides in presence of thioredoxin." Methods Enzymol 300: 219-226.

Chai, Y. C., S. S. Ashraf, et al. (1994). "S-thiolation of individual human neutrophil proteins including actin by stimulation of the respiratory burst: evidence against a role for glutathione disulfide." Arch Biochem Biophys 310(1): 273-281.

Chance, B., H. Sies, et al. (1979). "Hydroperoxide metabolism in mammalian organs." Physiol Rev 59(3): 527-605.

Chen, Z., D. A. Putt, et al. (2000). "Enrichment and functional reconstitution of glutathione transport activity from rabbit kidney mitochondria: further evidence for the role of the dicarboxylate and 2-oxoglutarate carriers in mitochondrial glutathione transport." Arch Biochem Biophys 373(1): 193-202.

Cherqui, S., V. Kalatzis, et al. (2001). "The targeting of cystinosin to the lysosomal membrane requires a tyrosine-based signal and a novel sorting motif." J Biol Chem 276(16): 13314-13321.

Chiarugi, P. (2005). "PTPs versus PTKs: the redox side of the coin." Free Radic Res 39(4): 353-364.

Choi, H., S. Kim, et al. (2001). "Structural basis of the redox switch in the OxyR transcription factor." Cell 105(1): 103-113.

Chung, K. K., B. Thomas, et al. (2004). "S-nitrosylation of parkin regulates ubiquitination and compromises parkin's protective function." Science 304(5675): 1328-1331.

Ckless, K., N. L. Reynaert, et al. (2004). "In situ detection and visualization of S-nitrosylated proteins following chemical derivatization: identification of Ran GTPase as a target for S-nitrosylation." Nitric Oxide 11(3): 216-227.

Claiborne, A., H. Miller, et al. (1993). "Protein-sulfenic acid stabilization and function in enzyme catalysis and gene regulation." FASEB J 7(15): 1483-1490.

Claiborne, A., J. I. Yeh, et al. (1999). "Protein-sulfenic acids: diverse roles for an unlikely player in enzyme catalysis and redox regulation." Biochemistry 38(47): 15407-15416.

Clarke, W. M. (1960). The standard hydrogen half-cell and the standardization of oxidation-reduction potentials and pH numbers Oxidation-Reduction Potentials of Organic Systems. Baltimore, MD, Waverly Press: 248-272.

Cleaver, J. E. and J. C. States (1997). "The DNA damage-recognition problem in human and other eukaryotic cells: the XPA damage binding protein." Biochem J 328 (Pt 1): 1-12.

Clemmons, D. R. (2007). "Value of insulin-like growth factor system markers in the assessment of growth hormone status." Endocrinol Metab Clin North Am 36(1): 109-129.

Clive, D. R. and J. J. Greene (1996). "Cooperation of protein disulfide isomerase and redox environment in the regulation of NF-kappaB and AP1 binding to DNA." Cell Biochem Funct 14(1): 49-55.

Colvin, R. A., C. P. Fontaine, et al. (2003). "Zn2+ transporters and Zn2+ homeostasis in neurons." Eur J Pharmacol 479(1-3): 171-185.

Comporti, M., C. Signorini, et al. (2002). "Iron release, oxidative stress and erythrocyte ageing." Free Radic Biol Med 32(7): 568-576.

Conrad, M. (2009). "Transgenic mouse models for the vital selenoenzymes cytosolic thioredoxin reductase, mitochondrial thioredoxin reductase and glutathione peroxidase 4." Biochim Biophys Acta 1790(11): 1575-1585.

Conrad, M., C. Jakupoglu, et al. (2004). "Essential role for mitochondrial thioredoxin reductase in hematopoiesis, heart development, and heart function." Mol Cell Biol 24(21): 9414-9423.

Crawford, J. H., B. K. Chacko, et al. (2004). "Transduction of NO-bioactivity by the red blood cell in sepsis: novel mechanisms of vasodilation during acute inflammatory disease." Blood 104(5): 1375-1382.

Cross, J. V. and D. J. Templeton (2006). "Regulation of signal transduction through protein cysteine oxidation." Antioxid Redox Signal 8(9-10): 1819-1827.

Crowe, E., C. Sell, et al. (2009). "Activation of proteasome by insulin-like growth factor-I may enhance clearance of oxidized proteins in the brain." Mech Ageing Dev 130(11-12): 793-800.

Cruzado, M. C., N. R. Risler, et al. (2005). "Vascular smooth muscle cell NAD(P)H oxidase activity during the development of hypertension: Effect of angiotensin II and role of insulinlike growth factor-1 receptor transactivation." Am J Hypertens 18(1): 81-87.

Czech, M. P. (1976). "Differential effects of sulfhydryl reagents on activation and deactivation of the fat cell hexose transport system." J Biol Chem 251(4): 1164-1170.

Cuozzo, J. W. and C. A. Kaiser (1999). "Competition between glutathione and protein thiols for disulfide-bond formation." Nat Cell Biol 1(3): 130-135.

D'Autreaux, B. and M. B. Toledano (2007). "ROS as signaling molecules: mechanisms that generate specificity in ROS homeostasis." Nat Rev Mol Cell Biol 8(10): 813-824.

Daiber, A. (2010). "Redox signaling (cross-talk) from and to mitochondria involves mitochondrial pores and reactive oxygen species." Biochim Biophys Acta 1797(6-7): 897-906.

Dalle-Donne, I., G. Colombo, et al. (2011). "S-glutathiolation in life and death decisions of the cell." Free Radic Res 45(1): 3-15.

Dalle-Donne, I., R. Rossi, et al. (2009). "Protein S-glutathionylation: a regulatory device from bacteria to humans." Trends Biochem Sci 34(2): 85-96.

Dalle-Donne, I., R. Rossi, et al. (2007). "S-glutathionylation in protein redox regulation." Free Radic Biol Med 43(6): 883-898.

Dardalhon, M., C. Kumar, et al. (2012). "Redox-sensitive YFP sensors monitor dynamic nuclear and cytosolic glutathione redox changes." Free Radic Biol Med 52(11-12): 2254-2265.

Davis, F. A., L. A. Jenkins, et al. (1986). "Chemistry of sulfenic acids. 7. Reason for the high reactivity of sulfenic acids. Stabilization by intramolecular hydrogen bonding and electronegativity effects." The Journal of Organic Chemistry 51(7): 1033-1040.

De Wolf, E., R. Gill, et al. (1996). "Solution structure of a mini IGF-1." Protein Sci 5(11): 2193-2202.

Delafontaine, P. and L. Ku (1997). "Reactive oxygen species stimulate insulin-like growth factor I synthesis in vascular smooth muscle cells." Cardiovasc Res 33(1): 216-222.

Delafontaine, P., Y. H. Song, et al. (2004). "Expression, regulation, and function of IGF-1, IGF-1R, and IGF-1 binding proteins in blood vessels." Arterioscler Thromb Vasc Biol 24(3): 435-444.

DeYulia, G. J., Jr., J. M. Carcamo, et al. (2005). "Hydrogen peroxide generated extracellularly by receptor-ligand interaction facilitates cell signaling." Proc Natl Acad Sci U S A 102(14): 5044-5049.

Diaz-Cruz, M. S., J. Mendieta, et al. (1998). "Study of the zinc-binding properties of glutathione by differential pulse polarography and multivariate curve resolution." Journal of Inorganic Biochemistry 70(2): 91-98.

Dickinson, D. A. and H. J. Forman (2002). "Cellular glutathione and thiols metabolism." Biochem Pharmacol 64(5-6): 1019-1026.

Dooley, C. T., T. M. Dore, et al. (2004). "Imaging dynamic redox changes in mammalian cells with green fluorescent protein indicators." J Biol Chem 279(21): 22284-22293.

Dormer, U. H., J. Westwater, et al. (2002). "Oxidant regulation of the Saccharomyces cerevisiae GSH1 gene." Biochim Biophys Acta 1576(1-2): 23-29.

Du, J., T. Peng, et al. (1999). "Angiotensin II activation of insulin-like growth factor 1 receptor transcription is mediated by a tyrosine kinase-dependent redox-sensitive mechanism." Arterioscler Thromb Vasc Biol 19(9): 2119-2126.

Dutton, P. L. (1978). "Redox potentiometry: determination of midpoint potentials of oxidation-reduction components of biological electron-transfer systems." Methods Enzymol 54: 411-435.

Eide, D. J. (2004). "The SLC39 family of metal ion transporters." Pflugers Arch 447(5): 796-800.

Eshghi, A., K. Lourdault, et al. (2012). "Leptospira interrogans catalase is required for resistance to H2O2 and for virulence." Infect Immun 80(11): 3892-3899.

Eu, J. P., J. Sun, et al. (2000). "The skeletal muscle calcium release channel: coupled O2 sensor and NO signaling functions." Cell 102(4): 499-509.
Fabisiak, J. P., G. G. Borisenko, et al. (2002). "Redox sensor function of metallothioneins." Methods Enzymol 353: 268-281.
Fagarasanu, A., M. Fagarasanu, et al. (2007). "Maintaining peroxisome populations: a story of division and inheritance." Annu Rev Cell Dev Biol 23: 321-344.
Filomeni, G., G. Rotilio, et al. (2002). "Cell signaling and the glutathione redox system." Biochem Pharmacol 64(5-6): 1057-1064.
Filomeni, G., G. Rotilio, et al. (2005). "Disulfide relays and phosphorylative cascades: partners in redox-mediated signaling pathways." Cell Death Differ 12(12): 1555-1563.
Finkel, T. (2000). "Redox-dependent signal transduction." FEBS Lett 476(1-2): 52-54.
Finkel, T. (2012). "Signal transduction by mitochondrial oxidants." J Biol Chem 287(7): 4434-4440.
Flohe, L., S. Toppo, et al. (2011). "A comparison of thiol peroxidase mechanisms." Antioxid Redox Signal 15(3): 763-780.
Forman, H. J. (2007). "Use and abuse of exogenous H2O2 in studies of signal transduction." Free Radic Biol Med 42(7): 926-932.
Forman, H. J. and I. Fridovich (1973). "Superoxide dismutase: a comparison of rate constants." Arch Biochem Biophys 158(1): 396-400.
Forman, H. J., J. M. Fukuto, et al. (2008). "The chemistry of cell signaling by reactive oxygen and nitrogen species and 4-hydroxynonenal." Arch Biochem Biophys 477(2): 183-195.
Forman, H. J., J. M. Fukuto, et al. (2004). "Redox signaling: thiol chemistry defines which reactive oxygen and nitrogen species can act as second messengers." Am J Physiol Cell Physiol 287(2): C246-256.
Forman, H. J., M. Maiorino, et al. (2010). "Signaling functions of reactive oxygen species." Biochemistry 49(5): 835-842.
Foster, M. W., D. T. Hess, et al. (2009). "Protein S-nitrosylation in health and disease: a current perspective." Trends Mol Med 15(9): 391-404.
Foster, M. W., T. J. McMahon, et al. (2003). "S-nitrosylation in health and disease." Trends Mol Med 9(4): 160-168.
Fourquet, S., M. E. Huang, et al. (2008). "The dual functions of thiol-based peroxidases in H2O2 scavenging and signaling." Antioxid Redox Signal 10(9): 1565-1576.
Fratelli, M., H. Demol, et al. (2002). "Identification by redox proteomics of glutathionylated proteins in oxidatively stressed human T lymphocytes." Proc Natl Acad Sci U S A 99(6): 3505-3510.

Fratelli, M., H. Demol, et al. (2003). "Identification of proteins undergoing glutathionylation in oxidatively stressed hepatocytes and hepatoma cells." Proteomics 3(7): 1154-1161.
Frederickson, C. J., J. Y. Koh, et al. (2005). "The neurobiology of zinc in health and disease." Nat Rev Neurosci 6(6): 449-462.
Gaetke, L. M. and C. K. Chow (2003). "Copper toxicity, oxidative stress, and antioxidant nutrients." Toxicology 189(1-2): 147-163.
Gallogly, M. M. and J. J. Mieyal (2007). "Mechanisms of reversible protein glutathionylation in redox signaling and oxidative stress." Curr Opin Pharmacol 7(4): 381-391.
Galter, D., S. Mihm, et al. (1994). "Distinct effects of glutathione disulfide on the nuclear transcription factor kappa B and the activator protein-1." Eur J Biochem 221(2): 639-648.
Gaston, B., J. Reilly, et al. (1993). "Endogenous nitrogen oxides and bronchodilator S-nitrosothiols in human airways." Proc Natl Acad Sci U S A 90(23): 10957-10961.
Georgiou, G. (2002). "How to flip the (redox) switch." Cell 111(5): 607-610.
Gilbert, H. F. (1990). "Molecular and cellular aspects of thiol-disulfide exchange." Adv Enzymol Relat Areas Mol Biol 63: 69-172.
Giorgio, M., M. Trinei, et al. (2007). "Hydrogen peroxide: a metabolic by-product or a common mediator of ageing signals?" Nat Rev Mol Cell Biol 8(9): 722-728.
Giustarini, D., R. Rossi, et al. (2004). "S-glutathionylation: from redox regulation of protein functions to human diseases." J Cell Mol Med 8(2): 201-212.
Go, Y. M. and D. P. Jones (2005). "Intracellular proatherogenic events and cell adhesion modulated by extracellular thiol/disulfide redox state." Circulation 111(22): 2973-2980.
Go, Y. M. and D. P. Jones (2008). "Redox compartmentalization in eukaryotic cells." Biochim Biophys Acta 1780(11): 1273-1290.
Gon, Y., T. Sasada, et al. (2001). "Expression of thioredoxin in bleomycin-injured airway epithelium: possible role of protection against bleomycin induced epithelial injury." Life Sci 68(16): 1877-1888.
Goto, K., M. Holler, et al. (1997). "Synthesis, Structure, and Reactions of a Sulfenic Acid Bearing a Novel Bowl-Type Substituent: The First Synthesis of a Stable Sulfenic Acid by Direct Oxidation of a Thiol." Journal of the American Chemical Society 119(6): 1460-1461.
Gow, A. J., Q. Chen, et al. (2002). "Basal and stimulated protein S-nitrosylation in multiple cell types and tissues." J Biol Chem 277(12): 9637-9640.

Griffith, O. W. and A. Meister (1985). "Origin and turnover of mitochondrial glutathione." Proc Natl Acad Sci U S A 82(14): 4668-4672.
Gromer, S., S. Urig, et al. (2004). "The thioredoxin system--from science to clinic." Med Res Rev 24(1): 40-89.
Gross, E., C. S. Sevier, et al. (2006). "Generating disulfides enzymatically: reaction products and electron acceptors of the endoplasmic reticulum thiol oxidase Ero1p." Proc Natl Acad Sci U S A 103(2): 299-304.
Gutscher, M., A. L. Pauleau, et al. (2008). "Real-time imaging of the intracellular glutathione redox potential." Nat Methods 5(6): 553-559.
Hagg, D., M. C. Englund, et al. (2006). "Oxidized LDL induces a coordinated up-regulation of the glutathione and thioredoxin systems in human macrophages." Atherosclerosis 185(2): 282-289.
Hainaut, P. and J. Milner (1993). "Redox modulation of p53 conformation and sequence-specific DNA binding in vitro." Cancer Res 53(19): 4469-4473.
Hall, A., D. Parsonage, et al. (2010). "Structural evidence that peroxiredoxin catalytic power is based on transition-state stabilization." J Mol Biol 402(1): 194-209.
Halliwell, B., M. V. Clement, et al. (2000). "Hydrogen peroxide in the human body." FEBS Lett 486(1): 10-13.
Halliwell, B., M. V. Clement, et al. (2000). "Hydrogen peroxide. Ubiquitous in cell culture and in vivo?" IUBMB Life 50(4-5): 251-257.
Halliwell, B. and J. M. C. Gutteridge (2007). Free radicals in biology and medicine. Oxford ; New York, Oxford University Press.
Halliwell, B. and M. Whiteman (2004). "Measuring reactive species and oxidative damage in vivo and in cell culture: how should you do it and what do the results mean?" Br J Pharmacol 142(2): 231-255.
Halvey, P. J., W. H. Watson, et al. (2005). "Compartmental oxidation of thiol-disulfide redox couples during epidermal growth factor signaling." Biochem J 386(Pt 2): 215-219.
Hansen, J. M., Y. M. Go, et al. (2006). "Nuclear and mitochondrial compartmentation of oxidative stress and redox signaling." Annu Rev Pharmacol Toxicol 46: 215-234.
Hansen, J. M., H. Zhang, et al. (2006). "Differential oxidation of thioredoxin-1, thioredoxin-2, and glutathione by metal ions." Free Radic Biol Med 40(1): 138-145.
Hansen, J. M., H. Zhang, et al. (2006). "Mitochondrial thioredoxin-2 has a key role in determining tumor necrosis factor-alpha-induced reactive

oxygen species generation, NF-kappaB activation, and apoptosis." Toxicol Sci 91(2): 643-650.
Hansen, R. E., D. Roth, et al. (2009). "Quantifying the global cellular thiol-disulfide status." Proc Natl Acad Sci U S A 106(2): 422-427.
Harman, D. (1956). "Aging: a theory based on free radical and radiation chemistry." J Gerontol 11(3): 298-300.
Harris, C. and J. M. Hansen (2012). "Oxidative stress, thiols, and redox profiles." Methods Mol Biol 889: 325-346.
Hausladen, A., C. T. Privalle, et al. (1996). "Nitrosative stress: activation of the transcription factor OxyR." Cell 86(5): 719-729.
Hawkins, B. J., M. Madesh, et al. (2007). "Superoxide flux in endothelial cells via the chloride channel-3 mediates intracellular signaling." Mol Biol Cell 18(6): 2002-2012.
He, T., A. Banach-Latapy, et al. (2012). "Peroxiredoxin 1 knockdown potentiates beta-lapachone cytotoxicity through modulation of reactive oxygen species and mitogen-activated protein kinase signals." Carcinogenesis.
Heeren, G., S. Jarolim, et al. (2004). "The role of respiration, reactive oxygen species and oxidative stress in mother cell-specific ageing of yeast strains defective in the RAS signaling pathway." FEMS Yeast Res 5(2): 157-167.
Heneberg, P. and P. Draber (2005). "Regulation of cys-based protein tyrosine phosphatases via reactive oxygen and nitrogen species in mast cells and basophils." Curr Med Chem 12(16): 1859-1871.
Hess, D. T., A. Matsumoto, et al. (2005). "Protein S-nitrosylation: purview and parameters." Nat Rev Mol Cell Biol 6(2): 150-166.
Hess, D. T., A. Matsumoto, et al. (2001). "S-nitrosylation: spectrum and specificity." Nat Cell Biol 3(2): E46-49.
Hess, N. J., G. W. Buchko, et al. (1998). "Human nucleotide excision repair protein XPA: extended X-ray absorption fine-structure evidence for a metal-binding domain." Protein Sci 7(9): 1970-1975.
Hildebrandt, W., R. Kinscherf, et al. (2002). "Plasma cystine concentration and redox state in aging and physical exercise." Mech Ageing Dev 123(9): 1269-1281.
Hilt, W. and D. H. Wolf (1996). "Proteasomes: destruction as a programme." Trends Biochem Sci 21(3): 96-102.
Hober, S., A. Hansson, et al. (1994). "Folding of insulin-like growth factor I is thermodynamically controlled by insulin-like growth factor binding protein." Biochemistry 33(22): 6758-6761.
Hogg, D. R. (2010). Chemistry of sulphenic acids and esters. Sulfenic Acids and Derivatives (1990), John Wiley & Sons, Ltd.: 361-402.

Holmgren, A. (1989). "Thioredoxin and glutaredoxin systems." J Biol Chem 264(24): 13963-13966.
Holmgren, A. and M. Luthman (1978). "Tissue distrubution and subcellular localization of bovine thioredoxin determined by radioimmunoassay." Biochemistry 17(19): 4071-4077.
Hoshino, Y., K. Shioji, et al. (2007). "From oxygen sensing to heart failure: role of thioredoxin." Antioxid Redox Signal 9(6): 689-699.
Hou, Y., Z. Guo, et al. (1996). "Seleno compounds and glutathione peroxidase catalyzed decomposition of S-nitrosothiols." Biochem Biophys Res Commun 228(1): 88-93.
Howie, J. K., J. J. Houts, et al. (1977). "Oxidation-reduction chemistry of DL-alpha-lipoic acid, propanedithiol, and trimethylene disulfide in aprotic and in aqueous media." J Am Chem Soc 99(19): 6323-6326.
Hu, J., L. Dong, et al. (2008). "The redox environment in the mitochondrial intermembrane space is maintained separately from the cytosol and matrix." J Biol Chem 283(43): 29126-29134.
Huber-Wunderlich, M. and R. Glockshuber (1998). "A single dipeptide sequence modulates the redox properties of a whole enzyme family." Fold Des 3(3): 161-171.
Hugo, M., L. Turell, et al. (2009). "Thiol and sulfenic acid oxidation of AhpE, the one-cysteine peroxiredoxin from Mycobacterium tuberculosis: kinetics, acidity constants, and conformational dynamics." Biochemistry 48(40): 9416-9426.
Hutter, D. E., B. G. Till, et al. (1997). "Redox state changes in density-dependent regulation of proliferation." Exp Cell Res 232(2): 435-438.
Hwang, C., A. J. Sinskey, et al. (1992). "Oxidized redox state of glutathione in the endoplasmic reticulum." Science 257(5076): 1496-1502.
Ilbert, M., J. Horst, et al. (2007). "The redox-switch domain of Hsp33 functions as dual stress sensor." Nat Struct Mol Biol 14(6): 556-563.
Jacob, C., I. Knight, et al. (2006). "Aspects of the biological redox chemistry of cysteine: from simple redox responses to sophisticated signaling pathways." Biol Chem 387(10-11): 1385-1397.
Jacobsen, K. T., L. Adlerz, et al. (2010). "Insulin-like growth factor-1 (IGF-1)-induced processing of amyloid-beta precursor protein (APP) and APP-like protein 2 is mediated by different metalloproteinases." J Biol Chem 285(14): 10223-10231.
Jaffrey, S. R., H. Erdjument-Bromage, et al. (2001). "Protein S-nitrosylation: a physiological signal for neuronal nitric oxide." Nat Cell Biol 3(2): 193-197.

Jarvis, K., P. Assis-Nascimento, et al. (2007). "Beta-amyloid toxicity and reversal in embryonic rat septal neurons." Neurosci Lett 423(3): 184-188.

Jensen, K. S., R. E. Hansen, et al. (2009). "Kinetic and thermodynamic aspects of cellular thiol-disulfide redox regulation." Antioxid Redox Signal 11(5): 1047-1058.

Jeong, W., S. J. Park, et al. (2006). "Molecular mechanism of the reduction of cysteine sulfinic acid of peroxiredoxin to cysteine by mammalian sulfiredoxin." J Biol Chem 281(20): 14400-14407.

Jiang, L. J., W. Maret, et al. (1998). "The glutathione redox couple modulates zinc transfer from metallothionein to zinc-depleted sorbitol dehydrogenase." Proc Natl Acad Sci U S A 95(7): 3483-3488.

Jiang, S., S. E. Moriarty-Craige, et al. (2005). "Oxidant-induced apoptosis in human retinal pigment epithelial cells: dependence on extracellular redox state." Invest Ophthalmol Vis Sci 46(3): 1054-1061.

Jimenez-Del-Rio, M. and C. Velez-Pardo (2012). "The bad, the good, and the ugly about oxidative stress." Oxid Med Cell Longev 2012: 163913.

Jocelyn, P. C. (1972). Biochemistry of the SH group; the occurrence, chemical properties, metabolism and biological function of thiols and disulfides. London, New York, Academic Press.

Jonas, C. R., L. H. Gu, et al. (2003). "Glutamine and KGF each regulate extracellular thiol/disulfide redox and enhance proliferation in Caco-2 cells." Am J Physiol Regul Integr Comp Physiol 285(6): R1421-1429.

Jonas, C. R., A. B. Puckett, et al. (2000). "Plasma antioxidant status after high-dose chemotherapy: a randomized trial of parenteral nutrition in bone marrow transplantation patients." Am J Clin Nutr 72(1): 181-189.

Jones, D. P. (2006). "Redefining oxidative stress." Antioxid Redox Signal 8(9-10): 1865-1879.

Jones, D. P., J. L. Carlson, et al. (2000). "Redox state of glutathione in human plasma." Free Radic Biol Med 28(4): 625-635.

Jones, D. P., L. Eklow, et al. (1981). "Metabolism of hydrogen peroxide in isolated hepatocytes: relative contributions of catalase and glutathione peroxidase in decomposition of endogenously generated H2O2." Arch Biochem Biophys 210(2): 505-516.

Jones, D. P., Y. M. Go, et al. (2004). "Cysteine/cystine couple is a newly recognized node in the circuitry for biologic redox signaling and control." FASEB J 18(11): 1246-1248.

Jones, D. P., V. C. Mody, Jr., et al. (2002). "Redox analysis of human plasma allows separation of pro-oxidant events of aging from decline in antioxidant defenses." Free Radic Biol Med 33(9): 1290-1300.

Jones, J. I. and D. R. Clemmons (1995). "Insulin-like growth factors and their binding proteins: biological actions." Endocr Rev 16(1): 3-34.

Jourd'heuil, D., L. Gray, et al. (2000). "S-nitrosothiol formation in blood of lipopolysaccharide-treated rats." Biochem Biophys Res Commun 273(1): 22-26.

Jourd'heuil, D., F. S. Laroux, et al. (1999). "Effect of superoxide dismutase on the stability of S-nitrosothiols." Arch Biochem Biophys 361(2): 323-330.

Ju, T. C., S. D. Chen, et al. (2005). "Protective effects of S-nitrosoglutathione against amyloid beta-peptide neurotoxicity." Free Radic Biol Med 38(7): 938-949.

Juarez, J. C., M. Manuia, et al. (2008). "Superoxide dismutase 1 (SOD1) is essential for H2O2-mediated oxidation and inactivation of phosphatases in growth factor signaling." Proc Natl Acad Sci U S A 105(20): 7147-7152.

Jung, C. H. and J. A. Thomas (1996). "S-glutathiolated hepatocyte proteins and insulin disulfides as substrates for reduction by glutaredoxin, thioredoxin, protein disulfide isomerase, and glutathione." Arch Biochem Biophys 335(1): 61-72.

Jung, J. W., A. Yee, et al. (2005). "Solution structure of YKR049C, a putative redox protein from Saccharomyces cerevisiae." J Biochem Mol Biol 38(5): 550-554.

Katakai, K., J. Liu, et al. (2001). "Nitric oxide induces metallothionein (MT) gene expression apparently by displacing zinc bound to MIT." Toxicology Letters 119(2): 103-108.

Kemp, M., Y. M. Go, et al. (2008). "Nonequilibrium thermodynamics of thiol/disulfide redox systems: a perspective on redox systems biology." Free Radic Biol Med 44(6): 921-937.

Kettenhofen, N. J. and M. J. Wood (2010). "Formation, reactivity, and detection of protein sulfenic acids." Chem Res Toxicol 23(11): 1633-1646.

Khan, M., Y. B. Im, et al. (2009). "Administration of S-nitrosoglutathione after traumatic brain injury protects the neurovascular unit and reduces secondary injury in a rat model of controlled cortical impact." J Neuroinflammation 6: 32.

Khan, M., B. Sekhon, et al. (2005). "S-Nitrosoglutathione reduces inflammation and protects brain against focal cerebral ischemia in a rat model of experimental stroke." J Cereb Blood Flow Metab 25(2): 177-192.

Kim, S. O., K. Merchant, et al. (2002). "OxyR: a molecular code for redox-related signaling." Cell 109(3): 383-396.
Kirlin, W. G., J. Cai, et al. (1999). "Glutathione redox potential in response to differentiation and enzyme inducers." Free Radic Biol Med 27(11-12): 1208-1218.
Kluge, I., U. Gutteck-Amsler, et al. (1997). "S-nitrosoglutathione in rat cerebellum: identification and quantification by liquid chromatography-mass spectrometry." J Neurochem 69(6): 2599-2607.
Kopera, E., T. Schwerdtle, et al. (2004). "Co(II) and Cd(II) substitute for Zn(II) in the zinc finger derived from the DNA repair protein XPA, demonstrating a variety of potential mechanisms of toxicity." Chem Res Toxicol 17(11): 1452-1458.
Korichneva, I. (2006). "Zinc dynamics in the myocardial redox signaling network." Antioxid Redox Signal 8(9-10): 1707-1721.
Korichneva, I., B. Hoyos, et al. (2002). "Zinc release from protein kinase C as the common event during activation by lipid second messenger or reactive oxygen." J Biol Chem 277(46): 44327-44331.
Kosower, N. S. and E. M. Kosower (1978). "The glutathione status of cells." Int Rev Cytol 54: 109-160.
Krause, G. and A. Holmgren (1991). "Substitution of the conserved tryptophan 31 in Escherichia coli thioredoxin by site-directed mutagenesis and structure-function analysis." J Biol Chem 266(7): 4056-4066.
Krezel, A., Q. Hao, et al. (2007). "The zinc/thiolate redox biochemistry of metallothionein and the control of zinc ion fluctuations in cell signaling." Arch Biochem Biophys 463(2): 188-200.
Krezel, A. and W. Maret (2006). "Zinc-buffering capacity of a eukaryotic cell at physiological pZn." J Biol Inorg Chem 11(8): 1049-1062.
Kroncke, K. D. (2007). "Cellular stress and intracellular zinc dyshomeostasis." Arch Biochem Biophys 463(2): 183-187.
Kroncke, K. D. and L. O. Klotz (2009). "Zinc fingers as biologic redox switches?" Antioxid Redox Signal 11(5): 1015-1027.
Kurosawa, K., N. Hayashi, et al. (1990). "Transport of glutathione across the mitochondrial membranes." Biochem Biophys Res Commun 167(1): 367-372.
Lai, T. S., A. Hausladen, et al. (2001). "Calcium regulates S-nitrosylation, denitrosylation, and activity of tissue transglutaminase." Biochemistry 40(16): 4904-4910.
Laity, J. H., B. M. Lee, et al. (2001). "Zinc finger proteins: new insights into structural and functional diversity." Curr Opin Struct Biol 11(1): 39-46.

Lash, L. H. (2006). "Mitochondrial glutathione transport: physiological, pathological and toxicological implications." Chem Biol Interact 163(1-2): 54-67.
Lee, C., S. M. Lee, et al. (2004). "Redox regulation of OxyR requires specific disulfide bond formation involving a rapid kinetic reaction path." Nat Struct Mol Biol 11(12): 1179-1185.
Li, L., S. J. Elledge, et al. (1994). "Specific association between the human DNA repair proteins XPA and ERCC1." Proc Natl Acad Sci U S A 91(11): 5012-5016.
Li, Q. and J. Ren (2007). "Influence of cardiac-specific overexpression of insulin-like growth factor 1 on lifespan and aging-associated changes in cardiac intracellular Ca2+ homeostasis, protein damage and apoptotic protein expression." Aging Cell 6(6): 799-806.
Lillig, C. H., C. Berndt, et al. (2008). "Glutaredoxin systems." Biochim Biophys Acta 1780(11): 1304-1317.
Lillig, C. H. and A. Holmgren (2007). "Thioredoxin and related molecules--from biology to health and disease." Antioxid Redox Signal 9(1): 25-47.
Lin, T. Y. and P. S. Kim (1989). "Urea dependence of thiol-disulfide equilibria in thioredoxin: confirmation of the linkage relationship and a sensitive assay for structure." Biochemistry 28(12): 5282-5287.
Linke, K. and U. Jakob (2003). "Not every disulfide lasts forever: disulfide bond formation as a redox switch." Antioxid Redox Signal 5(4): 425-434.
Liu, L., A. Hausladen, et al. (2001). "A metabolic enzyme for S-nitrosothiol conserved from bacteria to humans." Nature 410(6827): 490-494.
Liu, L., Y. Yan, et al. (2004). "Essential roles of S-nitrosothiols in vascular homeostasis and endotoxic shock." Cell 116(4): 617-628.
Lopez-Mirabal, H. R. and J. R. Winther (2008). "Redox characteristics of the eukaryotic cytosol." Biochim Biophys Acta 1783(4): 629-640.
Loughran, P. A., D. B. Stolz, et al. (2005). "Monomeric inducible nitric oxide synthase localizes to peroxisomes in hepatocytes." Proc Natl Acad Sci U S A 102(39): 13837-13842.
Lund, P. K. (1994). "Insulin-like growth factor I: molecular biology and relevance to tissue-specific expression and action." Recent Prog Horm Res 49: 125-148.
Lundberg, M., C. Johansson, et al. (2001). "Cloning and expression of a novel human glutaredoxin (Grx2) with mitochondrial and nuclear isoforms." J Biol Chem 276(28): 26269-26275.
Ma, Y., L. Zhang, et al. (2006). "Angiotensin II stimulates transcription of insulin-like growth factor I receptor in vascular smooth muscle

cells: role of nuclear factor-kappaB." Endocrinology 147(3): 1256-1263.
Mackay, J. P. and M. Crossley (1998). "Zinc fingers are sticking together." Trends Biochem Sci 23(1): 1-4.
Mahadev, K., X. Wu, et al. (2001). "Hydrogen peroxide generated during cellular insulin stimulation is integral to activation of the distal insulin signaling cascade in 3T3-L1 adipocytes." J Biol Chem 276(52): 48662-48669.
Mahmood, D. F., A. Abderrazak, et al. (2012). "THE THIOREDOXIN SYSTEM AS A THERAPEUTIC TARGET IN HUMAN HEALTH AND DISEASE." Antioxid Redox Signal.
Malinouski, M., Y. Zhou, et al. (2011). "Hydrogen peroxide probes directed to different cellular compartments." PLoS One 6(1): e14564.
Mandal, P. K., M. Schneider, et al. (2010). "Loss of thioredoxin reductase 1 renders tumors highly susceptible to pharmacologic glutathione deprivation." Cancer Res 70(22): 9505-9514.
Maret, W. (2003). "Cellular zinc and redox states converge in the metallothionein/thionein pair." J Nutr 133(5 Suppl 1): 1460S-1462S.
Maret, W. (2004). "Zinc and sulfur: a critical biological partnership." Biochemistry 43(12): 3301-3309.
Maret, W. (2006). "Zinc coordination environments in proteins as redox sensors and signal transducers." Antioxid Redox Signal 8(9-10): 1419-1441.
Maret, W. (2009). "Molecular aspects of human cellular zinc homeostasis: redox control of zinc potentials and zinc signals." Biometals 22(1): 149-157.
Maret, W. (2011). "Redox biochemistry of mammalian metallothioneins." J Biol Inorg Chem 16(7): 1079-1086.
Marri, L., P. Trost, et al. (2008). "Spontaneous assembly of photosynthetic supramolecular complexes as mediated by the intrinsically unstructured protein CP12." J Biol Chem 283(4): 1831-1838.
Massy, Z. A., C. Fumeron, et al. (2004). "Increased pasma S-nitrosothiol concentrations predict cardiovascular outcomes among patients with end-stage renal disease: a prospective study." J Am Soc Nephrol 15(2): 470-476.
Matsuda, T., M. Saijo, et al. (1995). "DNA repair protein XPA binds replication protein A (RPA)." J Biol Chem 270(8): 4152-4157.
Matsumoto, A., K. E. Comatas, et al. (2003). "Screening for nitric oxide-dependent protein-protein interactions." Science 301(5633): 657-661.

Matsushita, K., C. N. Morrell, et al. (2003). "Nitric oxide regulates exocytosis by S-nitrosylation of N-ethylmaleimide-sensitive factor." Cell 115(2): 139-150.
McCall, K. A. and C. A. Fierke (2000). "Colorimetric and fluorimetric assays to quantitate micromolar concentrations of transition metals." Anal Biochem 284(2): 307-315.
McNally, J. S., M. E. Davis, et al. (2003). "Role of xanthine oxidoreductase and NAD(P)H oxidase in endothelial superoxide production in response to oscillatory shear stress." Am J Physiol Heart Circ Physiol 285(6): H2290-2297.
Meier, B., H. H. Radeke, et al. (1989). "Human fibroblasts release reactive oxygen species in response to interleukin-1 or tumour necrosis factor-alpha." Biochem J 263(2): 539-545.
Meng, D., X. Shi, et al. (2007). "Insulin-like growth factor-I (IGF-I) induces epidermal growth factor receptor transactivation and cell proliferation through reactive oxygen species." Free Radic Biol Med 42(11): 1651-1660.
Meza, J. E., G. K. Scott, et al. (2003). "Essential cysteine-alkylation strategies to monitor structurally altered estrogen receptor as found in oxidant-stressed breast cancers." Anal Biochem 320(1): 21-31.
Meyer, A. J. and T. P. Dick (2010). "Fluorescent protein-based redox probes." Antioxid Redox Signal 13(5): 621-650.
Mieyal, J. J., M. M. Gallogly, et al. (2008). "Molecular mechanisms and clinical implications of reversible protein S-glutathionylation." Antioxid Redox Signal 10(11): 1941-1988.
Miranda-Vizuete, A., A. E. Damdimopoulos, et al. (1999). "cDNA cloning, expression and chromosomal localization of the mouse mitochondrial thioredoxin reductase gene(1)." Biochim Biophys Acta 1447(1): 113-118.
Miwa, K., C. Kishimoto, et al. (2005). "Serum thioredoxin and alpha-tocopherol concentrations in patients with major risk factors." Circ J 69(3): 291-294.
Morgan, B., D. Ezerina, et al. (2012). "Multiple glutathione disulfide removal pathways mediate cytosolic redox homeostasis." Nat Chem Biol.
Morgan, B., M. C. Sobotta, et al. (2011). "Measuring E(GSH) and H2O2 with roGFP2-based redox probes." Free Radic Biol Med 51(11): 1943-1951.
Moriarty, S. E., J. H. Shah, et al. (2003). "Oxidation of glutathione and cysteine in human plasma associated with smoking." Free Radic Biol Med 35(12): 1582-1588.

Mueller, C. F., J. D. Widder, et al. (2005). "The role of the multidrug resistance protein-1 in modulation of endothelial cell oxidative stress." Circ Res 97(7): 637-644.

Mukherjee, S. P., R. H. Lane, et al. (1978). "Endogenous hydrogen peroxide and peroxidative metabolism in adipocytes in response to insulin and sulfhydryl reagents." Biochem Pharmacol 27(22): 2589-2594.

Mukherjee, S. P. and C. Mukherjee (1982). "Similar activities of nerve growth factor and its homologue proinsulin in intracellular hydrogen peroxide production and metabolism in adipocytes. Transmembrane signaling relative to insulin-mimicking cellular effects." Biochem Pharmacol 31(20): 3163-3172.

Nagy, P., A. Karton, et al. (2011). "Model for the exceptional reactivity of peroxiredoxins 2 and 3 with hydrogen peroxide: a kinetic and computational study." J Biol Chem 286(20): 18048-18055.

Nakamura, H., S. C. De Rosa, et al. (2001). "Chronic elevation of plasma thioredoxin: inhibition of chemotaxis and curtailment of life expectancy in AIDS." Proc Natl Acad Sci U S A 98(5): 2688-2693.

Nakamura, H., L. A. Herzenberg, et al. (2001). "Circulating thioredoxin suppresses lipopolysaccharide-induced neutrophil chemotaxis." Proc Natl Acad Sci U S A 98(26): 15143-15148.

Nakamura, T. and S. A. Lipton (2013). "Emerging role of protein-protein transnitrosylation in cell signaling pathways." Antioxid Redox Signal 18(3): 239-249.

Narhi, L. O., Q. X. Hua, et al. (1993). "Role of native disulfide bonds in the structure and activity of insulin-like growth factor 1: genetic models of protein-folding intermediates." Biochemistry 32(19): 5214-5221.

Nath, N., O. Morinaga, et al. (2010). "S-nitrosoglutathione a physiologic nitric oxide carrier attenuates experimental autoimmune encephalomyelitis." J Neuroimmune Pharmacol 5(2): 240-251.

Nelson, K. J., D. Parsonage, et al. (2008). "Cysteine pK(a) values for the bacterial peroxiredoxin AhpC." Biochemistry 47(48): 12860-12868.

Ng, E. S. and P. Kubes (2003). "The physiology of S-nitrosothiols: carrier molecules for nitric oxide." Can J Physiol Pharmacol 81(8): 759-764.

Nikitovic, D. and A. Holmgren (1996). "S-nitrosoglutathione is cleaved by the thioredoxin system with liberation of glutathione and redox regulating nitric oxide." J Biol Chem 271(32): 19180-19185.

Nomura, K., H. Imai, et al. (1999). "Mitochondrial phospholipid hydroperoxide glutathione peroxidase suppresses apoptosis mediated

by a mitochondrial death pathway." J Biol Chem 274(41): 29294-29302.
Nordberg, J. and E. S. Arner (2001). "Reactive oxygen species, antioxidants, and the mammalian thioredoxin system." Free Radic Biol Med 31(11): 1287-1312.
Ohtake, Y. and S. Yabuuchi (1991). "Molecular cloning of the gamma-glutamylcysteine synthetase gene of Saccharomyces cerevisiae." Yeast 7(9): 953-961.
Ostergaard, H., C. Tachibana, et al. (2004). "Monitoring disulfide bond formation in the eukaryotic cytosol." J Cell Biol 166(3): 337-345.
Outten, F. W. and E. C. Theil (2009). "Iron-based redox switches in biology." Antioxid Redox Signal 11(5): 1029-1046.
Paget, M. S. and M. J. Buttner (2003). "Thiol-based regulatory switches." Annu Rev Genet 37: 91-121.
Palmiter, R. D. and S. D. Findley (1995). "Cloning and functional characterization of a mammalian zinc transporter that confers resistance to zinc." EMBO J 14(4): 639-649.
Palmiter, R. D. and L. Huang (2004). "Efflux and compartmentalization of zinc by members of the SLC30 family of solute carriers." Pflugers Arch 447(5): 744-751.
Palumaa, P. (2009). "Biological redox switches." Antioxid Redox Signal 11(5): 981-983.
Park, C. H., D. Mu, et al. (1995). "The general transcription-repair factor TFIIH is recruited to the excision repair complex by the XPA protein independent of the TFIIE transcription factor." J Biol Chem 270(9): 4896-4902.
Pastore, A., G. Tozzi, et al. (2003). "Actin glutathionylation increases in fibroblasts of patients with Friedreich's ataxia: a potential role in the pathogenesis of the disease." J Biol Chem 278(43): 42588-42595.
Patwari, P. and R. T. Lee (2007). "Thioredoxins, mitochondria, and hypertension." Am J Pathol 170(3): 805-808.
Paulsen, C. E. and K. S. Carroll (2010). "Orchestrating redox signaling networks through regulatory cysteine switches." ACS Chem Biol 5(1): 47-62.
Perez-Mato, I., C. Castro, et al. (1999). "Methionine adenosyltransferase S-nitrosylation is regulated by the basic and acidic amino acids surrounding the target thiol." J Biol Chem 274(24): 17075-17079.
Piantadosi, C. A. (2012). "Regulation of mitochondrial processes by protein S-nitrosylation." Biochim Biophys Acta 1820(6): 712-721.
Piemonte, F., A. Pastore, et al. (2001). "Glutathione in blood of patients with Friedreich's ataxia." Eur J Clin Invest 31(11): 1007-1011.

Piotukh, K., D. Kosslick, et al. (2007). "Reversible disulfide bond formation of intracellular proteins probed by NMR spectroscopy." Free Radic Biol Med 43(9): 1263-1270.
Pirev, E., C. Calles, et al. (2008). "Ultraviolet-A irradiation but not ultraviolet-B or infrared-A irradiation leads to a disturbed zinc homeostasis in cells." Free Radic Biol Med 45(1): 86-91.
Popken, G. J., M. Dechert-Zeger, et al. (2005). "Brain development." Adv Exp Med Biol 567: 187-220.
Prasad, A. S. (1995). "Zinc: an overview." Nutrition 11(1 Suppl): 93-99.
Ramirez, A., B. Ramadan, et al. (2007). "Extracellular cysteine/cystine redox potential controls lung fibroblast proliferation and matrix expression through upregulation of transforming growth factor-beta." Am J Physiol Lung Cell Mol Physiol 293(4): L972-981.
Ravichandran, V., T. Seres, et al. (1994). "S-thiolation of glyceraldehyde-3-phosphate dehydrogenase induced by the phagocytosis-associated respiratory burst in blood monocytes." J Biol Chem 269(40): 25010-25015.
Rebrin, I. and R. S. Sohal (2004). "Comparison of thiol redox state of mitochondria and homogenates of various tissues between two strains of mice with different longevities." Exp Gerontol 39(10): 1513-1519.
Rechler, M. M. (1993). "Insulin-like growth factor binding proteins." Vitam Horm 47: 1-114.
Rhee, S. G. (1999). "Redox signaling: hydrogen peroxide as intracellular messenger." Exp Mol Med 31(2): 53-59.
Rhee, S. G. (2006). "Cell signaling. H2O2, a necessary evil for cell signaling." Science 312(5782): 1882-1883.
Rhee, S. G., T. S. Chang, et al. (2003). "Cellular regulation by hydrogen peroxide." J Am Soc Nephrol 14(8 Suppl 3): S211-215.
Rhee, S. G. and H. A. Woo (2011). "Multiple functions of peroxiredoxins: peroxidases, sensors and regulators of the intracellular messenger H(2)O(2), and protein chaperones." Antioxid Redox Signal 15(3): 781-794.
Rigoulet, M., E. D. Yoboue, et al. (2011). "Mitochondrial ROS generation and its regulation: mechanisms involved in H(2)O(2) signaling." Antioxid Redox Signal 14(3): 459-468.
Rink, L. and P. Gabriel (2000). "Zinc and the immune system." Proc Nutr Soc 59(4): 541-552.
Rojkind, M., J. A. Dominguez-Rosales, et al. (2002). "Role of hydrogen peroxide and oxidative stress in healing responses." Cell Mol Life Sci 59(11): 1872-1891.
Romeo, A. A., J. A. Capobianco, et al. (2003). "Superoxide dismutase targets NO from GSNO to Cysbeta93 of oxyhemoglobin in

concentrated but not dilute solutions of the protein." J Am Chem Soc 125(47): 14370-14378.
Roy, S., S. Khanna, et al. (2008). "Redox regulation of the VEGF signaling path and tissue vascularization: Hydrogen peroxide, the common link between physical exercise and cutaneous wound healing." Free Radic Biol Med 44(2): 180-192.
Ruoppolo, M., J. Lundstrom-Ljung, et al. (1997). "Effect of glutaredoxin and protein disulfide isomerase on the glutathione-dependent folding of ribonuclease A." Biochemistry 36(40): 12259-12267.
Russo, V. C., P. D. Gluckman, et al. (2005). "The insulin-like growth factor system and its pleiotropic functions in brain." Endocr Rev 26(7): 916-943.
Sabel, C. E., J. M. Neureuther, et al. (2010). "A spectrophotometric method for the determination of zinc, copper, and cobalt ions in metalloproteins using Zincon." Anal Biochem 397(2): 218-226.
Sagher, D., D. Brunell, et al. (2006). "Selenocompounds can serve as oxidoreductants with the methionine sulfoxide reductase enzymes." J Biol Chem 281(42): 31184-31187.
Sahaf, B. and A. Rosen (2000). "Secretion of 10-kDa and 12-kDa thioredoxin species from blood monocytes and transformed leukocytes." Antioxid Redox Signal 2(4): 717-726.
Sainsbury, S., J. Ren, et al. (2010). "The structure of a reduced form of OxyR from Neisseria meningitidis." BMC Struct Biol 10: 10.
Salmeen, A., J. N. Andersen, et al. (2003). "Redox regulation of protein tyrosine phosphatase 1B involves a sulphenyl-amide intermediate." Nature 423(6941): 769-773.
Salsbury, F. R., Jr., S. T. Knutson, et al. (2008). "Functional site profiling and electrostatic analysis of cysteines modifiable to cysteine sulfenic acid." Protein Sci 17(2): 299-312.
Samiec, P. S., C. Drews-Botsch, et al. (1998). "Glutathione in human plasma: decline in association with aging, age-related macular degeneration, and diabetes." Free Radic Biol Med 24(5): 699-704.
Santos, C. X., N. Anilkumar, et al. (2011). "Redox signaling in cardiac myocytes." Free Radic Biol Med 50(7): 777-793.
Scarbrough, P. M., K. A. Mapuskar, et al. (2012). "Simultaneous inhibition of glutathione- and thioredoxin-dependent metabolism is necessary to potentiate 17AAG-induced cancer cell killing via oxidative stress." Free Radic Biol Med 52(2): 436-443.
Schafer, F. Q. and G. R. Buettner (2001). "Redox environment of the cell as viewed through the redox state of the glutathione disulfide/glutathione couple." Free Radic Biol Med 30(11): 1191-1212.

Schonhoff, C. M., M. Matsuoka, et al. (2006). "S-nitrosothiol depletion in amyotrophic lateral sclerosis." Proc Natl Acad Sci U S A 103(7): 2404-2409.
Schrader, M. and H. D. Fahimi (2006). "Peroxisomes and oxidative stress." Biochim Biophys Acta 1763(12): 1755-1766.
Schreck, R., P. Rieber, et al. (1991). "Reactive oxygen intermediates as apparently widely used messengers in the activation of the NF-kappa B transcription factor and HIV-1." EMBO J 10(8): 2247-2258.
Schwerdtle, T., I. Walter, et al. (2003). "Arsenite and its biomethylated metabolites interfere with the formation and repair of stable BPDE-induced DNA adducts in human cells and impair XPAzf and Fpg." DNA Repair (Amst) 2(12): 1449-1463.
Sen, C. K. (2000). "Cellular thiols and redox-regulated signal transduction." Curr Top Cell Regul 36: 1-30.
Sengupta, R. and A. Holmgren (2012). "The role of thioredoxin in the regulation of cellular processes by S-nitrosylation." Biochim Biophys Acta 1820(6): 689-700.
Shelton, M. D. and J. J. Mieyal (2008). "Regulation by reversible S-glutathionylation: molecular targets implicated in inflammatory diseases." Mol Cells 25(3): 332-346.
Shenton, D. and C. M. Grant (2003). "Protein S-thiolation targets glycolysis and protein synthesis in response to oxidative stress in the yeast Saccharomyces cerevisiae." Biochem J 374(Pt 2): 513-519.
Shi, Q., J. Feng, et al. (2008). "A proteomic study of S-nitrosylation in the rat cardiac proteins in vitro." Biol Pharm Bull 31(8): 1536-1540.
Silberstein, D. S., S. McDonough, et al. (1993). "Human eosinophil cytotoxicity-enhancing factor. Eosinophil-stimulating and dithiol reductase activities of biosynthetic (recombinant) species with COOH-terminal deletions." J Biol Chem 268(12): 9138-9142.
Snoeyink, V. L., Ed. (1980). Water chemistry. New-York, John Wiley and Sons.
Spahl, D. U., D. Berendji-Grun, et al. (2003). "Regulation of zinc homeostasis by inducible NO synthase-derived NO: nuclear metallothionein translocation and intranuclear Zn2+ release." Proc Natl Acad Sci U S A 100(24): 13952-13957.
Spyrou, G., E. Enmark, et al. (1997). "Cloning and expression of a novel mammalian thioredoxin." J Biol Chem 272(5): 2936-2941.
Staab, C. A., J. Alander, et al. (2008). "Reduction of S-nitrosoglutathione by alcohol dehydrogenase 3 is facilitated by substrate alcohols via direct cofactor recycling and leads to GSH-controlled formation of glutathione transferase inhibitors." Biochem J 413(3): 493-504.

Stadtman, E. R. (2004). "Role of oxidant species in aging." Curr Med Chem 11(9): 1105-1112.
Stadtman, E. R. and B. S. Berlett (1998). "Reactive oxygen-mediated protein oxidation in aging and disease." Drug Metab Rev 30(2): 225-243.
Stamler, J. S., O. Jaraki, et al. (1992). "Nitric oxide circulates in mammalian plasma primarily as an S-nitroso adduct of serum albumin." Proc Natl Acad Sci U S A 89(16): 7674-7677.
Stamler, J. S., L. Jia, et al. (1997). "Blood flow regulation by S-nitrosohemoglobin in the physiological oxygen gradient." Science 276(5321): 2034-2037.
Stamler, J. S., S. Lamas, et al. (2001). "Nitrosylation. the prototypic redox-based signaling mechanism." Cell 106(6): 675-683.
Stamler, J. S., D. J. Singel, et al. (1992). "Biochemistry of nitric oxide and its redox-activated forms." Science 258(5090): 1898-1902.
Stamler, J. S., E. J. Toone, et al. (1997). "(S)NO signals: translocation, regulation, and a consensus motif." Neuron 18(5): 691-696.
Steffen, M., T. M. Sarkela, et al. (2001). "Metabolism of S-nitrosoglutathione in intact mitochondria." Biochem J 356(Pt 2): 395-402.
Stephen, D. W. and D. J. Jamieson (1997). "Amino acid-dependent regulation of the Saccharomyces cerevisiae GSH1 gene by hydrogen peroxide." Mol Microbiol 23(2): 203-210.
Stewart, C. E. and P. Rotwein (1996). "Growth, differentiation, and survival: multiple physiological functions for insulin-like growth factors." Physiol Rev 76(4): 1005-1026.
Sticozzi, C., G. Belmonte, et al. (2012). "Cigarette smoke affects keratinocytes SRB1 expression and localization via H2O2 production and HNE protein adducts formation." PLoS One 7(3): e33592.
Stone, J. R. (2004). "An assessment of proposed mechanisms for sensing hydrogen peroxide in mammalian systems." Arch Biochem Biophys 422(2): 119-124.
Stone, J. R. and S. Yang (2006). "Hydrogen peroxide: a signaling messenger." Antioxid Redox Signal 8(3-4): 243-270.
Stroher, E. and K. J. Dietz (2006). "Concepts and approaches towards understanding the cellular redox proteome." Plant Biol (Stuttg) 8(4): 407-418.
Stubauer, G., A. Giuffre, et al. (1999). "Mechanism of S-nitrosothiol formation and degradation mediated by copper ions." J Biol Chem 274(40): 28128-28133.

Sugasawa, K., J. M. Ng, et al. (1998). "Xeroderma pigmentosum group C protein complex is the initiator of global genome nucleotide excision repair." Mol Cell 2(2): 223-232.

Sun, J., L. Xu, et al. (2003). "Nitric oxide, NOC-12, and S-nitrosoglutathione modulate the skeletal muscle calcium release channel/ryanodine receptor by different mechanisms. An allosteric function for O2 in S-nitrosylation of the channel." J Biol Chem 278(10): 8184-8189.

Sundaresan, M., Z. X. Yu, et al. (1995). "Requirement for generation of H2O2 for platelet-derived growth factor signal transduction." Science 270(5234): 296-299.

Zahedi Avval, F. and A. Holmgren (2009). "Molecular mechanisms of thioredoxin and glutaredoxin as hydrogen donors for Mammalian s phase ribonucleotide reductase." J Biol Chem 284(13): 8233-8240.

Zaman, K., L. A. Palmer, et al. (2004). "Concentration-dependent effects of endogenous S-nitrosoglutathione on gene regulation by specificity proteins Sp3 and Sp1." Biochem J 380(Pt 1): 67-74.

Zapf, J., C. Hauri, et al. (1995). "Intravenously injected insulin-like growth factor (IGF) I/IGF binding protein-3 complex exerts insulin-like effects in hypophysectomized, but not in normal rats." J Clin Invest 95(1): 179-186.

Zhang, D. X. and D. D. Gutterman (2007). "Mitochondrial reactive oxygen species-mediated signaling in endothelial cells." Am J Physiol Heart Circ Physiol 292(5): H2023-2031.

Zhang, Y. and N. Hogg (2004). "Formation and stability of S-nitrosothiols in RAW 264.7 cells." Am J Physiol Lung Cell Mol Physiol 287(3): L467-474.

Zhang, Y. and N. Hogg (2005). "S-Nitrosothiols: cellular formation and transport." Free Radic Biol Med 38(7): 831-838.

Zheng, M., F. Aslund, et al. (1998). "Activation of the OxyR transcription factor by reversible disulfide bond formation." Science 279(5357): 1718-1721.

Zinkevich, N. S. and D. D. Gutterman (2011). "ROS-induced ROS release in vascular biology: redox-redox signaling." Am J Physiol Heart Circ Physiol 301(3): H647-653.

Zovo, K. and P. Palumaa (2009). "Modulation of redox switches of copper chaperone Cox17 by Zn(II) ions determined by new ESI MS-based approach." Antioxid Redox Signal 11(5): 985-995.

Tanaka, K., N. Miura, et al. (1990). "Analysis of a human DNA excision repair gene involved in group A xeroderma pigmentosum and containing a zinc-finger domain." Nature 348(6296): 73-76.

Tanaka, K. and R. D. Wood (1994). "Xeroderma pigmentosum and nucleotide excision repair of DNA." Trends Biochem Sci 19(2): 83-86.

Tarrago, L., E. Laugier, et al. (2009). "Regeneration mechanisms of Arabidopsis thaliana methionine sulfoxide reductases B by glutaredoxins and thioredoxins." J Biol Chem 284(28): 18963-18971.

Tellez-Sanz, R., E. Cesareo, et al. (2006). "Calorimetric and structural studies of the nitric oxide carrier S-nitrosoglutathione bound to human glutathione transferase P1-1." Protein Sci 15(5): 1093-1105.

Thomas, J. A., B. Poland, et al. (1995). "Protein sulfhydryls and their role in the antioxidant function of protein S-thiolation." Arch Biochem Biophys 319(1): 1-9.

Toledano, M. B., A. Delaunay, et al. (2004). "Microbial H2O2 sensors as archetypical redox signaling modules." Trends Biochem Sci 29(7): 351-357.

Toppo, S., L. Flohe, et al. (2009). "Catalytic mechanisms and specificities of glutathione peroxidases: variations of a basic scheme." Biochim Biophys Acta 1790(11): 1486-1500.

Trachootham, D., J. Alexandre, et al. (2009). "Targeting cancer cells by ROS-mediated mechanisms: a radical therapeutic approach?" Nat Rev Drug Discov 8(7): 579-591.

Trachootham, D., W. Lu, et al. (2008). "Redox regulation of cell survival." Antioxid Redox Signal 10(8): 1343-1374.

Trotter, E. W. and C. M. Grant (2003). "Non-reciprocal regulation of the redox state of the glutathione-glutaredoxin and thioredoxin systems." EMBO Rep 4(2): 184-188.

Trujillo, M., M. N. Alvarez, et al. (1998). "Xanthine oxidase-mediated decomposition of S-nitrosothiols." J Biol Chem 273(14): 7828-7834.

Turan, B., H. Fliss, et al. (1997). "Oxidants increase intracellular free Zn2+ concentration in rabbit ventricular myocytes." Am J Physiol 272(5 Pt 2): H2095-2106.

Uriu-Adams, J. Y. and C. L. Keen (2005). "Copper, oxidative stress, and human health." Mol Aspects Med 26(4-5): 268-298.

Valko, M., D. Leibfritz, et al. (2007). "Free radicals and antioxidants in normal physiological functions and human disease." Int J Biochem Cell Biol 39(1): 44-84.

Vallee, B. C. J. A. D. (1991). "Zinc Fingers, Zinc Clusters, and Zinc Twists In Dna-Binding Protein Domains." Proc. Natl. Acad. Sci. U. S. A. 88(3): 999.

Vallee, B. L. (1995). "The Function Of Metallothionein." Neurochem. Int. 27(1): 23.

Vallee, B. L. and D. S. Auld (1990). "Zinc coordination, function, and structure of zinc enzymes and other proteins." Biochemistry 29(24): 5647-5659.

Vallee, B. L. and K. H. Falchuk (1993). "The biochemical basis of zinc physiology." Physiol. Rev. 73(1): 79-118.

van Montfort, R. L., M. Congreve, et al. (2003). "Oxidation state of the active-site cysteine in protein tyrosine phosphatase 1B." Nature 423(6941): 773-777.

Wanders, R. J. and H. R. Waterham (2006). "Biochemistry of mammalian peroxisomes revisited." Annu Rev Biochem 75: 295-332.

Westwater, J., N. F. McLaren, et al. (2002). "The adaptive response of Saccharomyces cerevisiae to mercury exposure." Yeast 19(3): 233-239.

Wiseman, D. A., S. M. Wells, et al. (2007). "Alterations in zinc homeostasis underlie endothelial cell death induced by oxidative stress from acute exposure to hydrogen peroxide." Am J Physiol Lung Cell Mol Physiol 292(1): L165-177.

Wong, P. S., J. Hyun, et al. (1998). "Reaction between S-nitrosothiols and thiols: generation of nitroxyl (HNO) and subsequent chemistry." Biochemistry 37(16): 5362-5371.

Wood, Z. A., L. B. Poole, et al. (2003). "Peroxiredoxin evolution and the regulation of hydrogen peroxide signaling." Science 300(5619): 650-653.

Wouters, M. A., S. W. Fan, et al. (2010). "Disulfides as redox switches: from molecular mechanisms to functional significance." Antioxid Redox Signal 12(1): 53-91.

Wunderlich, M., R. Jaenicke, et al. (1993). "The redox properties of protein disulfide isomerase (DsbA) of Escherichia coli result from a tense conformation of its oxidized form." J Mol Biol 233(4): 559-566.

Yang, K. S., S. W. Kang, et al. (2002). "Inactivation of human peroxiredoxin I during catalysis as the result of the oxidation of the catalytic site cysteine to cysteine-sulfinic acid." J Biol Chem 277(41): 38029-38036.

Yao, D., Z. Gu, et al. (2004). "Nitrosative stress linked to sporadic Parkinson's disease: S-nitrosylation of parkin regulates its E3 ubiquitin ligase activity." Proc Natl Acad Sci U S A 101(29): 10810-10814.

Yeh, J. I., A. Claiborne, et al. (1996). "Structure of the native cysteine-sulfenic acid redox center of enterococcal NADH peroxidase refined at 2.8 A resolution." Biochemistry 35(31): 9951-9957.

ACKNOWLEDGEMENT

These studies were carried out between 2004-2012 at the Department of Gene Technology, Tallinn University of Technology (TUT), Estonia.

I would like to express my sincere gratitude to my supervisor, Professor Peep Palumaa, for providing me with the opportunity to perform research in the fascinating fields of Proteomics and Mass Spectrometry. His support started when he encouraged me to pursue this thesis has not wained throughout the course of these studies.

My very special thanks go to my polish supervisor, Professor Wojciech Bal, whose help, stimulating suggestions, and encouragement have helped me during two Marie Curie fellowships at the Institute of Biochemistry and Biophysics Polish Academy of Sciences (IBB PAS). I also thank Professor Wojciech's family for their hospitality and his little princess Zuzja for her warm smiles.

I would like to thank all of my coauthors from the Proteomics lab at TUT, IBB PAS, and also Andrea Hartwig from the Institute of Food Technology and Food Chemistry at the Technical University of Berlin.

My colleagues from TUT and IBB PAS supported me in my research work. I want to thank all of my colleagues from the Proteomics Laboratory for all of their help, support, interest, and valuable hints. Special thanks go to Maria Borissova from the Department of Analytical Chemistry for support with ESI-MS and also for cheering me up. I also want to thank Edyta Kopera and Aleksandra Witkiewicz-Kucharczyk from the lab at IBB PAS in Poland for their patience and valuable help during experimental work. My deepest thanks go to Liliya Zhukova, also from this lab, for her outstanding support during my stay in Poland and also for discussions concerning HPLC techniques. I would also like to thank people from the remarkable MS lab at IBB PAS, headed by Michal Dadlez, for showing me the fascinating world of mass spectrometry and for their endless inspiration, cheerfulness and help. Last, but not least, I thank Vello Tõugu for his valuable advice during the review process of my latest publication.

I thank Professor Nigulas Samel for reviewing the thesis.

I am indebted to the World Federation of Scientists for financial support, and also to the Polish Ministry of Science, and the Estonian Science Foundation for financial support with both Marie Curie fellowships. I am also grateful to the Archimedes Foundation and the DoRa program for enabling me to introduce my results and broaden my knowledge at conferences and seminars.

My warmest thanks go to my family, relatives, and friends, who believed in me and supported me throughout these years. I am especially grateful to my beloved husband Vassili, whose patient love enabled me to complete this work, and my son Mihhail, who has been a major source of inspiration and happiness for the last five years.

SUMMARY

The oxidative modification of proteins is now considered to be an essential part of redox regulation within biological systems, and several ROS and RNS are crucial for the maintenance of life. The overproduction of these species leads to oxidative stress, which is a common cause of many diseases and disease symptoms and play a crucial role in aging. Moreover, the redox potential within cells is created to a large degree by low molecular weight thiols whose concentration largely determines the environment where redox reactions occur.

Determining the properties of redox-active proteins is of particular interest, for understanding the redox homeostasis of these proteins. In the current work, a rapid and efficient *in vitro* method - ESI-MS was applied to study various aspects of redox signaling using zinc finger proteins, and the hormone IGF-1. Zinc finger proteins are of particular interest due to their importance in gene regulation and because their structure enables them to act as biological redox switches. ESI-MS was found to be a suitable analytical technique to study the kinetics of oxidation of Cys_4 type XPA zinc finger with two different oxidative agents, known to be biologically relevant: H_2O_2 and GSNO. The zinc finger of XPA was found to be susceptible to oxidation by both H_2O_2 and GSNO with subsequent release of a Zn(II) ion. The initial reaction rate for oxidation of XPA zinc fingers by GSNO was higher as compared with H_2O_2. The final reaction products in both cases were zinc fingers with two disulfide bridges, however, a transiently S-nitrosylated zinc finger with Zn(II) bound is proposed to exist at low micromolar GSNO concentrations, characteristic for cells. These results presuppose that at lower oxidant exposures under normal physiological conditions Cys_4 type zinc fingers may undergo reversible regulation without Zn(II) release. It is important to mention that the reactivity of a particular zinc finger depends to a great extent on the tertiary structure of the protein, as well as on the local cellular redox environment. ESI-MS was also used to study the redox properties of human hormone IGF-1, which is folded in the ER and secreted into blood. The range of environmental redox potential values of different redox pairs for different cell organelles was collected from the literature, which demonstrates that the redox environment is more oxidative within the ER and in the extracellular environment. The midpoint redox potential for natively folded hIGF-1 is -332 mV which suggests that fully oxidized state for hIGF-1 with all three disulfides exists within ER and extracellular milieu.

The results of this work demonstrate that ESI-MS serves as a powerful tool for the investigation of redox properties of redox-active proteins and provides unique information about reaction intermediates and the release of metals from proteins under oxidative stimuli. It also enables determination of the redox state

of particular proteins within different redox environments. A comprehensive data set of this nature could serve as a valuable tool in solving various biological questions that involve redox chemistry.

KOKKUVÕTE

Valkude oksüdatiivne modifitseerimine on väga oluline bioloogiliste süsteemide regulatsiooni vahend. Mõned ROS ja RNS ühendid on füsioloogiliselt hädavajalikud, kuid nende ületootmine viib oksüdatiivse stressini, mis omakorda on paljude haiguste ja organismi vananemise peamiseks põhjuseks. Samal ajal mängib rakkude redoks potentsiaal, mille väärtus on määratud peamiselt madalamolekulaarsete tioolide poolt, määravat rolli nii ensümaatiliste kui ka spontaansete redoks reaktsioonide kulgemiseks.

Valkude redoks omaduste uurimine aitab kaasa nende redoks homeostaasiga ja selle rikkumisega seotud probleemide lahendamisele. Käesolevas töös rakendati valkude uurimiseks kiiret ja efektiivset *in vitro* metoodikat - ESI-MS, mis võimaldab erinevate redoksvormide kiiret ja täpset määramist, ning uuriti erinevaid redoks signaali ülekande aspekte, mis on seotud tsink-sõrm-valkude ja IGF-1 hormooniga. Tsink-sõrm-valgud osalevad geeniregulatsioonis ning nende struktuur võimaldab neil käituda bioloogiliste redoks lülititena. ESI-MS osutus sobivaks kahe erineva bioloogiliselt tähtsa oksüdeeriva agendi (H_2O_2 ja GSNO) mõju uurimiseks Cys_4-tüüpi XPA tsink-sõrm-valgu (XPA zf) oksüdatsiooni kineetikale. H_2O_2 ja GSNO oksüdeerivad XPA zf valku, millele järgnes Zn(II) vabanemine. GSNO reageeris XPA zf-ga kiiremini võrreldes H_2O_2-ga. Mõlemate oksüdantide puhul moodustus reaktsiooni lõppproduktina kahe disulfiid sillaga tsink-sõrm-valk. Näidati, et madalate, mikromolaarsete GSNO kontsentratsioonide puhul, mis on iseloomulikud rakkudele, võib ajutiselt tekkida S-nitrosüleeritud Zn(II) sisaldav produkt. See näitab et füsioloogilistes tingimustel võivad Cys_4 tüüpi tsink-sõrm-valgud olla ka pöörduvalt reguleeritud ilma Zn(II) vabastamiseta. Kindla tsink-sõrm-valgu reaktiivsus sõltub aga suurel määral ka valgu ruumilisest struktuurist ning rakulisest redoks keskkonnast. ESI-MS kasutati ka inimese hormooni IGF-1 redoks omaduste uurimiseks. IGF-1 ruumiline struktuur volditatakse kokku endoplasmaatilises võrgustikus (ER) enne tema sekreteerimist verre. Vastavalt kirjanduses leiduvatele keskkonna redoks potentsiaalide väärtustele, mis on erinevates organellides genereeritud erinevate redoks paaride poolt, on ER ja rakuväline keskkond kõige oksüdeerivamad. Natiivselt volditud IGF-1 redoks potentsiaal on -332 mV, mis näitab, et IGF-1 on rakuvälises keskkonnas täielikult oksüdeeritud, moodustades kolm disulfiid silda, mis on olulised hormooni seondumiseks oma retseptoriga raku pinnal.

Saadud tulemused näitavad, et ESI-MS on informatiivne metoodika redoks-aktiivsete valkude redoks omaduste uurimisteks, andes rikkaliku ja unikaalset informatsiooni metallide vabastamisest oksüdatiivsetes tingimustes ning erinevate valkude redoks olekutest erinevates tingimustes. Selline informatsioon võib osutuda oluliseks keeruliste redoks probleemide lahendamisel.

PUBLICATION I

Smirnova, J., Zhukova, L., Witkiewicz-Kucharczyk, A., Kopera, E., Oledzki, J., Wyslouch-Cieszynska, A., Palumaa, P., Hartwig, A., Bal, W. "Quantitative electrospray ionization mass spectrometry of zinc finger oxidation: the reaction of XPA zinc finger with H(2)O(2)" (2007) Anal Biochem.; 369(2):226-31

Available online at www.sciencedirect.com
ScienceDirect
Analytical Biochemistry 369 (2007) 226–231
ANALYTICAL BIOCHEMISTRY
www.elsevier.com/locate/yabio

Quantitative electrospray ionization mass spectrometry of zinc finger oxidation: The reaction of XPA zinc finger with H_2O_2

Julia Smirnova [a], Liliya Zhukova [b], Aleksandra Witkiewicz-Kucharczyk [b], Edyta Kopera [b], Jacek Olędzki [b], Aleksandra Wysłouch-Cieszyńska [b], Peep Palumaa [a], Andrea Hartwig [c], Wojciech Bal [b,d,*]

[a] *Institute of Gene Technology, Tallinn Technical University, 12618 Tallinn, Estonia*
[b] *Institute of Biochemistry and Biophysics, Polish Academy of Sciences, 02-106 Warsaw, Poland*
[c] *Institute of Food Technology and Food Chemistry, Technical University Berlin, D-13355 Berlin, Germany*
[d] *Central Institute for Labour Protection–National Research Institute, 00-701 Warsaw, Poland*

Received 14 April 2007
Available online 26 May 2007

Abstract

Oxidation plays an important role in the functioning of zinc fingers (ZFs). Electrospray ionization mass spectrometry (ESI–MS) is a very useful technique to study products of ZF oxidation, but its application has been limited largely to qualitative analysis of reaction products. On the other hand, ESI–MS has been applied successfully on several occasions to determine binding constants in metalloproteins. We used a synthetic 37-residue peptide acetyl-DYVICEECGKEFMDSYLMNHFDLPTCDNCRDADDKHK-amide (XPAzf), which corresponds to the Cys4 ZF sequence of human nucleotide excision repair protein XPA, to find out whether ESI–MS might be used quantitatively to study ZF reaction kinetics. For this purpose, we studied oxidation of the Zn(II) complex of XPAzf (ZnXPAzf) by H_2O_2 using three techniques in parallel: high-performance liquid chromatography (HPLC) of covalent reaction products, 4-(2-pyridylazo)-resorcinol monosodium salt (PAR)-based spectrophotometric zinc release assay, and ESI–MS. Single and double intrapeptide disulfides were detected by ESI–MS to be the sole reaction products. All three techniques yielded independently the same reaction rate, thereby demonstrating that ESI–MS may indeed be used in quantitative kinetic studies of ZF reactions. The comparison of experimental information demonstrated that the formation of the Cys5–Cys8 single disulfide was responsible for zinc release.

Keywords: Zinc finger; Hydrogen peroxide; Oxidation; Electrospray mass spectrometry

Zinc finger (ZF)[1] domains comprise one of the most abundant families of protein motifs in the eukaryotic genome, with multiple cellular functions. At least 3% of identified human proteins contain one or more ZF domains [1]. Functions of ZF proteins include the binding and recognition of nucleic acids and the formation of multiprotein complexes [2,3]. The Zn(II) ion is bonded in ZF domains in a tetrahedral geometry, with the involvement of at least two cysteine thiolates. The remaining two ligands are provided by two Cys residues, by one Cys residue and one His residue, or by two His residues.

The Zn(II) ion is not directly involved in interactions conveyed by a ZF, but it ensures the proper folding of the domain and its release leads to a loss of the ZF structure and function. It is suggested that many ZF proteins are regulated by reversible or irreversible oxidation of

* Corresponding author. Fax: +48 22 6584636.
E-mail address: wbal@ibb.waw.pl (W. Bal).

[1] *Abbreviations used:* ZF, Zinc finger; ESI–MS, Electrospray ionization mass spectrometry; HPLC, High-performance liquid chromatography; NMR, Nuclear magnetic resonance; EXAFS, Extended X-ray absorption fine structure; XPAzf, Acetyl-DYVICEECGKEFMDSYLMNHFDLPTCDNCRDADDKHK-amide peptide; ROS, Reactive oxygen species; ZnXPAzf, Zn(II) complex of XPAzf; PAR, 4-(2-pyridylazo)-resorcinol monosodium salt; MMTS, Methylmethanethiosulfonate; DMF, Dimethyl formamide; Hepes, *N*-2-hydroxyethylpiperazine-*N*′-2-ethanesulfonic acid; TFA, Trifluoroacetic acid; EDTA, Ethylenediaminetetraacetic acid; MS/MS, Tandem mass spectrometry.

0003-2697/$ - see front matter
doi:10.1016/j.ab.2007.05.019

zinc-binding cysteine thiols [4–6]. Such reactions usually are studied by single indirect methods, providing information about cysteine oxidation state or about zinc release, and results obtained rarely are correlated. In particular, those methods do not allow one to follow the fate of the native zinc-loaded ZF. Therefore, it is far from obvious which oxidation phenomena are responsible for the release of the Zn(II) ion and thereby the ultimate loss of ZF function.

Electrospray ionization mass spectrometry (ESI–MS) is used routinely in mechanistic studies of ZF oxidation to identify covalent reaction products in conjunction with separation methods such as high-performance liquid chromatography (HPLC). However, a direct kinetic application of this technique, for the detection of a Zn(II)–ZF complex, might yield much richer information than does any other experimental method used currently. Besides Zn(II) complexes, ESI–MS can simultaneously detect other species, such as labile intermediates, present in the sample. Moreover, this method is characterized by low consumption of the material. However, the ability of ESI–MS to provide quantitative information on the course of ZF reaction remains to be established.

XPA is a member of nucleotide excision repair multiprotein complex [7]. A loss of XPA function leads to xeroderma pigmentosum type A, a severe human disorder characterized by UV hypersensitivity and enhanced cancer risk [8]. The XPA activity was inhibited in cellular assays by several redox-capable metal ions, [9, 10]. The single ZF of XPA, of a Cys4 type, is essential for the XPA function. Its solution structure was determined by nuclear magnetic resonance (NMR) and extended X-ray absorption fine structure (EXAFS) [11,12]. In previous studies, we demonstrated a suitability of the synthetic 37-residue peptide acetyl-DYVICEECGKEFMDSYLMNHFDLPTCD NCRDADDKHK-amide (XPAzf), representing the XPA ZF sequence 101 to 137, as a model to study molecular mechanisms of XPA damage by metal ions and oxidants [13–15].

H_2O_2, the main long-lived by-product of oxygen metabolism in mitochondria, easily penetrates biomembranes and is present in various cellular compartments. As such, H_2O_2 is implicated in cellular signal transduction, neoplastic transformation, and apoptosis [16–18]. Therefore, H_2O_2 is used in numerous in vitro studies as a major biological reactive oxygen species (ROS). In the current work, we used the reaction of H_2O_2 oxidation of our Zn(II) complex of XPAzf (ZnXPAzf) model to determine whether ESI–MS is suitable to study kinetics of ZF oxidative reactions. In particular, we were interested in obtaining direct insight into the zinc release step for its biological relevance. We achieved this goal by comparing the results of direct noncovalent ESI–MS studies with those obtained by traditional methods, namely, HPLC of covalent reaction products and indirect monitoring of zinc release.

Materials and methods

Materials

The N-terminally acetylated and C-terminally amidated 37-residue peptide XPAzf was custom synthesized by Schafer-N (Copenhagen, Denmark). The identity of this peptide was verified by ESI–MS, and its purity was assessed by HPLC to exceed 98%. 4-(2-Pyridylazo)-resorcinol monosodium salt (PAR), methylmethanethiosulfonate (MMTS), ammonium acetate, and neocuproine were purchased from Sigma–Aldrich Chemical. H_2O_2 (30%, w/v) was obtained from POCH (Gliwice, Poland). Dimethyl formamide (DMF) and *N*-2-hydroxyethylpiperazine-*N*′-2-ethanesulfonic acid (Hepes) were purchased from Carl Roth (Karlsruhe, Germany). Acetonitrile was obtained from Lab-Scan Analytical Sciences (Dublin, Ireland). Trifluoroacetic acid (TFA), ethylenediaminetetraacetic acid (EDTA), and $ZnSO_4{\cdot}7H_2O$ were purchased from Merck (Darmstadt, Germany). Stock solutions of $ZnSO_4$ were calibrated spectrophotometrically with PAR using the differential absorption coefficient at 500 nm of 46,000 M^{-1} cm^{-1} [19].

Reaction kinetics

Weighed solid samples of XPAzf were dissolved in 10 mM ammonium acetate buffer (pH 7.4), previously saturated with argon, to prepare 100 μM stock solutions, which were immediately reconstituted with equimolar amounts of Zn(II) ions and filtered. The stocks of 10 mM H_2O_2 were prepared fresh before each experiment.

Reaction mixtures containing 10 μM ZnXPAzf and 100 μM H_2O_2 in 10 mM ammonium acetate buffer (pH 7.4) were incubated at 25 °C for several hours. Aliquots were studied by ESI–MS or assayed spectrophotometrically for the release of Zn(II) ions, as described below. For HPLC studies, batches of reaction mixtures were aliquoted into autosampler vials and analyzed separately at given times.

Zinc release

The release of Zn(II) ions from the ZnXPAzf complex was followed spectrophotometrically (Cary 3E) at 25 °C in 1-cm cuvettes using PAR as a Zn(II) indicator according to a published procedure with slight modifications [19]. This method was previously found to be suitable for studies of zinc release from ZnXPAzf [15]. Aliquots of reaction mixtures were diluted 10-fold with 50 μM PAR in 10 mM ammonium acetate buffer, and their absorption spectra were recorded immediately. Control experiments indicated that PAR and its Zn(II) complex were resistant to concentrations of H_2O_2 used within the time scale of these experiments.

HPLC and derivatization procedures

The analytical samples, typically 100 μl, were analyzed on a Breeze HPLC system (Waters, Milford, MA, USA)

equipped with an autosampler using a 218TP54 C18 column (300 Å, 5 μm, 4.6 mm i.d. × 250 mm, Grace Vydac, Columbia, MD, USA). Solvent A was 0.1% (v/v) TFA solution in water, and solvent B was 0.1% (v/v) TFA solution in acetonitrile. The samples were eluted for 5 min at 10% solvent B, followed by a steep linear gradient to 35% solvent B for 1 min and by another gradient to 50% solvent B over 30 min. The peaks were detected at 220 nm. The samples selected for fraction collection (500–1000 μl) were injected manually and analyzed by the same HPLC method. The fractions were collected manually and derivatized using MMTS, according to the published procedure [20]. The collected peaks were lyophilized and stored at 4 °C until analysis on ESI–MS as described below.

ESI–MS

Samples in 10 mM ammonium acetate buffer (pH 7.4) were injected into a Q-TOF1 mass spectrometer (Waters/Micromass, Manchester, UK) at 4 μl/min using a Hamilton syringe pump. The spectrometer parameters were as follows: cone voltage, 35 V; source block temperature, 80 °C; analyzer vacuum pressure, 5.8 nB. The time span of one scan was 5 s, and typically 30 to 50 scans were accumulated. Bovine pancreatic trypsin inhibitor was used as an internal mass standard. Positive ion spectra were deconvoluted using the MaxEnt module of the MassLynx suite (Micromass). Peptide sequencing was performed according to a standard procedure; the lyophilized fractions were resuspended in H_2O/acetonitrile (50:50) with an addition of 0.2% HCOOH and were injected using a Hamilton syringe pump. The tandem mass spectrometry (MS/MS) data were analyzed using the PepSeq module of MassLynx.

Results

HPLC studies

The reaction of ZnXPAzf with 100 μM H_2O_2 in 10 mM ammonium acetate was studied by following the decay of XPAzf (formed by acidic dissociation of ZnXPAzf) monitored by HPLC for several hours, similarly to our previous studies performed in 50 mM phosphate buffer [13,14]. The examples of chromatograms are shown in Fig. 1. The collected HPLC fractions were treated with MMTS to transform free –SH groups into $SSCH_3$ moieties. This reaction left –SS– groups intact [20]. The thiol modifications obtained in this fashion were assigned successfully for three major peaks. The MMTS derivatization of the starting material yielded an average mass of 4626.5 Da, corresponding to a 4× –$SSCH_3$ derivative of XPAzf. The intermediate product exhibited a mass of 4532.75 Da, corresponding to a 2× –$SSCH_3$ derivative with one disulfide bridge. The final product was characterized with a mass of 4439.0 Da, corresponding to XPAzf containing two disulfide bridges. ESI–MS/MS peptide sequencing experiments

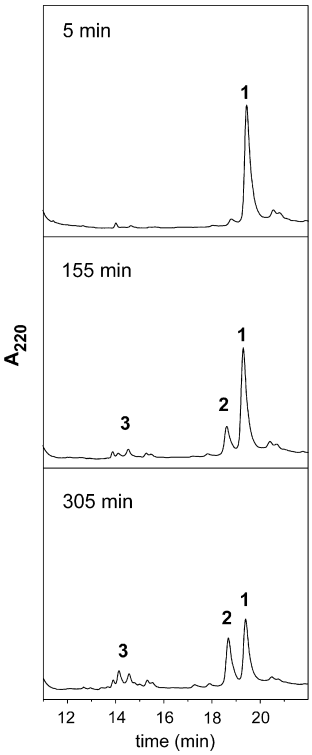

Fig. 1. Examples of chromatograms of products of oxidation of 10 μM ZnXPAzf by 100 μM H_2O_2 at various reaction times. Peaks: 1, XPAzf; 2, XPAzf(–SS–); 3, XPAzf(–SS–)$_2$.

were performed to establish the position of the disulfides formed. Even though only partial sequence information was obtained due to the large size of these peptides, it was nevertheless confirmed that the intermediate product contained the Cys5–Cys8 disulfide bridge. This bridge was also retained in the final product. The sequencing results are presented in the supplementary material. It should be noted that the low pH of the HPLC running buffer successfully stops the H_2O_2 oxidation due to thiol protonation in parallel with the dissociation of Zn(II) complexes. The HPLC experiment was analyzed quantitatively by integrating three principal peaks as shown in Fig. 2. Similar to our previous studies [13, 14], the oxidation of ZnXPAzf to disulfides by H_2O_2 progressed linearly with time.

Zn(II) release from ZnXPAzf monitored by PAR

The release of Zn(II) ions from ZnXPAzf induced by H_2O_2 was confirmed by spectrophotometric studies using a standard highly absorbing Zn(II) chelator, namely, PAR. The characteristic band of the Zn(PAR)$_2$ complex was monitored at 500 nm [19]. No free Zn(II) was detected in ZnXPAzf samples prior to the addition of oxidants. The

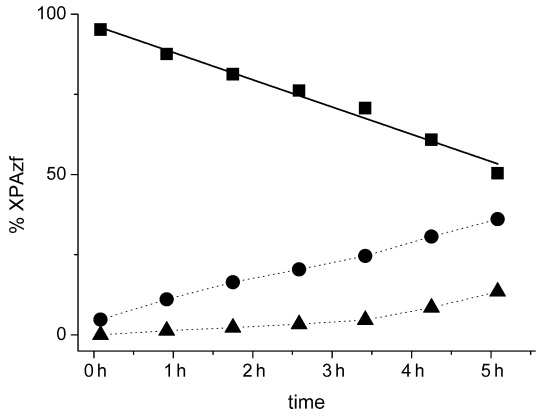

Fig. 2. Kinetics of oxidation of 10 μM ZnXPAzf by 100 μM H_2O_2, calculated by HPLC peak integration. ■, XPAzf; ●, XPAzf(–SS–); ▲, XPAzf(–SS–)$_2$. The solid line represents the linear fit of XPAzf decay.

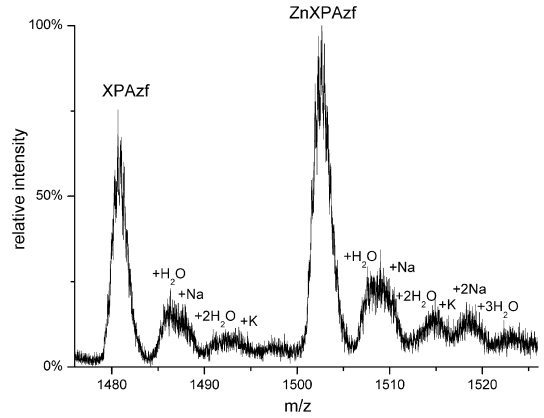

Fig. 4. Fragment of ESI mass spectrum of 10 μM ZnXPAzf incubated with 100 μM H_2O_2 for 117 min. Peaks correspond to 3^+ molecular ions.

decomposition of ZnXPAzf was linear, in agreement with MS and HPLC results. The extent of release of Zn(II) at the end of the experiment (340 min) was 37% (Fig. 3).

MS studies

ESI–MS experiments at a neutral pH value allowed the simultaneous detection of the ZnXPAzf complex and its oxidation products. The 3^+ and 4^+ ions were the only detectable forms of XPAzf and its derivatives and adducts. A typical MS spectrum demonstrating the presence of the ZnXPAzf is shown in Fig. 4. A number of noncovalent adducts were accompanying major peaks. They were identified on the basis of their masses to be formed by water molecules, sodium and potassium ions, as presented in Fig. 4. Their formation is a typical consequence of mild electrospray conditions. Major peaks assigned to XPAzf and ZnXPAzf had average masses of 4444.0 and 4506.3, respectively, agreeing with the corresponding theoretical values of 4442.96 and 4506.35. The mass-based assignments of peaks were supported by theoretical isotopic distributions, characteristic of the appropriate elemental compositions of the peptides. Each isotopic cluster corresponding to an identified species was integrated separately. Then the integrals for those 3^+ and 4^+ ions that corresponded to the same species, including its identified adducts, were summed. Finally, integrals for individual species were expressed as fractions of the total separately for each time point. The overlapping isotopic peaks for apo-XPAzf and its disulfide derivatives were deconvoluted prior to integration using theoretical isotopic distributions distinct for these three forms. The relative error of this procedure can be estimated at 20%. Fig. 5 presents the time-

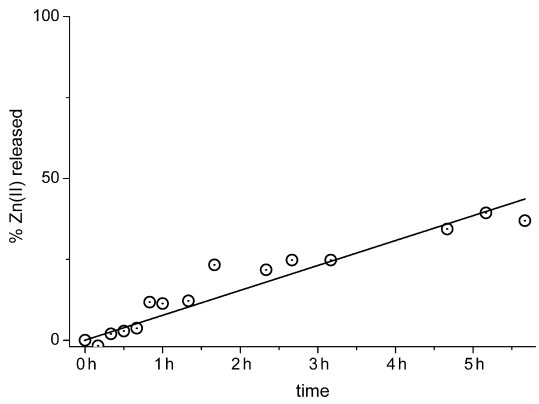

Fig. 3. Kinetics of release of Zn(II) from 10 μM ZnXPAzf to Zn(PAR)$_2$ by 100 μM H_2O_2 (○). The line represents the linear fit of Zn(PAR)$_2$ formation.

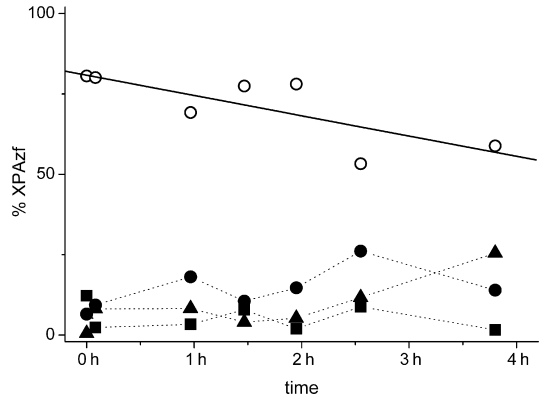

Fig. 5. Time course of oxidation of 10 μM ZnXPAzf by 100 μM H_2O_2, calculated by integration of ESI–MS peaks. ○, ZnXPAzf; ■, XPAzf; ●, XPAzf(–SS–); ▲, XPAzf(–SS–)$_2$. The solid line represents the linear fit of ZnXPAzf decay.

dependent changes in fractional contents of individual XPAzf species.

The mass spectra of samples containing 10 μM XPAzf and 10 μM Zn(II), recorded as controls prior to the addition of the oxidant (time point 0), reproducibly contained approximately 97% of the ZnXPAzf complex accompanied by approximately 3% of XPAzf apopeptide and traces of its disulfides.

Discussion

ESI–MS data are not inherently quantitative because of a complicated character of ESI processes, but all species compared in this analysis are derivatives of the same 37-amino-acid peptide, which might have similar ionization properties. Moreover, the content of individual species in consecutive spectra might be useful for studying the reaction kinetics. The comparison of kinetic data obtained by MS and other methodologies is crucial for the confirmation of suitability of the quantitative MS-based approach for kinetic studies. Table 1 gathers linear reaction velocities for ZnXPAzf oxidation by H_2O_2. We used two traditional experimental methods as well as noncovalent ESI–MS. These methods were specific for various aspects of the oxidation process. HPLC served to monitor the formation of disulfide species, PAR assay reported the loss of Zn(II) binding abilities, and ESI–MS provided direct detection of individual reaction substrates and products, particularly the starting ZnXPAzf complex. All three approaches yielded rates that were identical within their experimental errors. The higher relative error of the MS result was due to a lower accuracy of peak integration in this method, as seen in the spread of data points in Fig. 5. The applicability of ESI–MS for quantitative research in metalloproteins was demonstrated previously in binding constant determination [21,22], but this is the first time that ESI–MS has been shown to be equivalent to standard techniques in quantitation of the ZF reaction kinetics. At the same time, ESI–MS carries more information than do other techniques because the fate of reaction partners can be followed in their native states and artifacts resulting from specific aspects of indirect methods are avoided. In addition, only ESI–MS could demonstrate that the formation of a single disulfide was both required and sufficient to release zinc by the absence of metallated disulfides in the spectra.

Table 1
Rates calculated for oxidation of ZnXPAzf studied by various methods

Oxidant:	100 μM H_2O_2	
	Rate × 10^{10} (M s^{-1})	R^2
Method		
HPLC: decay of XPAzf	2.3 ± 0.1	0.98
Spectrophotometry: formation of $Zn(PAR)_2$ complex	2.1 ± 0.1	0.91
ESI–MS: decay of ZnXPAzf	1.8 ± 0.4	0.60

The use of ESI–MS combined with chemical derivatization allowed us to confirm the formation of a single intramolecular disulfide between Cys5 and Cys8 in XPAzf as the initial reaction product. ESI–MS results also indicate that the formation of this product is primarily responsible and sufficient for zinc release. No Zn(II)-containing disulfides were seen in ESI–MS spectra. The XPAzf monodisulfide was further oxidized to the final product containing two disulfide bridges. HPLC demonstrated that several minor peaks accompanied the major double disulfide product, suggesting a partial disulfide rearrangement (Fig. 1). However, the major peak contained Cys5–Cys8 and Cys26–Cys29 bridges, as demonstrated by MS/MS-based peptide sequencing. Direct injection MS experiments demonstrated that XPAzf oxidation by H_2O_2 was limited to disulfide formation; no evidence for oxidation of other residues was found. Similar sequence-specific preferences in the formation of disulfide bridges were also observed previously in the oxidation of the Cys3–His-type ZF domains of NCp7 viral protein by 3-nitrosobenzamide or Cu(II) [23] as well as in the oxidation of the Cys4-type ZF motifs in the estrogen receptor DNA binding domain by diamide or H_2O_2 [24].

Conclusion

The quantitative agreement of rates yielded by HPLC, zinc release assay, and ESI–MS yields two important conclusions. The general conclusion of our study, based on the agreement of reaction rates presented in Table 1, is that ESI–MS can be applied as a quantitative tool to study kinetics of ZF oxidation. With respect to the reaction mechanism, ESI–MS demonstrated the absence of Zn(II)-containing disulfides. This information, unique for ESI–MS, indicates that the formation of the single disulfide species is responsible for zinc release. Therefore, at least three thiolate ligands are required to complex the Zn(II) ion with XPAzf. Recent studies have demonstrated that a mixture of three- and four-thiolate coordination modes is present in Cys4 ZF [25, 26]. Therefore, such ZF can be particularly susceptible even to one-electron oxidation.

Acknowledgments

This work was sponsored in part by the Polish Ministry of Science (grant 3 T09A 009 26) and by the Estonian Science Foundation (grant 7191). J.S. acknowledges two Marie Curie fellowships at the Institute of Biochemistry and Biophysics, Polish Academy of Sciences (contract HPMT-CT-2001-00276).

Appendix A. Supplementary data

Supplementary data associated with this article can be found, in the online version, at doi:10.1016/j.ab.2007.05.019.

References

[1] W. Maret, Cellular zinc and redox states converge in the metallothionein/thionein pair, J. Nutr. 133 (2003) 1460S–1462S.

[2] J.P. Mackay, M. Crossley, Zinc fingers are sticking together, Trends Biochem. Sci. 23 (1998) 1–4.

[3] J.H. Laity, B.M. Lee, P.E. Wright, Zinc finger proteins: New insights into structural and functional diversity, Curr. Opin. Struct. Biol. 11 (2001) 39–46.

[4] A. Witkiewicz-Kucharczyk, W. Bal, Damage of zinc fingers in DNA repair proteins, a novel molecular mechanism in carcinogenesis, Toxicol. Lett. 162 (2006) 29–42.

[5] W. Maret, Zinc and sulfur: A critical biological partnership, Biochemistry 43 (2004) 3301–3309.

[6] D.E. Wilcox, A.D. Schenk, B.M. Feldman, Y. Xu, Oxidation of zinc-binding cysteine residues in transcription factor proteins, Antioxid. Redox Signal. 3 (2001) 549–564.

[7] K. Tanaka, N. Miura, I. Satokata, I. Miyamoto, M.C. Yoshida, Y. Satoh, S. Kondo, A. Yasui, H. Okayama, Y. Okada, Analysis of a human DNA excision repair gene involved in group A xeroderma pigmentosum and containing a zinc-finger domain, Nature 348 (1990) 73–76.

[8] J.E. Cleaver, J.C. States, The DNA damage-recognition problem in human and other eukaryotic cells: The XPA damage binding protein, Biochem. J. 328 (1997) 1–12.

[9] M. Asmuss, L.H. Mullenders, A. Hartwig, Interference by toxic metal compounds with isolated zinc finger DNA repair protein, Toxicol. Lett. 112/113 (2000) 227–231.

[10] M. Asmuss, L.H. Mullenders, A. Eker, A. Hartwig, Differential effects of toxic metal compounds on the activities of fpg and XPA, two zinc-finger proteins involved in DNA repair, Carcinogenesis 21 (2000) 2097–2104.

[11] G.W. Buchko, S. Ni, B.D. Thrall, M.A. Kennedy, Structural features of the minimal DNA binding domain (M98–F219) of human nucleotide excision repair protein XPA, Nucleic Acids Res. 26 (1998) 2779–2788.

[12] G.W. Buchko, L.M. Iakoucheva, M.A. Kennedy, E.J. Ackerman, N.J. Hess, Extended X-ray absorption fine structure evidence for a single metal binding domain in *Xenopus laevis* nucleotide excision repair protein XPA, Biochem. Biophys. Res. Commun. 254 (1999) 109–113.

[13] W. Bal, T. Schwerdtle, A. Hartwig, Mechanism of nickel assault on the zinc finger of DNA repair protein XPA, Chem. Res. Toxicol. 16 (2003) 242–248.

[14] E. Kopera, T. Schwerdtle, A. Hartwig, W. Bal, Co(II) and Cd(II) substitute for Zn(II) in the zinc finger derived from the DNA repair protein XPA, demonstrating a variety of potential mechanisms of toxicity, Chem. Res. Toxicol. 17 (2004) 1452–1458.

[15] H. Blessing, S. Krauss, P. Heindl, W. Bal, A. Hartwig, Interaction of selenium compounds with zinc finger proteins involved in DNA repair, Eur. J. Biochem. 271 (2004) 3190–3199.

[16] S. Immenschuh, E. Baumgart-Vogt, Peroxiredoxins, oxidative stress, and cell proliferation, Antioxid. Redox. Signal. 7 (2005) 768–777.

[17] H. Nohl, L. Gille, K. Staniek, Intracellular generation of reactive oxygen species by mitochondria, Biochem. Pharmacol. 69 (2005) 719–723.

[18] C. Le Goffe, G. Vallette, L. Charrier, T. Candelon, C. Bou-Hanna, J-F. Bouhours, C-L. Laboisse, Metabolic control of resistance of human epithelial cells to H_2O_2 and NO stresses, Biochem. J. 364 (2002) 349–359.

[19] K.A. McCall, C.A. Fierke, Colorimetric and fluorimetric assays to quantitate micromolar concentrations of transition metals, Anal. Biochem. 284 (2000) 307–315.

[20] J.E. Meza, G.K. Scott, C.C. Benz, M.A. Baldwin, Essential cysteine-alkylation strategies to monitor structurally altered estrogen receptor as found in oxidant-stressed breast cancers, Anal. Biochem. 320 (2003) 21–31.

[21] P. Palumaa, L. Kangur, A. Voronova, R. Sillard, Metal-binding mechanism of Cox17, a copper chaperone for cytochrome *c* oxidase, Biochem. J. 382 (2004) 307–314.

[22] L. Banci, I. Bertini, S. Ciofi-Baffoni, I. Leontari, M. Martinelli, P. Palumaa, R. Sillard, S.L. Wang, Human Sco1 functional studies and pathological implications of the P174L mutant, Proc. Natl. Acad. Sci. USA 104 (2007) 15–20.

[23] X. Yu, Y. Hathout, C. Fenselau, R.C. Sowder II, L.E. Henderson, W.G. Rice, J. Mendeleyev, E. Kun, Specific disulfide formation in the oxidation of HIV-1 zinc finger protein nucleocapsid p7, Chem. Res. Toxicol. 8 (1995) 586–590.

[24] R.M. Whittal, C.C. Benz, G. Scott, J. Semyonov, A.L. Burlingame, M.A. Baldwin, Preferential oxidation of zinc finger 2 in estrogen receptor DNA-binding domain prevents dimerization and, hence, DNA binding, Biochemistry 39 (2000) 8406–8417.

[25] U. Heinz, M. Kiefer, A. Tholey, H-W. Adolph, On the competition for available zinc, J. Biol. Chem. 280 (2005) 3197–3207.

[26] A.R. Reddi, B.R. Gibney, Role of protons in the thermodynamic contribution of a Zn(II)–Cys4 site toward metalloprotein stability, Biochemistry 46 (2007) 3745–3758.

PUBLICATION II

Smirnova, J., Zhukova, L., Witkiewicz-Kucharczyk, A., Kopera, E., Oledzki, J., Wyslouch-Cieszynska, A., Palumaa, P., Hartwig, A., Bal, W.
"Reaction of the XPA zinc finger with S-nitrosoglutathione" (2008)
Chem Res Toxicol.; 21(2):386-92

Reaction of the XPA Zinc Finger with *S*-Nitrosoglutathione

Julia Smirnova,[†] Liliya Zhukova,[‡] Aleksandra Witkiewicz-Kucharczyk,[‡] Edyta Kopera,[‡] Jacek Olędzki,[‡] Aleksandra Wysłouch-Cieszyńska,[‡] Peep Palumaa,[†] Andrea Hartwig,[§] and Wojciech Bal*[,‡,||]

Department of Gene Technology, Tallinn Technical University, Akadeemia tee 15, 12618 Tallinn, Estonia, Institute of Biochemistry and Biophysics, Polish Academy of Sciences, Pawińskiego 5a, 02-106 Warsaw, Poland, Institute of Food Technology and Food Chemistry, Technical University Berlin, Gustav-Meyer-Allee 25, D-13355 Berlin, Germany, and Central Institute for Labour Protection−National Research Institute, Czerniakowska 16, 00-701 Warsaw, Poland

Received August 20, 2007

S-Nitrosoglutathione (GSNO) is an intracellular redox signaling molecule, also implicated in nitrosative stress. GSNO actions include modifications of Cys thiols in proteins. In this study, we focused on a GSNO reaction with a Cys_4 zinc finger (ZF) sequence of human protein XPA, crucial to the nucleotide excision repair pathway of DNA repair. By using a corresponding synthetic 37-residue peptide acetyl-DYVICEECGKEFMDSYLMNHFDLPTCDNCRDADDKHK-amide (XPAzf) and combining the detection of noncovalent and covalent complexes by ESI-MS with zinc release monitored by the zinc-sensitive chromophore 4-(2-pyridylazo)resorcinol (PAR), we demonstrated that the reaction of XPAzf with GSNO yielded S-nitrosylated intermediates, intrapeptide disulfides, and mixed glutathione disulfides. The reaction started with the formation of a complex of GSNO with ZnXPAzf followed by thiol transnitrosylation reactions and the final formation of disulfides. The results obtained suggest that at low levels/transient exposures, GSNO may act as a reversible regulator of Cys_4 ZF activity, whereas transnitrosylation by GSNO, occurring at prolonged exposures, may cause deleterious effects to the functions of Cys_4 ZF proteins. In the case of XPA, this may lead to DNA repair inhibition.

Introduction

Zinc finger (ZF)[1] domains comprise one of the most abundant families of protein motifs in the eukaryotic genome, with multiple cellular functions. At least 3% of identified human proteins contain one or more ZF domains (*1*). Functions of ZF proteins include the binding and recognition of nucleic acids and the formation of multiprotein complexes (*2, 3*). The Zn(II) ion is bonded to the ZF sequence in a tetrahedral geometry, assured by the involvement of at least two cysteine thiolates in the binding. The remaining two ligands are two Cys, one Cys and one His, or two His residues.

The Zn(II) ion is not directly involved in interactions conveyed by a ZF, but it ensures the proper folding of the domain, and its release leads to a loss of the ZF function. It is suggested that many ZF proteins are regulated by reversible or irreversible oxidation of zinc-binding cysteine thiols (*4*−*6*). One may speculatively consider reversible oxidation to contribute to intracellular redox-dependent signaling systems, while irreversible oxidations leading to zinc release could contribute to toxic effects.

S-Nitrosothiols (RSNOs) are a prominent group of endogenous thiol modifying biomolecules. They were demonstrated to cause reversible site-specific protein thiol modifications, such as transnitrosylation, glutathionylation, and sulfinic acid formation, which provide a basis for intracellular NO-dependent signaling system (*7–9*). *S*-Nitrosoglutathione (GSNO), the most abundant intracellular RSNO (*10–12*), is regarded as the major intracellular NO carrier. It is formed spontaneously from GSH, the most abundant intracellular thiol, which readily accepts the NO group in the process of transnitrosylation (*13*). The importance of GSNO is further highlighted by the fact that there exists a dedicated enzyme, GSNO reductase, which controls its intracellular level (*14, 15*). Protein disulfide isomerase and Cu,Zn-superoxide dismutase are other ubiquitous enzymes implicated in the intracellular GSNO level control (*16–19*). In addition to intracellular roles, GSNO has recently been reported to also possess important extracellular tissue-specific regulatory functions (*20, 21*).

High levels of GSNO are implicated in irreversible effects of nitrosative stress (*9*); however, the border between signaling and stress-related levels of GSNO is not clear. The capacity of various cell types to accept high levels of GSNO without an overt cytotoxicity seems to depend strongly on cellular contexts such as their thiol levels. For example, GSNO in viable cultured NIH/3T3 fibroblasts could reach a 0.6 mM level in the presence of 1 mM GSH (*22*). The total levels of RSNO (largely GSNO,

* To whom correspondence should be addressed. Tel: +48-22-5922353. Fax: +48-22-6584636. E-mail: wbal@ibb.waw.pl.
[†] Tallinn Technical University.
[‡] Polish Academy of Sciences.
[§] Technical University Berlin.
[||] Central Institute for Labour Protection−National Research Institute.

[1] Abbreviations: GSNO, *S*-nitrosoglutathione; PAR, 4-(2-pyridylazo)resorcinol monosodium salt; XPAzf, acetyl-DYVICEECGKEFMDSYLMNHFDLPTCDNCRDADDKHK-amide peptide; XPAzf(NO), single *S*-nitrosylated XPAzf; $XPAzf(NO)_2$, double *S*-nitrosylated XPAzf; $XPAzf(SG)_2$, doubly *S*-glutathionylated XPAzf; XPAzf(NO)(SG), *S*-nitrosylated and *S*-glutathionylated XPAzf; XPAzf(−SS−), XPAzf intrapeptide single disulfide; $XPAzf(-SS-)_2$, XPAzf intrapeptide double disulfide; $XPAzf(-SS-)(NO)_2$, doubly *S*-nitrosylated XPAzf intrapeptide single disulfide; XPAzf(−SS−)(NO)(SG), *S*-nitrosylated and *S*-glutathionylated XPAzf intrapeptide single disulfide; XPAzf(−SS−)(SG), *S*-glutathionylated XPAzf intrapeptide single disulfide; $XPAzf(-SS-)(SG)_2$, doubly *S*-glutathionylated XPAzf intrapeptide single disulfide; ZF, zinc finger; ZnXPAzf, Zn(II) complex of XPAzf; ZnXPAzf[GSNO], *S*-nitrosoglutathione complex of ZnXPAzf; ZnXPAzf(NO), ZnXPAzf(NO)[GSH], glutathione complex of *S*-nitrosylated ZnXPAzf.

10.1021/tx700297f CCC: $40.75
Published on Web 01/03/2008

also *S*-nitrosylated proteins) in cultured RAW 264.7 cells were varied without affecting their viability by nearly 3 orders of magnitude, from ca. 6 μM up to 1.5 mM, depending on the availability of RSNO transport components in the medium (*23, 24*). Submillimolar RSNO levels were also induced in neuronal cells by nonthiol NO donors (*25, 26*). On the other hand, the lowering of GSNO from 6 to 3 μM resulted in significant adverse physiological effects in neuronal cell lines (*18*).

It is conceivable that GSNO also exerts its cellular effects via interactions with ZF transcription factors. It has been demonstrated that in a cellular system GSNO can regulate the activity of ZF transcription factors Sp3 and Sp1 (*27*); however, the molecular background of these interactions, which might have serious implications for cellular physiology, is currently unknown.

XPA is a member of nucleotide excision repair (NER) complex, participating in the recognition of DNA damage induced by many environmental mutagens (*28*). A loss of XPA function leads to xeroderma pigmentosum type A, a severe human disorder characterized by UV hypersensitivity and enhanced cancer risk (*29*). The XPA activity is inhibited by several metal ions, including carcinogenic Ni(II), Cd(II), and Co(II) (*30, 31*). These results provided strong evidence that DNA repair inhibition might be a major route in metal carcinogenesis. XPA is composed of 273 amino acid residues and contains a single Cys_4 ZF domain, which participates in the multiprotein NER complex formation. The solution structure of this domain was determined by NMR and EXAFS (*32, 33*). In previous studies, we demonstrated that the synthetic 37 residue peptide representing the XPA ZF sequence 101–137 (acetyl-DYVICEECGKEFMDSYLMNHFDLPTCDNCRDADDKHK-amide, XPAzf) and its Zn(II) complex (ZnXPAzf) are suitable and useful models to study molecular mechanisms of damage of XPA by metals and oxidants, which are relevant also for Cys_4 ZF domains in general (*34–38*). Recently, we successfully used ESI-MS to monitor the course of redox reactions of ZnXPAzf with hydrogen peroxide (*38*).

In the current work, we have used the same ZnXPAzf model and a similar methodology to study the reaction of Cys_4 ZF of XPA with GSNO. Our results, obtained by monitoring the zinc release in parallel with noncovalent ESI-MS, provide hints for a molecular mechanism for GSNO interaction with such ZF domains. The toxicological implications are discussed.

Materials and Methods

Materials. The N terminally acetylated and C terminally amidated 37 residue peptide XPAzf was custom-synthesized by Schafer-N Co. (Copenhagen, Denmark). The identity of this peptide was verified by ESI-MS, and its purity was assessed by HPLC to exceed 98%. GSH, 4-(2-pyridylazo)resorcinol monosodium salt (PAR), and ammonium acetate were purchased from Sigma-Aldrich Chemical Co.; sodium nitrite was obtained from POCH (Gliwice, Poland); acetonitrile was obtained from Laboratory-Scan Analytical Sciences (Dublin, Ireland); trifluoroacetic acid (TFA) and $ZnSO_4 \cdot 7H_2O$ were purchased from Merck KGaA (Darmstadt, Germany). GSNO was synthesized in the reaction of GSH with $NaNO_2$ in water in the dark under argon. The reaction mixtures were assayed by HPLC for completeness as described (*39*). For stability control, solutions containing 100 μM GSNO were incubated in a 10 mM ammonium acetate buffer, pH 7.4, for 24 h and measured periodically. Stock solutions of $ZnSO_4$ were calibrated spectrophotometrically with PAR, using the differential absorption coefficient at 500 nm of 46000 M^{-1} cm^{-1} (*40*).

Sample Preparation. Weighed solid samples of XPAzf were dissolved in a 10 mM ammonium acetate buffer, pH 7.4, previously saturated with argon, to prepare 100 μM stock solutions, which were immediately reconstituted with equimolar amounts of Zn(II) ions and filtered. The stocks of 10 mM GSNO were prepared fresh before each experiment.

Zinc Release. The release of Zn(II) ions from the ZnXPAzf complex was followed spectrophotometrically, using a published procedure with PAR as a Zn(II) indicator, with slight modifications (*40*). This method was previously found to be suitable for studies of zinc release from ZnXPAzf (*36–38*). Reaction mixtures, containing 10 μM ZnXPAzf and 100 μM GSNO in a 10 mM ammonium acetate buffer, pH 7.4, were incubated at 25 °C for several hours. Aliquots were diluted 10-fold with the same buffer containing 50 μM PAR. Their absorption spectra were recorded immediately in 1 cm cuvettes at 25 °C on a Cary 3E spectrophotometer (Varian, Australia) in the wavelength range of 250−600 nm. Control experiments indicated that neither PAR nor its Zn(II) complex reacted with GSNO within the time scale of these experiments.

ESI-MS. Samples in a 10 mM ammonium acetate buffer, pH 7.4, were injected into a Q-Tof1 mass spectrometer (Micromass, Manchester, United Kingdom) at 4 μL/min, using a Hamilton syringe pump. The spectrometer parameters were as follows: cone voltage, 35 V; source block temperature, 80 °C; and analyzer vacuum pressure, 5.8 nB. The time span of one scan was 5 s, and typically, 30–50 scans were accumulated. For *S*-nitrosylated peptides, the typical cone voltage of 35 V at the mass spectrometer source was either reduced (20 V) or increased (80 V) to ensure the stability or to induce the dissociation of S−NO bonds, respectively. Bovine pancreatic trypsin inhibitor was used as an internal mass standard. Positive ion spectra were deconvoluted using the MaxEnt module of MassLynx suite from Micromass.

Results

Stability of GSNO and Specificity of Its Reactivity toward XPAzf. Our previous work demonstrated that millimolar solutions of GSNO in HEPES buffer are relatively stable, contrary to a much lower stability reported for phosphate buffers (*41*). All experiments performed in this work were conducted in 10 mM ammonium acetate, because this volatile buffer permits detection of noncovalent complexes in ESI-MS at physiological pH. To check the stability of GSNO in this buffer, a 100 μM solution thereof was incubated at 25 °C, and its absorption at 334 nm, characteristic for the −SNO moiety, was recorded periodically. No significant changes were observed during the initial 10 h of incubation. A partial decomposition of the −SNO moiety (about 20%) was observed after 24 h. Therefore, the time span of further experiments was limited to less than 10 h, typically 5–6 h.

To provide a general view of the reactivity of GSNO against ZnXPAzf, the UV–vis spectra of samples containing 10 μM ZnXPAzf and 100 μM GSNO were recorded for 3 h in 20 min intervals. The changes in the spectra were confined to regions of 330–340 and 515–545 nm, which are regions characteristic for the −SNO moiety (*41, 42*).

Zn(II) Release from ZnXPAzf Monitored by ESI-MS. The kinetic experiment was conducted by direct injections of reaction mixtures into the mass spectrometer, under conditions that allowed for the detection of noncovalent species. Preliminary experiments demonstrated that nitrosothiols were stable at such conditions. Examples of MS spectra are shown in Figure 1, which demonstrates that the 3^+ and 4^+ ions were the only detectable forms of XPAzf, its covalent derivatives, and noncovalent adducts, including those with Na^+ and NH_4^+ ions. In the presence of 100 μM GSNO, the signal-to-noise ratios were much lower from those obtained without GSNO. Table 1 presents all identified XPAzf species. Their mass-based assignments were supported by theoretical isotopic distributions,

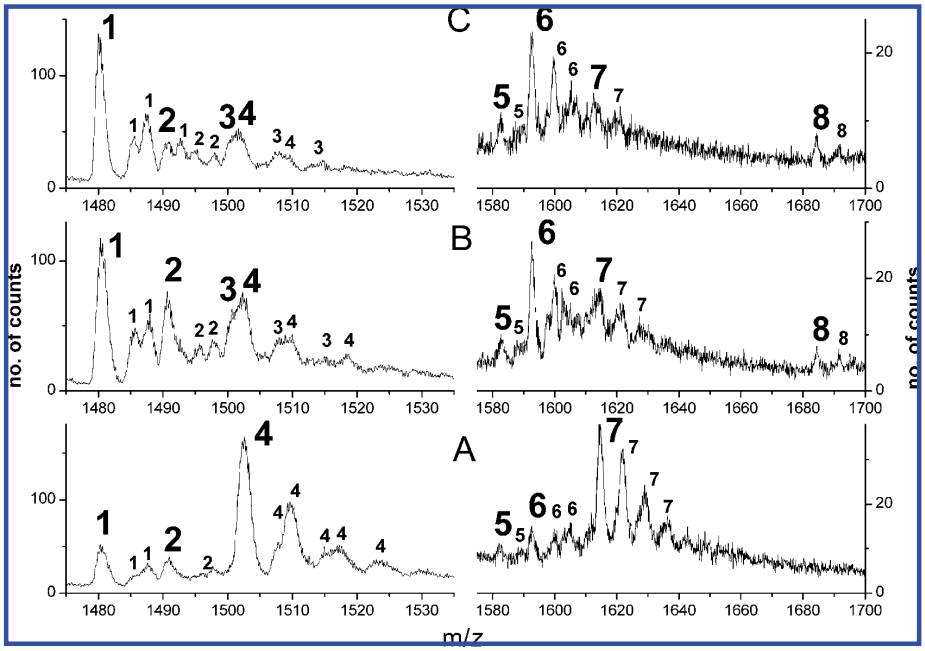

Figure 1. The 3+ region of ESI mass spectra of 10 μM ZnXPAzf incubated with 100 μM GSNO for 18 (A), 131 (B), and 312 (C) min. Peak labels correspond to those in Table 1, except for the (′) and (″) labels, which were omitted for clarity: 1, XPAzf, XPAzf(−SS−), XPAzf(−SS−)$_2$; 2, XPAzf(NO) + XPAzf(−SS−)(NO); 3, XPAzf(NO)$_2$ + XPAzf(−SS−)(NO)$_2$; 4, ZnXPAzf; 5, XPAzf(−SS−)(SG); 6, XPAzf(NO)(SG) + XPAzf(−SS−)(NO)(SG); 7, ZnXPAzf[GSNO] + ZnXPAzf(NO)[GSH]; and 8, XPAzf(SG)$_2$ + XPAzf(−SS−)(SG)$_2$. Smaller numbers denote secondary adducts with H_2O, NH_4^+, Na^+, and K^+ ions.

Table 1. Principal Peaks of XPAzf and Its Derivatives Identified in ESI-MS Spectra[a]

peak no.[b]	assignment	MW theoretical average	MW experimental[c]
1 + 1′ + 1″	XPAzf[d]	4442.96	4444.0 ± 0.3
2 + 2′	XPAzf(NO)[e]	4471.96	4471.3 ± 0.5
3 + 3′	XPAzf(NO)$_2$[e]	4500.96	4500.5 ± 0.5
4	ZnXPAzf	4506.35	4506.3 ± 0.8
5	XPAzf(−SS−)(SG)	4747.27	4746.4 ± 1.1
6 + 6′	XPAzf(SG)(NO)[e]	4777.27	4777.1 ± 0.3
7	ZnXPAzf[GSNO]/ZnXPAzf(NO)[GSH][f]	4842.66	4842.1 ± 0.5
8 + 8′	XPAzf(SG)$_2$[e]	5053.59	5053.0 ± 1.5

[a] These peaks were uniformly assisted by secondary adducts with H_2O, NH_4^+, Na^+, and K^+ ions. [b] Single and double intrapeptide XPAzf disulfides of respective species are marked with (′) and (″), respectively; their contributions increased with time. [c] Masses were calculated from positions of highest peaks of multiplets of isotopic peaks and averaged over time and over 3+ and 4+ molecular ions. [d] Contributions from intrapeptide XPAzf disulfides were quantified by deconvolution. [e] Contributions from intrapeptide XPAzf disulfides could not be quantified due to weak signals. [f] Species indistinguishable by MS.

characteristic for the appropriate elemental compositions of the peptides. Each isotopic cluster corresponding to an identified species was integrated separately. Then, the integrals for those 3^+ and 4^+ ions, which corresponded to the same species, including its NH_4^+ and Na^+ adducts, were summed up. Finally, integrals for individual species were expressed as fractions of the total, separately for each time point. The overlapping isotopic peaks for apo-XPAzf and its disulfide derivatives were deconvoluted prior to integration using theoretical isotopic distributions, distinct for these three forms (*38*). Figure 2 presents the time-dependent changes in fractional contents of individual XPAzf species detected by ESI-MS. Mass spectrometry data are not inherently quantitative, because of the complicated character of electrospray ionization processes. However, all species compared in this analysis are thiol derivatives of the same 37 aa-peptide, which could be expected to have similar ionization properties. Also, an excellent agreement between the values of rate constants of ZnXPAzf decay by H_2O_2, demonstrated in our recent study (*38*), provided a confirmation for the suitability of the quantitative MS-based approach for kinetic studies.

The mass spectra of samples containing 10 μM XPAzf and 10 μM Zn(II), recorded as controls prior to the addition of oxidants (time point 0), reproducibly contained at least 97% of the ZnXPAzf complex, accompanied by less than 3% of XPAzf apopeptide and traces of its disulfides. The spectra of the control sample of ZnXPAzf recorded at 0, 3, and 6 h of incubation indicated the absence of oxidation of the peptide by air.

A 10-fold molar excess of GSNO was not sufficient to decompose ZnXPAzf completely. An apparent equilibrium was attained at ca. 25% of the starting ZnXPAzf concentration. Higher GSNO concentrations could not be used because they suppressed the ESI signal.

We have also observed the fate of the second reaction partner, GSNO. Figure 3 presents the 600–700 *m*/*z* part of the spectrum, where several peaks corresponding to glutathione derivatives

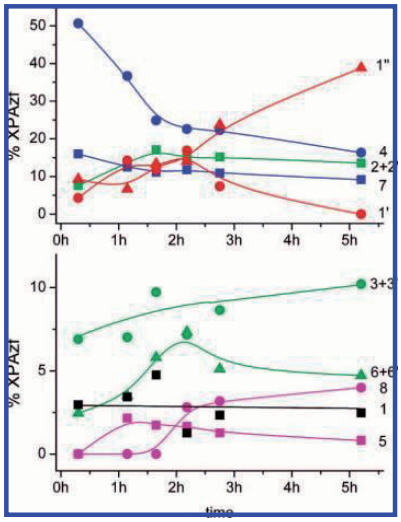

Figure 2. Time course of oxidation of 10 μM ZnXPAzf by 100 μM GSNO, calculated by integration of ESI-MS peaks. Top, major species; bottom, minor species. Color codes: blue, zinc holding species; green, *S*-nitrosylated species; red, intrapeptide disulfide species; magenta, glutathionylated species; and black, reduced apopeptide. Labels correspond to those in Table 1: 1, XPAzf; 1′, XPAzf(−SS−); 1″, XPAzf(−SS−)$_2$; 2 + 2′, XPAzf(NO) + XPAzf(−SS−)(NO); 3 + 3′, XPAzf(NO)$_2$ + XPAzf(−SS−)(NO)$_2$; 4, ZnXPAzf; 5, XPAzf(−SS−)(SG); 6 + 6′, XPAzf(NO)(SG) + XPAzf(−SS−)(NO)(SG); 7, ZnXPAzf[GSNO] + ZnXPAzf(NO)[GSH]; and 8 + 8′, XPAzf(SG)$_2$ + XPAzf(−SS−)(SG)$_2$.

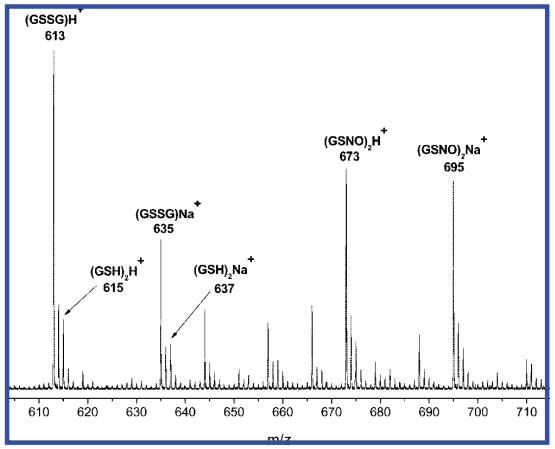

Figure 3. Low *m*/*z* region of ESI mass spectrum of 10 μM ZnXPAzf incubated with 100 μM GSNO for 69 min.

could be assigned. The most intense ones belong to monomeric $(GSSG)H^+$, dimeric $(GSNO)_2H^+$, and their Na^+ adducts. The signals of $(GSH)_2H^+$ and $(GSH)_2Na^+$ dimers were also detected among tail peaks of $(GSSG)H^+$ and $(GSSG)Na^+$, respectively, on a basis of theoretical isotopic distributions, and quantified. All of these peaks were detected previously in GSNO solutions (*43*). The formation of those noncovalent dimers is an electrospray artifact, and intensities of their signals are not necessarily proportional to solution concentrations. Nevertheless, these signals provide important semiquantitative information about the progress of reaction. Changes of their intensities in time are shown in Figure 4. The signal of $(GSNO)_2H^+$ decayed

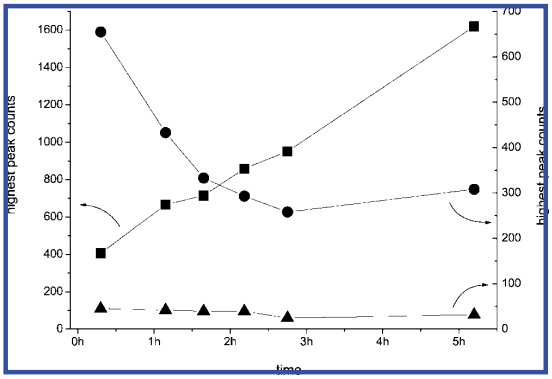

Figure 4. Time dependence of counts of low molecular mass peaks measured in the course of incubation of 10 μM ZnXPAzf by 100 μM GSNO: $(GSSG)H^+$, ■; $(GSNO)_2H^+$, ●; and $(GSH)_2H^+$, ▲.

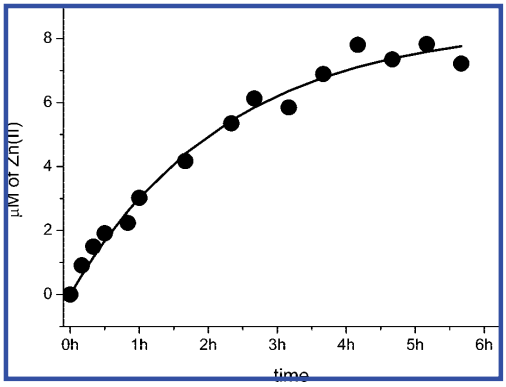

Figure 5. Time course of release of Zn(II) from 10 μM ZnXPAzf to $Zn(PAR)_2$ by 100 μM GSNO (●) and the fit of the data to an exponential function (−).

exponentially, similarly to the signal of ZnXPAzf, and a tentative equilibrium was reached at an apparent 40% of the initial GSNO level.

Zn(II) Release from ZnXPAzf Monitored by PAR. The release of Zn(II) ions from ZnXPAzf induced by GSNO was confirmed by spectrophotometry using PAR. The characteristic band of the $Zn(PAR)_2$ complex was monitored at 500 nm (*40*). No free Zn(II) ions were detected in ZnXPAzf samples prior to the addition of GSNO. The decomposition of ZnXPAzf by GSNO was incomplete also according to the PAR assay, which is in agreement with ESI-MS results. The extent of Zn(II) release at the end of the experiment (340 min) was 78% (Figure 5), and the maximum of Zn(II) release by GSNO at equilibrium, extrapolated from the experimental curve by an exponential function, was 84 ± 4%.

Discussion

General Features of Oxidation of ZnXPAzf by GSNO. Initially, the reaction of GSNO with ZnXPAzf proceeded relatively fast, as demonstrated by both the zinc release assay and ESI-MS. The initial linear reaction rate could be estimated as ca. $2 \pm 0.5 \times 10^{-9}$ M s^{-1} from both the PAR assay and ESI-MS; for the latter method, the extent of zinc release was quantified by integration of MS signals of zinc-binding species (peak 4, ZnXPAzf, + peak 7, ZnXPAzf[GSNO]). This rate is 10-fold higher from that measured previously for 100 μM H_2O_2

Table 2. Peaks Related to Glutathione Identified in the Low *m/z* Region of ESI-MS Spectra

assignment	MW theoretical	MW experimental
$(GSSG)H^+$	613.14	613.03
$(GSH)_2H^+$	615.16	615.03
$(GSSG)Na^+$	635.14	635.00
$(GSH)_2Na^+$	637.16	637.00
$(GSNO)_2H^+$	673.15	673.00
$(GSNO)_2Na^+$	695.14	694.98

as an oxidant (*38*). At longer incubation times, however, the GSNO reaction slowed down significantly. Approximations with an exponential (first-order kinetic) function of both the zinc release and the ESI-MS data suggested an equilibrium condition with respect to the starting ZnXPAzf complex, at a substoichiometric zinc release level of ca. 80%. The GSNO decay was also incomplete (Figure 4). In addition to internal disulfides, which are the most common products of ZF oxidations (*4*), also *S*-nitrosylated and *S*-glutathionylated derivatives of XPAzf were identified by ESI-MS (Table 2 and Figures 1 and 2). The primary process of XPAzf *S*-nitrosylation occurred largely within the first 2 h of incubation. At later times, when the decay of the ZnXPAzf complex slowed down, also *S*-nitrosylated products started to decay, accompanied by an accumulation of disulfide products, primarily $XPAzf(-SS-)_2$.

Complexation of GSNO to ZnXPAzf. The MS signal corresponding to the formula ZnXPAzf[GSNO] (peak 7) appeared immediately in MS spectra and was present at all time points studied. The intensity of its signal was proportional to that of ZnXPAzf (peak 4). The composition and stoichiometry of this species are consistent with the coordination of an intact GSNO molecule to XPAzf-bonded Zn(II). The tetrahedral Zn(II) ion in ZF has been considered to be coordinatively saturated. However, there is a -2 charge in the first coordination sphere of Zn(II) in Cys_4 ZF, which conceivably leads to a strong electrostatic repulsion between individual sulfur atoms and a weakening of Zn−S bonds. Indeed, the current literature showed two examples of Cys_4 ZF, which exhibited an equilibrium of 4S and 3S coordination modes: the LADH ZF peptide, studied by EXAFS (*44*), and a model hexadecapeptide, studied by a range of thermodynamic and spectroscopic techniques (*45*). These complementary reports strongly suggest that such equilibria are the common features of tetrathiolate ZFs. Therefore, GSNO can bind to the Zn(II) ion of the 3S coordination isomer of ZnXPAzf, using the amine and carboxylate groups of its Glu residue, as it does in binary Zn(II)−GSNO complexes (*41*). The apparent equilibrium constant of the corresponding reaction

$$\mathrm{ZnXPAzf} + \mathrm{GSNO} \overset{K}{\leftrightarrow} \mathrm{ZnXPAzf[GSNO]} \qquad (1)$$

could be tentatively estimated from the last three time points of the MS experiment at 131, 165, and 312 min, when other parallel and consecutive reactions had also nearly approached equilibrium. The concentration of GSNO for these calculations was assumed as 4 μM, and the value of $K = 1540 \pm 47\ M^{-1}$ was obtained ($\log K = 3.19 \pm 0.01$). This value is in striking agreement with the conditional stability constant for the $Zn(GSNO)^-$ complex at pH 7.4, 3.16 (recalculated from the $\log \beta$ value of 4.85 (*41*)), thus further supporting the above interpretation.

The quantitative coupling of ZnXPAzf and ZnXPAzf[GSNO] species suggests that the formation of the latter precedes *S*-nitrosylation of XPAzf. The coordination of GSNO to Zn(II) via the Glu residue, which is the only possible mode of interaction, makes the −SNO moiety of GSNO free to attack

Scheme 1. Reversible Steps of the Mechanism of Reaction of ZnXPAzf with GSNO[a]

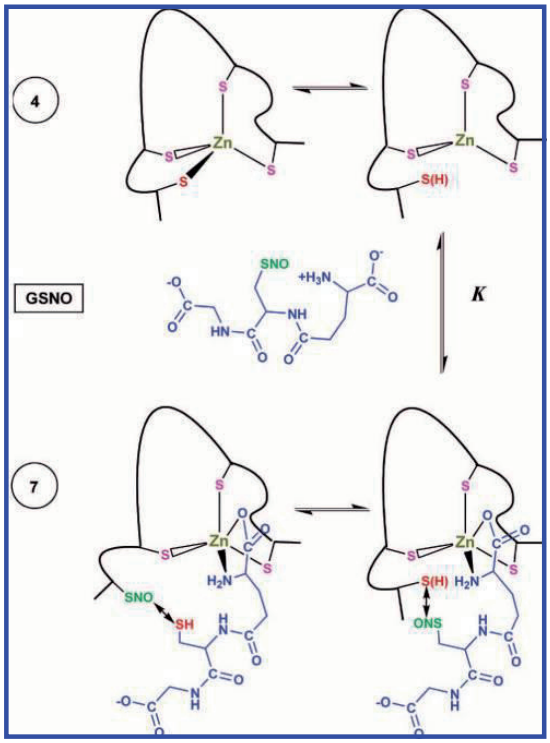

[a] Numbers in circles correspond to MS peak labels in Table 1 and Figure 5. The choice of the S-nitrosylation position is arbitrary.

the available thiolate in ZnXPAzf. Such transnitrosation reactions are reversible and yield GSH as the second product (*46–50*). This GSH molecule formed in situ is likely to remain complexed to ZnXPAzf(NO), forming a ZnXPAzf(NO)[GSH] species, indistinguishable from ZnXPAzf[GSNO] in ESI-MS. These reaction steps are presented in Scheme 1.

Zinc Release and Further Molecular Events. The nitrosylated products (peaks 2 + 2′, 3 + 3′, and 6 + 6′ in Table 1) were detected in ESI-MS spectra at all time points, while nonnitrosylated mixed glutathione disulfides (peaks 5 and 8 + 8′ in Table 1) were formed at longer incubation times. Therefore, disulfide formation follows rather than parallels transnitrosylation in the molecular mechanism of the reaction. The binding and initial transnitrosylation processes proposed in Scheme 1 would constitute the first phase of the overall reaction. This step is fast but, as argued above, reversible. Previously, we demonstrated that the oxidation of two thiolate donors is both required and sufficient for the release of the Zn(II) ion from ZnXPAzf (*38*). An attack of another GSNO molecule on the mononitrosylated species is therefore required for zinc release. The product of this process, $XPAzf(NO)_2$ (peak 3), is strongly susceptible to oxidation, yielding an internal disulfide (peak 3′). The mononitrosylated peptide, XPAzf(NO), and its disulfide (peak 2 + 2′), may result from NO elimination from $XPAzf(NO)_2$. The disulfide is a likely product of intrapeptide rearrangement, while the reduced species may be formed in a transnitrosation reaction with a GSH molecule. It may also be formed as a result of nonredox Zn(II) withdrawal from ZnXPAzf(NO)[GSH] by GSH, which is a relatively strong Zn(II) chelator (*51*). Sufficient amounts of GSH, evidenced

by ESI-MS, are formed in the autocatalytical process of GSNO decomposition (*19, 52*). The formation of nitrosylated XPAzf derivatives constitutes the second reaction phase, which occurs largely within the initial 2 h of incubation. The accumulation of nitrosylated species appears to be terminated upon the decrease of GSNO to the apparent 40% of its initial level. This indicates that the coordinative addition of a GSNO molecule to ZnXPAzf(NO) is the rate-determining step in the zinc release process, similarly to the formation of ZnXPAzf[GSNO].

Then, in the third phase of the reaction, −SNO groups in the peptide were converted into kinetically stable disulfides. Both intrapeptide and mixed disulphides with GSH were formed. These processes involve GSH and GSSG, which are the products of GSNO decomposition. A significant participation of another XPAzf molecule in the elimination of −SNO groups is unlikely, because no XPAzf dimers were observed.

Toxicological Implications of the Results. Intracellular GSNO levels, as mentioned in the Introduction section, can reach submicromolar as well as nearly millimolar concentrations, the latter being severalfold higher from those used in our experiments (*18, 22–26, 53*). Our experiments can be considered to represent intermediate GSNO levels, likely corresponding to mild nitrosative stress conditions. Similar GSNO exposures may occur locally as a result of therapeutic intervention, for example, GSNO supplementation in cystic fibrosis (*54*), although lower exposures, 5–10 μM, were demonstrated to be effective (*55*). Our results allow us to suggest that under such conditions Cys-rich ZF can be expected to be *S*-nitrosylated with the loss of Zn(II) ions and subsequently oxidized to intramolecular and mixed disulfides. However, our results indicate that at low, micromolar GSNO exposures, such ZF may be nitrosylated transiently and reversibly without zinc release, according to the mechanism proposed in Scheme 1. Such exposures seem to correspond to normal physiological conditions in many tissues. Our results clearly support the usage of lower, rather than higher, GSNO levels in therapeutic interventions whenever possible.

Also, the presence of thiols, mainly GSH, will control the ability of GSNO to transnitrosylate XPA and similar thiolate-rich ZF targets, so that the course of the reaction will effectively depend on a local GSH/GSNO ratio. While this principle is based on the fundamental chemistry of transnitrosylation (*42, 52*), it may be expected that ZF proteins in general, including transcription factors, nuclear receptors, and cell cycle guardians, can be reversibly regulated by GSH/GSNO. Further research is, however, necessary to understand the reactivity of different ZF toward GSNO more deeply. In particular, individual susceptibilities of various ZF domains to the GSNO signal may vary significantly, depending on both the type of Zn(II) environment and the whole protein context.

From the point of view of carcinogenesis, our results suggest that even mild nitrosative stress, induced by GSNO, may be deleterious to ZF proteins, including XPA. Therefore, more attention should be directed to the involvement of RNS in those mechanisms of carcinogenesis that include ZF proteins.

Acknowledgment. This work was sponsored in part by the Polish Ministry of Science, Grant No. 3 T09A 009 26, and by the Estonian Science Foundation, Grant No. 7191. J.S. acknowledges two Marie Curie fellowships at IBB PAS, Contract No. HPMT-CT-2001-00276.

References

(1) Maret, W. (2003) Cellular zinc and redox states converge in the metallothionein/thionein pair. *J. Nutr. 133*, 1460S–1462S.
(2) Mackay, J. P., and Crossley, M. (1998) Zinc fingers are sticking together. *Trends Biochem. Sci. 23*, 1–4.
(3) Laity, J. H., Lee, B. M., and Wright, P. E. (2001) Zinc finger proteins: New insights into structural and functional diversity. *Curr. Opin. Struct. Biol. 11*, 39–46.
(4) Witkiewicz-Kucharczyk, A., and Bal, W. (2006) Damage of zinc fingers in DNA repair proteins, a novel molecular mechanism in carcinogenesis. *Toxicol. Lett. 162*, 29–42.
(5) Maret, W. (2004) Zinc and sulfur: A critical biological partnership. *Biochemistry 43*, 3301–3309.
(6) Wilcox, D. E., Schenk, A. D., Feldman, B. M., and Xu, Y. (2001) Oxidation of zinc-binding cysteine residues in transcription factor proteins. *Antioxid. Redox Signaling 3*, 549–564.
(7) Stamler, J. S., Jia, L., Eu, J. P., McMahon, T. J., Demchenko, I. T., Bonaventura, J., Gernert, K., and Piantadosi, C. A. (1997) Blood flow regulation by S-nitrosohemoglobin in the physiological oxygen gradient. *Science 276*, 2034–2037.
(8) Stamler, J. S., and Hausladen, A. (1998) Oxidative modifications in nitrosative stress. *Nat. Struct. Biol. 5*, 247–249.
(9) Kim, S. O., Merchant, K., Nudelman, R., Beyer, W. F., Jr., Keng, T., Hausladen, A., and Stamler, J. S. (2002) OxyR: A molecular code for redox-related signaling. *Cell 109*, 383–396.
(10) Sandmann, J., Schwedhelm, K. S., and Tsikas, D. (2005) Specific transport of S-nitrosocysteine in human red blood cells: Implications for formation of S-nitrosothiols and transport of NO bioactivity within the vasculature. *FEBS Lett. 579*, 4119–4124.
(11) Hess, D. T., Matsumoto, A., Nudelman, R., and Stamler, J. S. (2001) S-nitrosylation: Spectrum and specifity. *Nat. Cell Biol. 3*, E1–E3.
(12) Jaffrey, S. R., Erdjument-Bromage, H., Ferris, C. D., Tempst, P., and Snyder, S. H. (2001) Protein S-nitrosylation: A physiological signal for neuronal nitric oxide. *Nat. Cell Biol. 3*, 193–197.
(13) Mayer, B., Pfeiffer, S., Schrammel, A., Koesling, D., Schmidt, K., and Brunner, F. (1998) A new pathway of nitric oxide/cyclic GMP signaling involving S-nitrosoglutathione. *J. Biol. Chem. 273*, 3264–3270.
(14) Jensen, D. E., Belka, G. K., Du, G., and Bois, C. (1998) *S*-nitrosoglutathione is a substrate for rat alcohol dehydrogenase class III isoenzyme. *Biochem. J. 331*, 659–668.
(15) Liu, L., Hausladen, A., Zeng, M., Que, L., Heitman, J., and Stamler, J. S. (2001) A metabolic enzyme for S-nitrosothiol conserved from bacteria to humans. *Nature 410*, 490–494.
(16) Sliskovic, I., Raturi, A., and Mutus, B. (2005) Characterization of the S-denitrosation activity of protein disulfide isomerase. *J. Biol. Chem. 280*, 8733–8741.
(17) Shah, C. M., Bell, S. E., Locke, I. C., Chowdrey, H. S., and Gordge, M. P. (2007) Interactions between cell surface protein disulphide isomerase and S-nitrosoglutathione during nitric oxide delivery. *Nitric Oxide 16*, 135–142.
(18) Schonhoff, C. M., Matsuoka, M., Tummala, H., Johnson, M. A., Estevéz, A. G., Wu, R., Kamaid, A., Ricart, K. C., Hashimoto, Y., Gaston, B., Macdonald, T. L., Xu, Z., and Mannick, J. B. (2006) S-nitrosothiol depletion in amyotrophic lateral sclerosis. *Proc. Natl. Acad. Sci. U.S.A. 103*, 2404–2409.
(19) Okado-Matsumoto, A., and Fridovich, I. (2007) Putative denitrosylase activity of Cu,Zn-superoxide dismutase. *Free Radical Biol. Med. 43*, 830–836.
(20) Joksovic, P. M., Doctor, A., Gaston, B., and Todorovic, S. M. (2007) Functional regulation of T-type calcium channels by S-nitrosothiols in the rat thalamus. *J. Neurophysiol. 97*, 2712–2721.
(21) Savidge, T. C., Newman, P., Pothoulakis, C., Ruhl, A., Neunlist, M., Bourreille, A., Hurst, R., and Sofroniew, M. V. (2007) Enteric glia regulate intestinal barrier function and inflammation via release of S-nitrosoglutathione. *Gastroenterology 132*, 1344–1358.
(22) Mallis, R. J., and Thomas, J. A. (2000) Effect of *S*-nitrosothiols on cellular glutathione and reactive protein sulfhydryls. *Arch. Biochem. Biophys. 383*, 60–69.
(23) Zhang, Y. H., and Hogg, N. (2004) The mechanism of transmembrane S-nitrosothiol transport. *Proc. Natl. Acad. Sci. U.S.A. 101*, 7891–7896.
(24) Zhang, Y. H., and Hogg, N. (2005) *S*-Nitrosothiols: cellular formation and transport. *Free Radical Biol. Med. 38*, 831–838.
(25) Solano, R. M., Menéndez, J., Casarejos, M. J., Rodriguez-Navarro, J. A., Garcia de Yébenes, J., and Mena, M. A. (2006) Midbrain neuronal cultures from parkin mutant mice are resistant to nitric oxide-induced toxicity. *Neuropharmacology 51*, 327–340.
(26) Baud, O., Li, J., Zhang, Y., Neve, R. L., Volpe, J. J., and Rosenberg, P. A. (2004) Nitric oxide-induced death in developing oligodendrocytes is associated with mitochondrial dysfunction and apoptosis-inducing factor translocation. *Eur. J. Neurosci. 20*, 1713–1726.
(27) Zaman, K., Palmer, M. A., Doctor, A., Hunt, J. F., and Gaston, B. (2004) Concentration-dependent effects of endogenous S-nitrosoglutathione on gene regulation by specificity proteins Sp3 and Sp1. *Biochem. J. 380*, 67–74.

(28) Tanaka, K., Miura, N., Satokata, I., Miyamoto, I., Yoshida, M. C., Satoh, Y., Kondo, S., Yasui, A., Okayama, H., and Okada, Y. (1990) Analysis of a human DNA excision repair gene involved in group A xeroderma pigmentosum and containing a zinc-finger domain. *Nature 348*, 73–76.

(29) Cleaver, J. E., and States, J. C. (1997) The DNA damage-recognition problem in human and other eukaryotic cells: The XPA damage binding protein. *Biochem. J. 328*, 1–12.

(30) Asmuss, M., Mullenders, L. H., and Hartwig, A. (2000) Interference by toxic metal compounds with isolated zinc finger DNA repair protein. *Toxicol. Lett. 112–113*, 227–231.

(31) Asmuss, M., Mullenders, L. H., Eker, A., and Hartwig, A. (2000) Differential effects of toxic metal compounds on the activities of fpg and XPA, two zinc-finger proteins involved in DNA repair. *Carcinogenesis 21*, 2097–2104.

(32) Buchko, G. W., Ni, S., Thrall, B. D., and Kennedy, M. A. (1998) Structural features of the minimal DNA binding domain (M98-F219) of human nucleotide excision repair protein XPA. *Nucleic Acids Res. 26*, 2779–2788.

(33) Buchko, G. W., Iakoucheva, L. M., Kennedy, M. A., Ackerman, E. J., and Hess, N. J. (1999) Extended X-ray absorption fine structure evidence for a single metal binding domain in *Xenopus laevis* nucleotide excision repair protein XPA. *Biochem. Biophys. Res. Commun. 254*, 109–113.

(34) Bal, W., Schwerdtle, T., and Hartwig, A. (2003) Mechanism of nickel assault on the zinc finger of DNA repair protein XPA. *Chem. Res. Toxicol. 16*, 242–248.

(35) Kopera, E., Schwerdtle, T., Hartwig, A., and Bal, W. (2004) Co(II) and Cd(II) substitute for Zn(II) in the zinc finger derived from the DNA repair protein XPA, demonstrating a variety of potential mechanisms of toxicity. *Chem. Res. Toxicol. 17*, 1452–1458.

(36) Blessing, H., Krauss, S., Heindl, P., Bal, W., and Hartwig, A. (2004) Interaction of selenium compounds with zinc finger proteins involved in DNA repair. *Eur. J. Biochem. 271*, 3190–3199.

(37) Schwerdtle, T., Walter, I., and Hartwig, A. (2003) Arsenite and its biomethylated metabolites interfere with the formation and repair of stable BPDE-induced DNA adducts in human cells and impair XPAzf and Fpg. *DNA Rep. (Amsterdam) 2*, 1449–1463.

(38) Smirnova, J., Zhukova, L., Witkiewicz-Kucharczyk, A., Kopera, E., Olędzki, J., Wysłouch-Cieszyńska, A., Palumaa, P., Hartwig, A., and Bal, W. (2007) Quantitative electrospray mass spectrometry of zinc finger oxidation: The reaction of XPA zinc finger with H_2O_2. *Anal. Biochem. 369*, 226–231.

(39) Zhukova, L., Zhukov, I., Bal, W., and Wysłouch-Cieszyńska, A. (2004) Redox modifications of the C-terminal cysteine residue cause structural changes in S100A1 and S100B proteins. *Biochem. Biophys. Acta 1742*, 191–201.

(40) McCall, K. A., and Fierke, C. A. (2000) Colorimetric and fluorimetric assays to quantitate micromolar concentrations of transition metals. *Anal. Biochem. 284*, 307–315.

(41) Krępel, A., and Bal, W. (2004) Contrasting effects of metal ions on S-nitrosoglutathione, related to coordination equilibria: GSNO decomposition assisted by Ni(II) versus stability increase in the presence of Zn(II) and Cd(II). *Chem. Res. Toxicol. 17*, 392–403.

(42) Stamler, J. S., and Toone, E. J. (2002) The decomposition of thionitrites. *Curr. Opin. Chem. Biol. 6*, 779–785.

(43) Tao, L., and English, A. M. (2004) Protein S-glutathionylation triggered by decomposed S-nitrosoglutathione. *Biochemistry 43*, 4028–4038.

(44) Heinz, U., Kiefer, M., Tholey, A., and Adolph, H.-W. (2005) On the competition for available zinc. *J. Biol. Chem. 280*, 3197–3207.

(45) Reddi, A. R., and Gibney, B. R. (2007) Role of protons in the thermodynamic contribution of a Zn(II)-Cys_4 site toward metalloprotein stability. *Biochemistry 46*, 3745–3758.

(46) Meyer, D. J., Kramer, H., Özerb, N., Coles, B., and Ketterer, B. (1994) Kinetics and equilibria of S-nitrosothiol-thiol exchange between glutathione, cysteine, penicillamines and serum albumin. *FEBS Lett. 345*, 177–180.

(47) Tsikas, D., Sandmann, J., Rossa, S., Gutzki, F.-M., and Frölich, J. C. (1999) Investigations of S-transnitrosylation reactions between low- and high-molecular-weight S-nitroso compounds and their thiols by high-performance liquid chromatography and gas chromatography-mass spectrometry. *Anal. Biochem. 270*, 231–241.

(48) Lee, J., Chen, L., West, A. H., and Richter-Addo, G. B. (2002) Interactions of organic nitroso compounds with metals. *Chem. Rev. 102*, 101Ø–1065.

(49) Barnett, D. J., McAninly, J., and Williams, D. L. H. (1994) Transnitrosation between nitrosothiols and thiols. *J. Chem. Soc., Perkin Trans. 2*, 1131–1133.

(50) Barnett, D. J., Rios, A., and Williams, D. L. H. (1995) NO-Group transfer (transnitrosation) between *S*-nitrosothiols and thiols. Part 2. *J. Chem. Soc., Perkin Trans. 2*, 1279–1282.

(51) Krępel, A., Wójcik, J., Maciejczyk, M., and Bal, W. (2003) May GSH and L-His contribute to intracellular binding of zinc? Thermodynamic and solution structural study of a ternary complex. *Chem. Commun.* 704–705.

(52) Singh, S. P., Wishnok, J. S., Keshive, M., Deen, W. M., and Tannenbaum, S. R. (1996) The chemistry of the *S*-nitrosoglutathione system. *Proc. Natl. Acad. Sci. U.S.A. 93*, 14428–14433.

(53) Marshall, H. E., Merchant, K., and Stamler, J. S. (2000) Nitrosation and oxidation in the regulation of gene expression. *FASEB J. 14*, 1889–1900.

(54) Servetnyk, Z., Krjukova, J., Gaston, B., Zaman, K., Hjelte, L., Roomans, G. M., and Dragomir, A. (2006) Activation of chloride transport in CF airway epithelial cell lines and primary CF nasal epithelial cells by S-nitrosoglutathione. *Respir. Res. 7*, 124.

(55) Zaman, K., Carraro, S., Doherty, J., Henderson, E. M., Lendermon, E., Liu, L., Verghese, G., Zigler, M., Ross, M., Park, E., Palmer, L. A., Doctor, A., Stamler, J. S., and Gaston, B. (2006) *S*-nitrosylating agents: A novel class of compounds that increase cystic fibrosis transmembrane conductance regulator expression and maturation in epithelial cells. *Mol. Pharmacol. 70*, 1435–1442.

TX700297F

PUBLICATION III

Smirnova, J., Muhhina, J., Tõugu, V., Palumaa, P.
"Redox and Metal Ion Binding Properties of Human Insulin-like Growth Factor 1 Determined by Electrospray Ionization Mass Spectrometry" (2012) Biochemistry; 51(29):5851-9

BIOCHEMISTRY
including biophysical chemistry & molecular biology

Article

pubs.acs.org/biochemistry

Redox and Metal Ion Binding Properties of Human Insulin-like Growth Factor 1 Determined by Electrospray Ionization Mass Spectrometry

Julia Smirnova, Jekaterina Muhhina, Vello Tõugu, and Peep Palumaa*

Department of Gene Technology, Tallinn University of Technology, Akadeemia tee 15, 12618 Tallinn, Estonia

ABSTRACT: Insulin-like growth factor 1 (IGF-1) is a 70-residue hormone containing three intramolecular disulfide bridges. IGF-1 and other growth factors are oxidatively folded in the endoplasmic reticulum and act primarily in the blood, under relatively oxidative conditions. It is known that IGF-1 exists in various intracellular and extracellular compartments in the oxidized form; however, the reduction potential of IGF-1 and the ability of fully reduced IGF-1, which contains six cysteine residues, to bind transition metal ions are not known. In this work, we determine that the redox potential of human IGF-1 is equal to −332 mV and the reduced form of hIGF-1 can bind cooperatively four Cu^+ ions, most probably into a tetracopper−hexathiolate cluster. The Cu^+ binding affinity of hIGF-1 is, however, approximately 3 times lower than that for the copper chaperones; thus, we can conclude that fully reduced hIGF-1 cannot compete with known Cu^+-binding proteins.

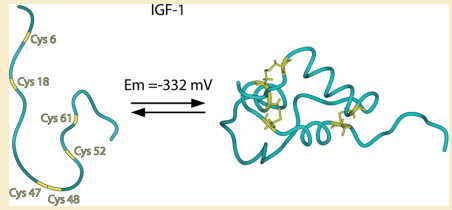

Insulin-like growth factor 1 (IGF-1), a 70-residue hormone (7649 Da) displaying a high degree of homology to insulin, consists of three intramolecular disulfide bridges.[1] Although small amounts of IGF-1 are synthesized in most peripheral tissues, it is mainly secreted by the liver. The secretion of IGF-1 is regulated by growth hormone (GH).[2] The major part of IGF-1 circulating in the bloodstream is in the complex with one of six IGF-binding proteins (insulin-like growth factor binding proteins 1−6 or IGFBP1−6),[3,4] and only a small amount of IGF-1, <1%, circulates in the free biologically active form that can bind to the IGF receptor.[5] All three native disulfide bridges in the IGF-1 molecule are crucial for this binding.[6]

Before it is released into the blood, IGF-1 is oxidatively folded in the endoplasmic reticulum (ER). Both these environments, blood and ER, are characterized by oxidative redox potentials. On the basis of the experimental determination of the GSH/GSSG ratio, the average redox potential in the ER is estimated to be equal to −189 mV.[7] The oxidative conditions in the ER guarantee the formation of structural disulfide bridges in the membrane and extracellular proteins during protein folding.[8] The redox potential values in the extracellular environments are also determined by thiol−disulfide equilibria. The main redox couple in this environment, Cys/CySS, plays a major role in the redox communication between cells and tissues.[9−12] The Cys/CySS buffering system keeps the mean plasma redox potential value at approximately −80 mV, whereas the mean plasma redox potential value, which is determined by the GSH/GSSG ratio, is approximately −140 mV.[13,14] Both values are substantially higher (more oxidizing) than the cytoplasmic redox potential values. The redox potential value of plasma becomes more oxidative during several diseases and aging, and these changes have been shown to affect the function of cell surface receptors, ion channels, and structural proteins.[13,15] It should be noted that the plasma Cys/CySS redox potential is not in equilibrium with the plasma GSH/GSSG pool.[16]

The disulfide bonds in the proteins can be classified as stable structural disulfide bridges with midpoint redox potentials reaching −470 mV[17] and as the more labile redox-active disulfides with corresponding midpoint redox potentials ranging from −95 to −330 mV.[18−21] The disulfide bonds in IGF-1 most probably belong to the structural ones; however, their reduction in the cellular cytosol cannot be ruled out. The highly reducing cellular redox potential with values as low as −289 mV[22] is maintained mainly by the redox couple of GSH and GSSG, with a total cellular concentration of 2−10 mM.[23] The cellular redox potential value is different in various organelles and fluctuates depending on the cell cycle and apoptotic processes, the presence of ROS and RNS, and the state of disease or aging.[14] The redox potential of the cytoplasm has been reported to be in the range from −193 mV for the red blood cells[24] to −220 mV for nondividing cells and −260 mV for proliferating cells.[14] The state of cellular thiols depends primarily on the environmental redox potential and the presence of ROS or RNS.

If IGF-1 becomes reduced, it can bind metal ions and, in particular, Cu^+ ions. It has been demonstrated that Cu^+ ions can bind to proteins containing six Cys residues with high affinity, forming tetracopper−hexathiolate clusters.[25−27] Fully reduced IGF-1 is a good model for such proteins, and the Cu^+

Received: April 17, 2012
Revised: June 29, 2012
Published: July 2, 2012

binding affinity of reduced IGF-1 allows the estimation of whether such proteins can compete with cellular Cu^+ proteins.

In this work, we applied a recently developed ESI-MS method[28] to IGF-1 and demonstrated that the disulfide bonds in this molecule are formed in a cooperative manner with a midpoint redox potential value equal to −332 mV. This value is sufficiently low in comparison with the redox potentials of the secretory pathway and extracellular environment for stabilizing hIGF-1 in its fully oxidized native fold that is required for IGFR binding. Fully reduced hIGF-1 binds four Cu^+ ions with very high cooperativity, suggesting the formation of a tetracopper−hexathiolate cluster. In principle, the interaction with metal ions can stabilize the reduced form of the peptide; however, the Cu^+ binding affinity of hIGF-1 is 3-fold weaker than that of the copper chaperone Cox17,[25] which has the lowest affinity for copper among the proteins forming the cellular copper proteome.[29] Thus, formation of the Cu^+−IGF-1 complex in the cellular environment is improbable.

MATERIALS AND METHODS

Chemicals. Human insulin-like growth factor 1 (hIGF-1) (ProSpec), DTT (Fluka), BME (Sigma), oxidized BME (Aldrich), Cu(II) acetate (Sigma), and ammonium acetate (Scharlau) were acquired. Oxidized DTT was synthesized from reduced DTT according to the protocol described in ref 30. Milli-Q quality water was used for the preparation of solutions.

Reduction of hIGF-1 with DTT. Fully oxidized human IGF-1_{3S-S} (2 μM) was incubated in argon-saturated 20 mM ammonium acetate (pH 7.5), containing 0.5, 1, and 5 mM DTT as a reducing agent. Separate reaction mixtures were incubated at 25 and 40 °C. For the measurement of kinetics of IGF-1_{3S-S} reduction, 50 μL aliquots from the reaction mixture were taken at various time points (1−120 min) and injected directly by a syringe pump at a rate of 10 μL/min into a QSTAR Elite ESI-Q-TOF mass spectrometer (Applied Biosystems, Foster City, CA). Mass spectra were recorded in the positive mode over 2−3 min in the region from 500 to 2000 Da. The following instrument parameters were used: ion spray voltage, 5500 V; source gas, 30 L/min; curtain gas, 20 L/min; declustering potential, 60 V; focusing potential, 320 V; ion release delay, 6; ion release width, 5; detector voltage, 2300 V. The obtained spectra were deconvoluted and analyzed using Bioanalyst version 2.0 from Applied Biosystems.

The rate constant (k) for hIGF-1_{3S-S} reduction with 0.5, 1, and 5 mM DTT was calculated from kinetic data at different temperatures using the exponential equation

$$y = A_1 - A_2 e^{-kt} \quad (1)$$

where k is the rate constant, y is the average molecular mass of hIGF-1, t is the incubation time, and A_1 and A_2 are constants. Data were fit using an A_1 of 7648.5 (molecular mass of hIGF-1_{3S-S}) and an A_2 of 7654.5 (molecular mass of hIGF-1_{0S-S}) with Origin 6.1 (Originlab Corp., Northampton, MA).

The half-life of the reaction is equal to

$$t_{1/2} = \ln(2)/k \quad (2)$$

Reduction of hIGF-1 with BME. Fully oxidized human IGF-1_{3S-S} (2 μM) was incubated in argon-saturated 20 mM ammonium acetate (pH 7.5), containing 5, 10, and 25 mM BME as a reducing agent.

The reaction mixtures were incubated at 25 or 40 °C. At various time points (1−300 min), aliquots from the reaction mixture were analyzed by ESI-MS as described above.

Measuring the Redox Potential of hIGF-1 in DTT/DTT_{ox} and BME/BME_{ox} Redox Buffers. For the measurement of the redox potential of hIGF-1, fully oxidized hIGF-1_{3S-S} (2 μM) was incubated in various DTT- and BME-based redox buffers to achieve the redox equilibrium between the protein forms. The equilibrium ratios of hIGF-1 redox forms were determined after incubation of hIGF-1_{3S-S} (2 μM) for 30 min at 40 °C in DTT/DTT_{ox} redox buffers ([DTT] + [DTT_{ox}] = 5 mM) or after incubation of hIGF-1_{3S-S} (2 μM) for 3 h at 40 °C in BME/BME_{ox} redox buffers ([BME] + 2[BME_{ox}] = 25 mM) by ESI-MS.

The fractional content of IGF-1_{0S-S} was determined by dividing the mass increment (average molecular mass of hIGF-1 minus molecular mass of IGF-1_{3S-S}) by 6 (maximal mass increment in the case of reduction of three S−S bonds).

The redox potential of redox buffers was adjusted by varying the ratio of reduced and oxidized forms of DTT and BME, and corresponding redox potentials were calculated from the following Nernst equations:

$$E' = E_0'(\mathrm{DTT}) - [(RT)/(nF)] \ln([\mathrm{DTT}]/[\mathrm{DTT_{ox}}]) \quad (3)$$

$$E' = E_0'(\mathrm{BME}) - [(RT)/(nF)] \ln([\mathrm{BME}^2]/[\mathrm{BME_{ox}}]) \quad (4)$$

where E_0'(DTT) = −0.323 V (pH 7.0 and 25 °C),[31] E_0'(BME) = −0.231 V (pH 7.0 and 25 °C),[32] R is the gas constant (8.315 J K^{-1} mol^{-1}), n is the number of electrons transferred in the reaction, and F is the Faraday constant (9.6485 × 10^{-4} C mol^{-1}). The E_0'(DTT) and E_0'(BME) values have been recalculated for 40 °C using eqs 3 and 4 and for pH 7.5 using the following equation:

$$E_{pH} = E_0' + (\mathrm{pH} - \mathrm{pH_0})(\Delta E/\Delta \mathrm{pH}) \quad (5)$$

where $\Delta E/\Delta$pH is the change in E if the pH is increased by 1 unit and is equal to 60.1 mV.[33]

The midpoint redox potential of the hIGF-1_{3S-S} → hIGF-1_{0S-S} reaction was determined by fitting the fractional content of hIGF-1_{0S-S} to the equation

$$y = (A_1 - A_2)/[1 + e^{(x-x_0)/dx}] + A_2 \quad (6)$$

where y is the fractional content of hIGF-1_{0S-S}, x is the environmental redox potential (E_h), A_1 and A_2 are constants, and x_0 is the midpoint redox potential (E_m). Data were fit using an A_1 of 0 (initial fractional content of hIGF-1_{0s-s}) and an A_2 of 1 (final fractional content of IGF-1_{0s-s}) with Origin 6.1 (Originlab Corp.).

Copper Binding Properties of hIGF-1 Reduced with DTT and BME and Stability of Cu^+−Protein Metallo-forms in the Presence of Increasing Concentrations of DTT. Human IGF-1 was reduced using one of the following schemes. hIGF-1 (2 μM) was fully reduced at 40 °C with 0.5 mM DTT for 90 min, and 10 μM hIGF-1 was partially reduced with 10 mM BME at 40 °C for 220 min. Reduction was confirmed by ESI-MS. Metal binding experiments were performed with partly reduced and fully reduced hIGF-1 forms. Reconstitution of various IGF-1 forms with copper was performed as follows. First, Cu(II) acetate was dissolved at a concentration of 100 μM in argon-saturated 20 mM ammonium acetate (pH 7.5), and Cu^{2+} was reduced to Cu^+ by the addition of 0.5 mM DTT or 1 mM BME. A freshly prepared metal salt

dx.doi.org/10.1021/bi300494s | Biochemistry 2012, 51, 5851−5859

solution (1−8 equiv) was added to apoIGF-1, and the mixture was incubated for 1 min at 25 °C. Samples were then diluted with 20 mM ammonium acetate (pH 7.5) to a final protein concentration of 1 μM (final concentration of reducing agent in the final sample for MS of 0.5 mM for DTT and 1 mM for BME) and infused with a syringe pump into a QSTAR Elite ESI-Q-TOF mass spectrometer at a rate of 10 μL/min.

The influence of DTT on copper binding by hIGF-1 was studied by adding of 0.5−7.5 mM reduced DTT to 1 μM Cu_nIGF-1. Cu_nIGF-1 was prepared by addition of 8 equiv of the Cu^+DTT complex to hIGF-1. The Cu^+DTT complex was prepared by addition of DTT to copper acetate at a concentration of 16 μM in argon-saturated 20 mM ammonium acetate (pH 7.5). Final mixtures contained 0.25−4 mM DTT and 1 μM Cu_nIGF-1. The obtained mixtures were injected into the QSTAR Elite ESI-Q-TOF instrument.

Characterization of hIGF-1 via High-Performance Liquid Chromatography (HPLC). hIGF-1 (25 μL of 30 μM hIGF-1) was applied to a reversed-phase HPLC column (Agilent Eclipse XDB-C18, 4.6 mm × 150 mm, 5 μm) and analyzed according to the method described by Miller and colleagues[34] with small modifications. The gradient used for all HPLC experiments was as follows: (i) equilibration of the column with 80% A [0.1% (v/v) aqueous trifluoroacetic acid] and 20% B [88% acetonitrile, 2% 2-propanol, 9.9% water, and 0.1% trifluoroacetic acid (all v/v)], (ii) a linear gradient to 30% B in 1 column volume (CV), (iii) a linear gradient to 38% B in 8.4 CV, and (iv) a linear gradient to 80% B in 6.2 CV. After each run, the column was washed with 100% B and re-equilibrated.

Disulfide rearrangement was performed according to the method described in ref 34 with small modifications. hIGF-1 (30 μM) was incubated with BME at a BME/IGF-1 ratio of 13/1 in 20 mM ammonium acetate (pH 7.5) at 25 °C for 23 h and subjected to HPLC.

For redox experiments, hIGF-1 was incubated in different DTT/DTT_{ox} redox buffers as described in the ESI-MS section and chromatographed after incubation for 1 h. E_h values of the samples were established via calculation of the DTT/DTT_{ox} ratios of the corresponding DTT and DTT_{ox} peaks, which had been resolved in each HPLC chromatogram. In the incubation mixtures, the concentration of DTT and DTT_{ox} was 75 mM, and the concentration of IGF-1 was 30 μM.

All peaks present in HPLC chromatograms were collected and identified using ESI-MS.

RESULTS

Reduction of hIGF-1 with DTT. The mass spectrum of isolated hIGF-1 showed three major peaks with charges of +5, +6, and +7 with different distributions in samples containing oxidized and reduced forms of the protein. The average molecular mass of hIGF-1 was calculated using all peaks corresponding to different ionization states in the particular sample. High-resolution ESI-MS spectra of hIGF-1 (Figure 1) show a small increase in the protein molecular mass in the presence of DTT.

The deconvolution of the spectrum in the absence of DTT gave a molecular mass of 7648.66 Da that agrees well with the theoretical molecular mass of oxidized hIGF-1 containing three disulfide bridges (7648.70 Da). Incubation of fully oxidized hIGF-1 with 0.5 mM DTT at 25 and 40 °C for 120 min resulted in gradual reduction of the protein reflected in progressive increase in its molecular mass. The increase in the average molecular mass of hIGF-1 was 6 Da (Figure 2), which

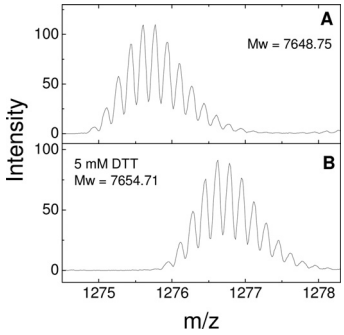

Figure 1. High-resolution ESI-MS spectra of hIGF-1 in the absence and presence of DTT. Conditions: 2 μM hIGF-1, 20 mM ammonium acetate, pH 7.5. (A) hIGF-1 or (B) hIGF-1 incubated with 5 mM DTT at 40 °C for 45 min. The +6 charge states are presented, and average molecular masses were calculated using Bioanalyst.

corresponds to the reduction of all three disulfide bonds. The incubation of hIGF-1_{3S-S} at higher concentrations of DTT at 25 and 40 °C led to the fast reduction of the protein (approximately 15 min for 5 mM DTT and 45 min for 1 mM DTT for the full reduction of the protein). Fully reduced hIGF-1 exposes four ion species (charges from +5 to +8) in the mass spectrum. Figure 2 shows that all three disulfide bonds are reduced simultaneously because the kinetic curve of the increase of the protein molecular mass can be fit to a single exponent. The half-life ($t_{1/2}$) of the reaction varied between 1.9 and 27.1 min depending on the incubation temperature and concentration of DTT.

Reduction of hIGF-1 with BME. The acquired ESI mass spectra of hIGF-1 displayed three main peaks with charges of +5, +6, and +7. In the presence of BME, an additional minor peak corresponding to the hIGF-1_{1S-S}−BME adduct was also detected. Incubation of hIGF-1_{3S-S} with 25 mM BME resulted in an increase in the average molecular mass of hIGF-1 of ∼5 Da (Figure 3), which corresponds to the reduction of two or three disulfide bonds.

Reduction of hIGF-1_{3S-S} with 5 mM BME occurs with a half-life of 22 min at 40 °C and 37 min at 25 °C, whereas increasing the BME concentration to 10 and 25 mM at 40 °C shortened the half-lives to 8 and 2.4 min, respectively.

The reduction of hIGF-1 by BME is considerably slower than its reduction by DTT under similar conditions; however, at a high (25 mM) concentration of BME and an elevated temperature (40 °C), the reaction occurs much faster (half-life of ∼2 min) and all disulfide bonds are reduced (Figure 3). Reduction occurs at a slightly lower rate comparable to that with DTT; however, disulfide bonds were reduced simultaneously, as in the case of DTT.

Determination of Midpoint Redox Potentials of hIGF-1 in DTT/DTT_{ox} and BME/BME_{ox} Redox Buffers. Figure 4A shows the dependence of the average mass of hIGF-1 on the redox potential in 5 mM DTT/DTT_{ox} redox buffers determined after incubation at 40 °C for 30 min. The average mass of hIGF-1_{3S-S} increased by 6 Da at environmental redox potential values of less than −300 mV, which reflects the equilibrium position between hIGF-1_{3S-S} and hIGF-1_{0S-S} forms. The midpoint redox potential value for the hIGF-1_{0S-S}−hIGF-1_{3S-S} transition was calculated from the dependence of the fractional

dx.doi.org/10.1021/bi300494s | Biochemistry 2012, 51, 5851−5859

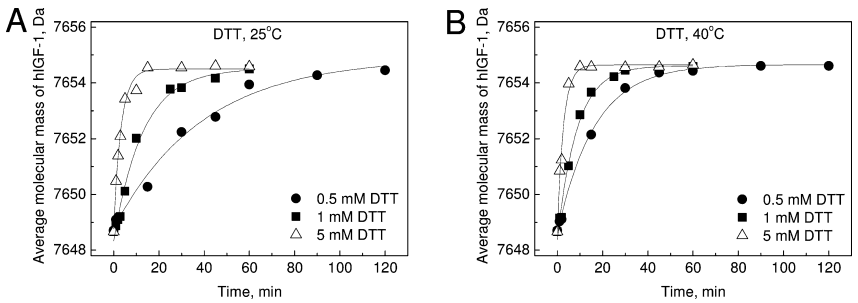

Figure 2. Kinetics of hIGF-1_{3S-S} reduction with DTT monitored by the increase in the average molecular mass of hIGF-1. Conditions: 2 μM hIGF-1_{3S-S}, 20 mM ammonium acetate, pH 7.5. (A) T = 25 °C, with 0.5, 1, and 5 mM DTT. (B) T = 40 °C, with 0.5, 1, and 5 mM DTT. Average molecular masses were calculated using Bioanalyst. Solid lines are fitted curves.

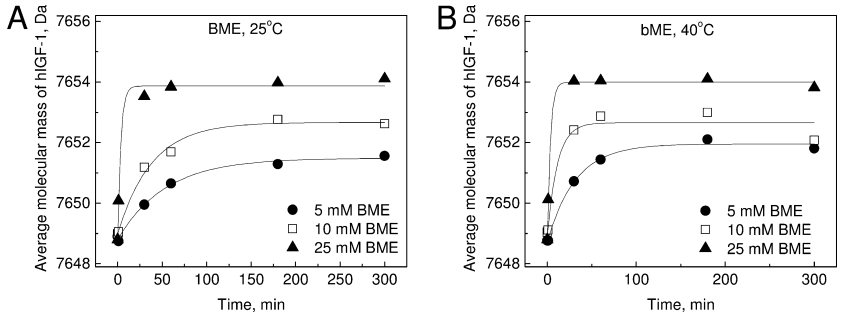

Figure 3. Kinetics of reduction of hIGF-1_{3S-S} by BME monitored by the increase in the average molecular mass of hIGF-1. Conditions: 2 μM hIGF-1_{3S-S}, 20 mM ammonium acetate, pH 7.5. (A) T = 25 °C, with 5, 10, and 25 mM BME. (B) T = 40 °C, with 5, 10, and 25 mM BME. Average molecular masses were calculated using Bioanalyst. Solid lines are fitted curves.

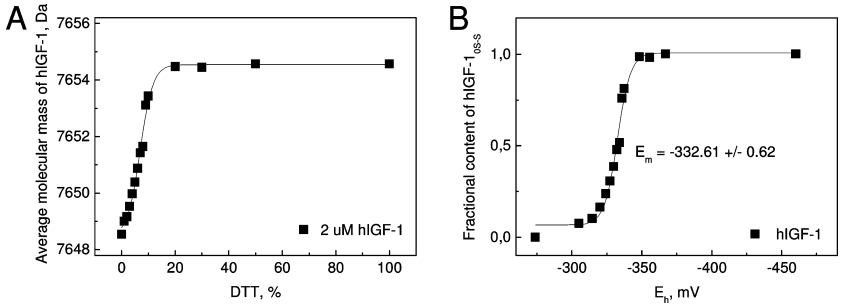

Figure 4. Determination of the redox midpoint potential of hIGF-1 in DTT/DTT_{ox} redox buffers. (A) Average molecular mass of hIGF-1 plotted vs increasing DTT concentrations in 5 mM DTT/DTT_{ox} redox buffers. (B) Fractional content of hIGF-1_{0S-S} at different E_h values generated by the DTT/DTT_{ox} couple.

content of hIGF-1_{0S-S} and E_h, presented in Figure 4B. The fitting of data to eq 6 yielded a midpoint redox potential equal to −332.61 ± 0.62 mV (pH 7.5 and 40 °C).

The average masses of hIGF-1 in 25 mM BME/BME_{ox} redox buffers determined after incubation at 40 °C for 3 h are presented in Figure 5A. At environmental redox potential values of less than −300 mV, the average mass of hIGF-1_{3S-S} increases 5−6 Da. The midpoint redox potential value for the hIGF-1_{0S-S}/hIGF-1_{3S-S} couple was calculated from the dependence of the fractional content of hIGF-1_{0S-S} from E_h, presented in Figure 5B. The fitting of the data to eq 6 yielded an E_m of −328.07 ± 1.01 mV (pH 7.5 and 40 °C), which is in agreement with the value observed in DTT/DTT_{ox} redox buffer because their confidence intervals overlap.

Copper Binding Properties of Reduced hIGF-1 and Stability of Cu^+−Protein Metalloforms in the Presence of Increasing Concentrations of DTT. Figure 6 shows the mass spectra of fully reduced IGF-1 at different concentrations of Cu^+ ions in the presence of 0.5 mM DTT. The addition of 1−2 equiv of Cu^+ ions to apoIGF-1 generated small amounts of two metalloforms of hIGF corresponding to Cu_4IGF-1 and Cu_4IGF-1-DTT (Figure 6A,B). After the addition of 4 and 6

dx.doi.org/10.1021/bi300494s | Biochemistry 2012, 51, 5851−5859

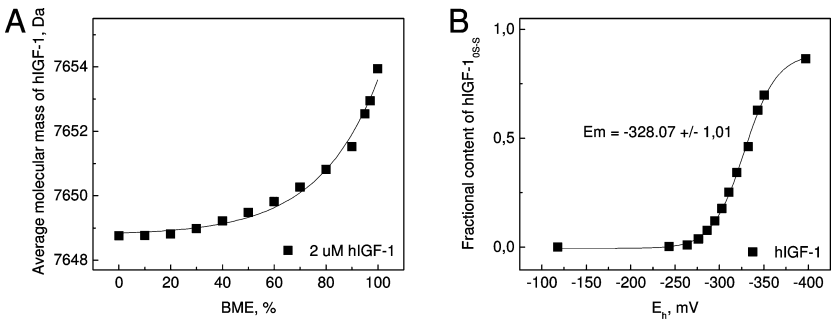

Figure 5. Determination of redox midpoint potentials of hIGF-1 in BME/BME_{ox} redox buffers. (A) Average molecular mass of hIGF-1 plotted vs increasing BME concentrations in 25 mM BME/BME_{ox} redox buffers. (B) Fractional content of $hIGF\text{-}1_{0S-S}$ at different E_h values generated by the BME/BME_{ox} couple.

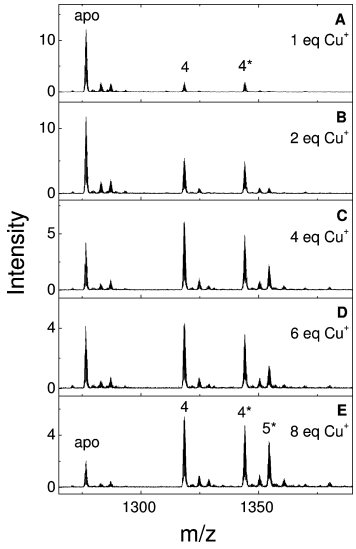

Figure 6. Binding of Cu^+ ions to hIGF-1 in the presence of DTT. Mass spectra of hIGF-1 (1 μM) reconstituted with 1−8 equiv of Cu^+ ions in the presence of 20 mM ammonium acetate (pH 7.5) and 0.5 mM DTT at 25 °C. Charge state +6 ions are presented, and numbers on the peaks denote the metal stoichiometry of the complex; asterisks denote DTT adducts.

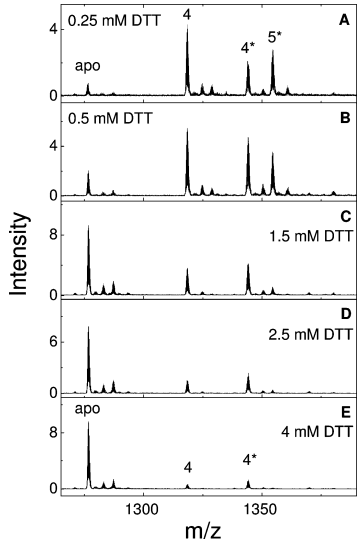

Figure 7. Release of Cu^+ ions in the presence of increasing concentrations of DTT. Mass spectra of hIGF-1 (1 μM) reconstituted with 8 equiv of Cu^+ ions in 20 mM ammonium acetate (pH 7.5) in the presence of DTT at various concentrations: (A) 0.25, (B) 0.5, (C) 1.5, (D) 2.5, and (E) 4 mM. Charge state +6 ions are presented, and numbers on the peaks denote the metal stoichiometry of the complex; asterisks denote DTT adducts.

equiv of Cu^+ ions, the MS spectrum exposes one dominant peak corresponding to Cu_4IGF-1 together with minor apoIGF-1, Cu_4IGF-1-DTT, and Cu_5IGF-1-DTT forms (Figure 6C,D). Addition of 8 equiv of Cu^+ ions leads to the relative increase in the magnitude of the Cu_5IGF-1-DTT peak and the decrease in the magnitude of the apoIGF-1 peak (Figure 6E). The experimentally determined molecular mass of Cu_4IGF-1 (7904.54 Da) indicates that the molecular mass of hIGF-1 in this complex is 7654.84 Da, which is very close to the theoretical value for the fully reduced hIGF-1 protein (7654.7 Da), demonstrating the absence of disulfide bridges in Cu_4IGF-1.

Figure 7 shows the mass spectra of hIGF-1 incubated with 8 equiv of Cu^+ in the presence of increasing concentrations of DTT. At 0.5 mM DTT, the peak corresponding to apoIGF-1 starts to increase (Figure 7B) and becomes dominant at 2.5 mM DTT (Figure 7D,E). The results demonstrate that DTT extracts metals from hIGF-1 at supramillimolar concentrations.

Mass spectra of hIGF-1, reduced with BME and reconstituted at pH 7.5 with increasing concentrations of Cu^+ ions in the presence of 1 mM BME, are presented in Figure 8. The MS spectrum in the presence of 1 equiv of Cu^+ exposes one major peak of Cu_4IGF-1 together with minor apoIGF-1 and Cu_4IGF-1-BME forms (Figure 8A). The magnitude of the apoIGF-1 peak decreases with elevated copper concentrations, and the peak became a minor form after the addition of 6 equiv of Cu^+ ions, where the MS spectrum exposes Cu_4IGF-1 as a major peak together with minor apoIGF-1, Cu_4IGF-1-BME, and Cu_5IGF-1 forms (Figure 8D). Further addition of Cu^+ ions leads to a relative increase in the magnitude of the Cu_5IGF-1

dx.doi.org/10.1021/bi300494s | Biochemistry 2012, 51, 5851−5859

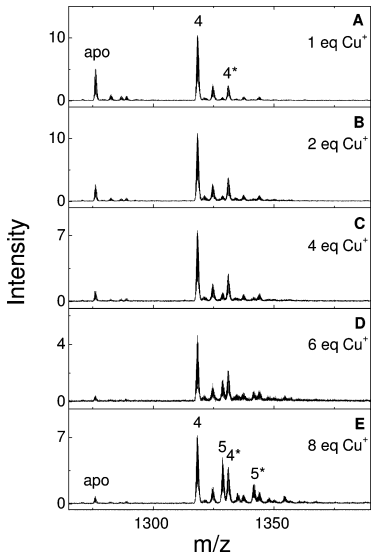

Figure 8. Binding of Cu^+ ions to hIGF-1 in the presence of BME. Mass spectra of hIGF-1 (1 μM) reconstituted with 1−8 equiv of Cu^+ ions in 20 mM ammonium acetate (pH 7.5) in the presence of 1 mM BME at 25 °C. Charge state +6 ions are presented, and numbers on the peaks denote the metal stoichiometry of the complex; asterisks denote BME adducts.

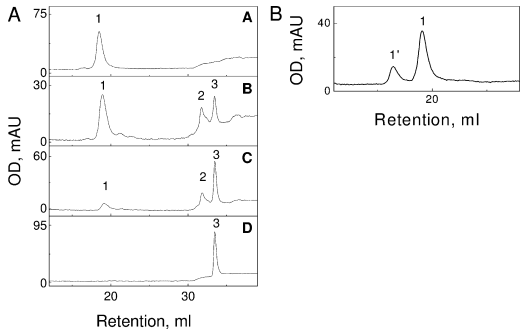

Figure 9. Disulfide rearrangement and redox properties of hIGF-1 monitored by HPLC. Conditions: 30 μM hIGF-1, 20 mM ammonium acetate, pH 7.5. (A) hIGF-1 (A), hIGF-1 incubated in DTT/DTT_{ox} redox buffer containing 2.6% DTT at 25 °C for 1 h (B), hIGF-1 incubated in DTT/DTT_{ox} redox buffers containing 5% DTT at 25 °C for 1 h (C), and hIGF-1 incubated with DTT at 25 °C for 1 h (D). (B) hIGF-1 incubated with BME at a BME/IGF-1 ratio of 13/1 at 25 °C for 23 h. (1) IGF-1_{3S-S}, (1′) IGF-swap, (2) IGF-1_{1S-S}, and (3) IGF-1_{0S-S}.

peak and a decrease in the magnitude of the apoIGF-1 peak; the minor peak of the Cu_5IGF-1-BME form has appeared in the mass spectrum (Figure 8E). Mass analysis of Cu_4IGF-1 (assuming that four Cu^+ ions are bound) demonstrates that there are no disulfides in Cu_4IGF-1.

Characterization of hIGF-1 with HPLC. The gradient and solvent composition used by Miller et al.[34] were used with an Agilent Eclipse XDB C-18 column, and different hIGF-1 species have been resolved, providing results similar to those described previously.[34] A fully oxidized hIGF-1 sample exposed one major peak with retention at 31.7% B in reversed phase HPLC (Figure 9A, panel A). After incubation with 75 mM DTT for 1 h, hIGF-1 was fully reduced and hIGF-1_{0S-S} eluted at 36.6% B (Figure 9A, panel D). Disulfide rearrangement was initiated under our experimental conditions according to the procedure described by Miller et al.[34]

Equilibration of hIGF-1 under various redox conditions, similar to those used in ESI-MS experiments, was monitored by HPLC (Figure 9A, panels B and C). Three peaks were identified by ESI-MS to be major products of the reaction: peak 1 corresponding to hIGF-1_{3S-S}, peak 3 corresponding to hIGF-1_{0S-S}, and peak 2 corresponding to IGF-1 containing one disulfide bond (hIGF-1_{1S-S}). Retention times of these species were as follows: 31.7% B for IGF-1_{3S-S}, 36.1% B for IGF-1_{1S-S}, and 36.6% B for IGF-1_{0S-S}. IGF-1_{1S-S} is the major intermediate of the reaction in DTT/DTT_{ox} redox buffers under our experimental conditions. IGF-1_{2S-S} peaks were not detected in the course of the experiment, which suggests that both native disulfides of hIGF-1, 47−52 and 6−48, are reduced simultaneously and cooperatively. It has been shown earlier that prolonged incubation of IGF-1 under the conditions of extensive thiol exchange leads to the appearance of IGF with incorrectly folded disulfide bridges.[34] As seen in Figure 9B, after incubation of the BME/IGF-1 mixture for 23 h, the additional peak was eluted at 30.8% B, which corresponds to fully oxidized IGF-swap, nonnative product containing disulfide pairing (6−47, 18−61, 48−52). Such a peak was not detected in any of the chromatograms after incubation for 1 h (Figure 9A), suggesting that incorrect folding does not occur during our ESI-MS experiments.

DISCUSSION

The principal characteristic of the redox switching properties of the protein is the midpoint redox potential (E_m) of the redox processes involved. The E_m values can be determined from the equilibrium between oxidized and reduced forms of the protein at different environmental redox potential values maintained by GSH/GSSG or DTT/oxidized DTT redox buffers.[35] Importantly, high-resolution MS instruments allow the determination of the molecular mass of small proteins with an accuracy sufficient for direct monitoring of disulfide bond formation; thus, the redox equilibrium can be monitored without chemical modification of Cys residues.[28] In this work, we used a BME-based redox buffer instead of natural GSH as additional buffer to verify data obtained from the DTT redox system, because the nonionic BME is compatible with ESI-MS measurements and its redox potential is similar to that of GSH (−253 mV for BME and −262 mV for GSH).[32,36]

The ESI-MS studies reported here help us to understand the interplay between different redox states of hIGF-1. In general, our results exhibited a single sigmoid in the titration curve depending on the environmental conditions, suggesting that human IGF-1 exists mainly in two states corresponding to the fully oxidized and the reduced protein with six thiol groups whereas the latter can bind four Cu^+ ions. The high cooperativity of oxidative folding was confirmed by HPLC, showing that only a small amount (<20%) of the peptide with one disulfide bridge is forming at intermediate E_m values whereas the intermediate with two disulfide bonds is missing in all spectra. HPLC analysis also demonstrated the absence of

misfolded hIGF-swap at redox equilibrium within the time course of the experiments.

We found that the E_m value of hIGF-1 oxidation is equal to −332 mV (at pH 7.5 and 40 °C). The extracellular redox environment in the living organisms is relatively oxidative: an E_h value of approximately −80 mV has been determined from the Cys/CySS ratio in the plasma of young healthy individuals.[16] The experimental midpoint redox potential value of IGF-1 is much lower than the extracellular E_h, which is in agreement with the presence of three disulfide bonds in the IGF-1 molecules in extracellular fluids.[6]

In several reports, a thermodynamic folding problem of IGF-1 in vitro[34,37] was observed under redox conditions with an E_h value for the GSH/GSSG system of around −335 mV. Our results show that under these conditions hIGF-1 is not fully oxidized and thus will not be able to acquire its native fold. Moreover, the redox state of the secretory pathway has recently been reported to be more oxidized, and the redox potential has been estimated to be −189 mV,[7] which ensures IGF-1 oxidation and complete disulfide formation in vivo.

Several attempts to study the structural aspects of IGF-1 and its interaction with the receptor and IGFBPs have been made. Three native disulfide bonds that were shown to be critical for binding of IGF-1 with the type I IGFR are between Cys6 and Cys48, Cys18 and Cys61, and Cys47 and Cys52.[6] The X-ray structure of the IGF-1 ternary complex with N- and C-terminal domain fragments of IGFBP-4 revealed the same disulfides in IGF-1.[38] Besides this, several other crystal structures (see for examples refs 39−41) and solution structures[42,43] of IGF-1 alone or in complex with IGFBPs have been published, and all these studies show that native disulfides are involved in the formation of the three-dimensional structure of hIGF-1, which is necessary for its recognition by other biomolecules.

The presence of thiol groups in reduced hIGF-1 suggests that it can potentially bind zinc and/or copper ions. Our results demonstrate clearly that fully reduced hIGF-1 does not bind Zn^{2+} ions (data not shown); however, the protein can bind four Cu^+ ions in a highly cooperative manner. The cooperative character of the binding is obvious from the absence of peaks corresponding to protein forms Cu_1IGF-1, Cu_2IGF-1, and Cu_3IGF-1 in the mass spectrum throughout the titration. These experiments show that fully reduced IGF-1 is a good model for proteins containing six Cys residues. It has been suggested that this type of protein preferentially binds four Cu^+ ions with tetracopper−hexathiolate cluster formation occurring during metal ion binding.[25−27] Our results confirm this suggestion and demonstrate that the binding of four copper ions requires the presence of six thiol groups in the protein and is sequence-independent.

Our results show that hIGF-1 can also form a complex with five Cu^+ ions. However, an additional thiol ligand is required for the binding of the fifth Cu^+ ion, because the peaks corresponding to five bound copper ions in the mass spectrum always contained DTT or BME (Figure 6C−E, peaks with asterisks). The results demonstrate that the Cu_5IGF-1 peak does not arise from the nonspecific binding of an excess of metal.

We used the titration of the metal form of the protein with DTT to estimate the affinity of hIGF-1 for copper ions. DDT at supramillimolar concentrations can extract metals from Cu_4IGF-1. On the basis of our results, the calculated $K_d(Cu^+$-hIGF-1) value is equal to $(3.00 \pm 0.86) \times 10^{-18}$ M. This value was calculated as previously described in ref 25 using the corrected $K_d(Cu^+$-DTT) value of 5×10^{-16} M.[44] To compare the Cu^+ binding affinity of fully reduced hIGF-1 with the copper chaperone for cytochrome *c* oxidase Cox17, the $K_d(Cu^+$-Cox17) from ref 25 was recalculated using the corrected $K_d(Cu^+$-DTT) and was found to be equal to 1.03×10^{-18} M. This comparison showed that the Cu^+ binding affinity of fully reduced hIGF-1 is 3-fold lower than that of Cox17, which has the lowest affinity among the cellular copper chaperones.[25]

Dietary copper has been shown to play a certain role in the regulation of IGF-1,[45,46] but there are no data about a direct interaction of hIGF-1 with Cu^+ ions. The majority of IGF-1, which circulates in extracellular fluids in complex with IGFBP-s or in an unbound fully oxidized form, is therefore unable to bind any metal ions. In the secretory pathway, the hIGF-1 molecules are most likely also oxidized considering the estimated redox potential of −189 mV for the ER.

The midpoint redox potential values are important determinants of the state of a protein within different compartments of the cell as well as in the extracellular matrix. It is important to note that intracellular and extracellular redox conditions are not absolutely stable and can fluctuate even under normal physiological conditions; usually, the potential becomes more oxidizing during different diseases and aging. In the case of IGF-1, the very low redox potential value keeps the protein in the native folded oxidized state; however, for a large number of proteins, the redox switches are physiologically very significant. In this paper, we demonstrate the applicability of the ESI-MS method for a complex investigation of the redox and metal binding properties using hIGF-1 as a relatively simple model protein. The observed results show that the method would be applicable also for more complex proteins.

AUTHOR INFORMATION

Corresponding Author

*Telephone: +372 620 4410. E-mail: peep.palumaa@ttu.ee.

Author Contributions

P.P. and J.S. designed the research. J.S. and J.M. performed the experiments. J.S., J.M., P.P., and V.T. analyzed the results, and the manuscript was written through contributions of all authors. All authors have given approval to the final version of the manuscript.

Funding

This work was supported by the Estonian Ministry of Education and Research (Grant SF0140055s08) and Estonian Science Foundation Grant 8811 (both to P.P.) and Estonian Science Foundation Grant 9318 to (V.T.).

Notes

The authors declare no competing financial interest.

ABBREVIATIONS

BME, 2β-mercaptoethanol; DTT, dithiothreitol; DTT_{ox}, oxidized dithiothreitol; ESI-MS, electrospray ionization mass spectrometry; GH, growth hormone; GSH, glutathione; hIGF-1, human insulin-like growth factor 1; IGF-1R, insulin-like growth factor 1 receptor; IGFBP, IGF binding proteins; ROS, reactive oxygen species; RNS, reactive nitrogen species; CyS/CySS, cysteine/cystine redox pair; ER, endoplasmic reticulum.

REFERENCES

(1) De Wolf, E., Gill, R., Geddes, S., Pitts, J., Wollmer, A., and Grotzinger, J. (1996) Solution structure of a mini IGF-1. *Protein Sci. 5*, 2193−2202.

(2) Lund, P. K. (1994) Insulin-like growth factor I: Molecular biology and relevance to tissue-specific expression and action. *Recent Prog. Horm. Res. 49*, 125−148.
(3) Jones, J. I., and Clemmons, D. R. (1995) Insulin-like growth factors and their binding proteins: Biological actions. *Endocr. Rev. 16*, 3−34.
(4) Baxter, R. C. (2000) Insulin-like growth factor (IGF)-binding proteins: Interactions with IGFs and intrinsic bioactivities. *Am. J. Physiol. 278*, E967−E976.
(5) Clemmons, D. R. (2007) Value of insulin-like growth factor system markers in the assessment of growth hormone status. *Endocrinol. Metab. Clin. North Am. 36*, 109−129.
(6) Narhi, L. O., Hua, Q. X., Arakawa, T., Fox, G. M., Tsai, L., Rosenfeld, R., Holst, P., Miller, J. A., and Weiss, M. A. (1993) Role of native disulfide bonds in the structure and activity of insulin-like growth factor 1: Genetic models of protein-folding intermediates. *Biochemistry 32*, 5214−5221.
(7) Hwang, C., Sinskey, A. J., and Lodish, H. F. (1992) Oxidized redox state of glutathione in the endoplasmic reticulum. *Science 257*, 1496−1502.
(8) Sen, C. K. (2000) Cellular thiols and redox-regulated signal transduction. *Curr. Top. Cell. Regul. 36*, 1−30.
(9) Hansen, J. M., Go, Y. M., and Jones, D. P. (2006) Nuclear and mitochondrial compartmentation of oxidative stress and redox signaling. *Annu. Rev. Pharmacol. Toxicol. 46*, 215−234.
(10) Jones, D. P. (2006) Redefining oxidative stress. *Antioxid. Redox Signaling 8*, 1865−1879.
(11) Moriarty-Craige, S. E., and Jones, D. P. (2004) Extracellular thiols and thiol/disulfide redox in metabolism. *Annu. Rev. Nutr. 24*, 481−509.
(12) Jones, D. P. (2006) Disruption of mitochondrial redox circuitry in oxidative stress. *Chem.-Biol. Interact. 163*, 38−53.
(13) Go, Y. M., and Jones, D. P. (2008) Redox compartmentalization in eukaryotic cells. *Biochim. Biophys. Acta 1780*, 1273−1290.
(14) Kemp, M., Go, Y. M., and Jones, D. P. (2008) Nonequilibrium thermodynamics of thiol/disulfide redox systems: A perspective on redox systems biology. *Free Radical Biol. Med. 44*, 921−937.
(15) Go, Y. M., and Jones, D. P. (2010) Redox clamp model for study of extracellular thiols and disulfides in redox signaling. *Methods Enzymol. 474*, 165−179.
(16) Blanco, R. A., Ziegler, T. R., Carlson, B. A., Cheng, P. Y., Park, Y., Cotsonis, G. A., Accardi, C. J., and Jones, D. P. (2007) Diurnal variation in glutathione and cysteine redox states in human plasma. *Am. J. Clin. Nutr. 86*, 1016−1023.
(17) Gilbert, H. F. (1990) Molecular and cellular aspects of thiol-disulfide exchange. *Adv. Enzymol. Relat. Areas Mol. Biol. 63*, 69−172.
(18) Huber-Wunderlich, M., and Glockshuber, R. (1998) A single dipeptide sequence modulates the redox properties of a whole enzyme family. *Folding Des. 3*, 161−171.
(19) Krause, G., and Holmgren, A. (1991) Substitution of the conserved tryptophan 31 in *Escherichia coli* thioredoxin by site-directed mutagenesis and structure-function analysis. *J. Biol. Chem. 266*, 4056−4066.
(20) Lin, T. Y., and Kim, P. S. (1989) Urea dependence of thiol-disulfide equilibria in thioredoxin: Confirmation of the linkage relationship and a sensitive assay for structure. *Biochemistry 28*, 5282−5287.
(21) Wunderlich, M., and Glockshuber, R. (1993) Redox properties of protein disulfide isomerase (DsbA) from *Escherichia coli*. *Protein Sci. 2*, 717−726.
(22) Ostergaard, H., Tachibana, C., and Winther, J. R. (2004) Monitoring disulfide bond formation in the eukaryotic cytosol. *J. Cell Biol. 166*, 337−345.
(23) Lopez-Mirabal, H. R., and Winther, J. R. (2008) Redox characteristics of the eukaryotic cytosol. *Biochim. Biophys. Acta 1783*, 629−640.
(24) Samiec, P. S., Drews-Botsch, C., Flagg, E. W., Kurtz, J. C., Sternberg, P., Jr., Reed, R. L., and Jones, D. P. (1998) Glutathione in human plasma: Decline in association with aging, age-related macular degeneration, and diabetes. *Free Radical Biol. Med. 24*, 699−704.
(25) Palumaa, P., Kangur, L., Voronova, A., and Sillard, R. (2004) Metal-binding mechanism of Cox17, a copper chaperone for cytochrome c oxidase. *Biochem. J. 382*, 307−314.
(26) Banci, L., Bertini, I., Ciofi-Baffoni, S., Janicka, A., Martinelli, M., Kozlowski, H., and Palumaa, P. (2008) A structural-dynamical characterization of human Cox17. *J. Biol. Chem. 283*, 7912−7920.
(27) Ahte, P., Palumaa, P., and Tamm, T. (2009) Stability and conformation of polycopper-thiolate clusters studied by density functional approach. *J. Phys. Chem. A 113*, 9157−9164.
(28) Zovo, K., and Palumaa, P. (2009) Modulation of redox switches of copper chaperone Cox17 by Zn(II) ions determined by new ESI MS-based approach. *Antioxid. Redox Signaling 11*, 985−995.
(29) Banci, L., Bertini, I., Ciofi-Baffoni, S., Kozyreva, T., Zovo, K., and Palumaa, P. (2010) Affinity gradients drive copper to cellular destinations. *Nature 465*, 645−648.
(30) Cleland, W. W. (1964) Dithiothreitol, a New Protective Reagent for SH Groups. *Biochemistry 3*, 480−482.
(31) Lees, W. J., and Whitesides, G. M. (1993) Equilibrium Constants for Thiol-Disulfide Interchange Reactions: A Coherent, Corrected Set. *J. Org. Chem. 58*, 642−647.
(32) Keire, D. A., Strauss, E., Guo, W., Noszal, B., and Rabenstein, D. L. (1992) Kinetics and equilibria of thiol-disulfide interchange reactions of selected biological thiols and related molecules with oxidized glutathione. *J. Org. Chem. 57*, 123−127.
(33) Schafer, F. Q., and Buettner, G. R. (2001) Redox environment of the cell as viewed through the redox state of the glutathione disulfide/glutathione couple. *Free Radical Biol. Med. 30*, 1191−1212.
(34) Miller, J. A., Narhi, L. O., Hua, Q. X., Rosenfeld, R., Arakawa, T., Rohde, M., Prestrelski, S., Lauren, S., Stoney, K. S., Tsai, L., et al. (1993) Oxidative refolding of insulin-like growth factor 1 yields two products of similar thermodynamic stability: A bifurcating protein-folding pathway. *Biochemistry 32*, 5203−5213.
(35) Dutton, P. L. (1978) Redox potentiometry: Determination of midpoint potentials of oxidation-reduction components of biological electron-transfer systems. *Methods Enzymol. 54*, 411−435.
(36) Millis, K. K., Weaver, K. H., and Rabenstein, D. L. (1993) Oxidation/reduction potential of glutathione. *J. Org. Chem. 58*, 4144−4146.
(37) Hober, S., Forsberg, G., Palm, G., Hartmanis, M., and Nilsson, B. (1992) Disulfide exchange folding of insulin-like growth factor I. *Biochemistry 31*, 1749−1756.
(38) Sitar, T., Popowicz, G. M., Siwanowicz, I., Huber, R., and Holak, T. A. (2006) Structural basis for the inhibition of insulin-like growth factors by insulin-like growth factor-binding proteins. *Proc. Natl. Acad. Sci. U.S.A. 103*, 13028−13033.
(39) Brzozowski, A. M., Dodson, E. J., Dodson, G. G., Murshudov, G. N., Verma, C., Turkenburg, J. P., de Bree, F. M., and Dauter, Z. (2002) Structural origins of the functional divergence of human insulin-like growth factor-I and insulin. *Biochemistry 41*, 9389−9397.
(40) Zeslawski, W., Beisel, H. G., Kamionka, M., Kalus, W., Engh, R. A., Huber, R., Lang, K., and Holak, T. A. (2001) The interaction of insulin-like growth factor-I with the N-terminal domain of IGFBP-5. *EMBO J. 20*, 3638−3644.
(41) Vajdos, F. F., Ultsch, M., Schaffer, M. L., Deshayes, K. D., Liu, J., Skelton, N. J., and de Vos, A. M. (2001) Crystal structure of human insulin-like growth factor-1: Detergent binding inhibits binding protein interactions. *Biochemistry 40*, 11022−11029.
(42) Cooke, R. M., Harvey, T. S., and Campbell, I. D. (1991) Solution structure of human insulin-like growth factor 1: A nuclear magnetic resonance and restrained molecular dynamics study. *Biochemistry 30*, 5484−5491.
(43) Sato, A., Nishimura, S., Ohkubo, T., Kyogoku, Y., Koyama, S., Kobayashi, M., Yasuda, T., and Kobayashi, Y. (1993) Three-dimensional structure of human insulin-like growth factor-I (IGF-I) determined by ^{1}H-NMR and distance geometry. *Int. J. Pept. Protein Res. 41*, 433−440.

(44) Xiao, Z., Brose, J., Schimo, S., Ackland, S. M., La Fontaine, S., and Wedd, A. G. (2011) Unification of the copper(I) binding affinities of the metallo-chaperones Atx1, Atox1, and related proteins: Detection probes and affinity standards. *J. Biol. Chem. 286*, 11047−11055.
(45) Roughead, Z. K., and Lukaski, H. C. (2003) Inadequate copper intake reduces serum insulin-like growth factor-I and bone strength in growing rats fed graded amounts of copper and zinc. *J. Nutr. 133*, 442−448.
(46) Jiang, Y., Reynolds, C., Xiao, C., Feng, W., Zhou, Z., Rodriguez, W., Tyagi, S. C., Eaton, J. W., Saari, J. T., and Kang, Y. J. (2007) Dietary copper supplementation reverses hypertrophic cardiomyopathy induced by chronic pressure overload in mice. *J. Exp. Med. 204*, 657−666.

CURRICULUM VITAE

Name: Julia Smirnova
Date of birth: 01.04.1980
Citizenship: Estonian

CONTACT INFORMATION
Address: Department of Gene Technology, Tallinn University of Technology, Akadeemia tee 15, 12618 Tallinn, Estonia
E-mail: jussmirnova@gmail.com

EDUCATION

2004-2012 Tallinn University of Technology, PhD student

2002-2004 M.Sc., Tallinn University of Technology, Department of Gene Technology
"Metal binding properties of metallothionein isoforms"

1998-2002 B.Sc., Tallinn University of Technology, Department of Food Technology
"Purification and analysis of recombinant human motiline"

SUPPLEMENT COURSES

- Electrospray Ionization Mass Spectrometry Seminar, Tallinn, November 8, 2006

AWARDS

- Marie Curie Ph.D. scholarship, IBB PAS, Warsaw, Poland, September 2005 - February 2006
- Marie Curie Ph.D. scholarship, IBB PAS, Warsaw, Poland, May - August 2005

CONFERENCES

- Oral presentation "ESI-MS helps to solve the redox enigma" in the Estonian Biochemical Society Spring School, Vanaõue holiday centre, May 2012
- Zn Signals 2006 Italy, Siena, September 2006
- Oral presentation "Quantitative electrospray ionization mass spectrometry of zinc finger oxidation: reaction of XPA zinc finger with H_2O_2 and GSNO" in the Estonian Biochemical Society Spring School, Nelijärve, May 2006
- Biometals 2004 Germany, Garmisch-Partenkirchen, September 2004
- Oral presentation "Metal binding properties of metallothionein isoforms" in "First Summer Meeting on proteomics", June 2004

EMPLOYMENT

2008 - …	Tallinn University of Technology, Department of Gene Technology, research scientist
2006 - 2008	Tallinn University of Technology, Department of Gene Technology, specialist
2005 - 2006	Tallinn University of Technology, Department of Gene Technology, technician
2000 - 2000	AS Tallinna Vesi (Järvevana tee 3, Tallinn, 10132; reg. kood: 10257326), engineer of chemical analysis

ELULOOKIRJELDUS

Nimi: Julia Smirnova
Sünniaeg: 01.04.1980
Kodakontsus: Estonian

KONTAKTANDMED
Aadress: Geenitehnoloogia instituut, Tallinna Tehnikaülikool, Akadeemia tee 15, 12618 Tallinn, Eesti
E-mail: jussmirnova@gmail.com

HARIDUS

2004-2012	Tallinna Tehnikaülikool, doktorant
2002-2004	M.Sc., Tallinna Tehnikaülikool, Geenitehnoloogia instituut "Metallotioneiini isovormide metallide sidumisomaduste võrdlev analüüs"
1998-2002	B.Sc., Tallinna Tehnikaülikool, Bio- ja toiduainete tehnoloogia õppetool "Rekombinantsete inimese motiliini puhastamine ja analüüs"

TÄIENDKOOLITUS

- Elektropihustus ionisatsiooni mass-spektromeetria kursus, QSTAR Elite instrumendi tutvustus, Tallinn, november 8, 2006

TUNNUSTUS

- Marie Curie Ph.D. stipendium, IBB PAS, Varssavi, Poola, september 2005 - veebruar 2006
- Marie Curie Ph.D. stipendium, IBB PAS, Varssavi, Poola, mai - august 2005

OSALEMINE KONVERENTSIDEL

- Suuline ettekanne "ESI-MS helps to solve the redox enigma" Eesti Biokeemia Seltsi Kevadkooli raames, Vanaõue puhkeküla, mai 2012
- Zn Signals 2006 Itaalia, Siena, september 2006
- Suuline ettekanne "Quantitative electrospray ionization mass spectrometry of zinc finger oxidation: reaction of XPA zinc finger with H_2O_2 and GSNO" Eesti Biokeemia Seltsi Kevadkooli raames, Nelijärve, mai 2006
- Biometals 2004 Saksamaa, Garmisch-Partenkirchen, september 2004
- Suuline ettekanne "Metal binding properties of metallothionein isoforms" in "First Summer Meeting on proteomics", juuni 2004

TÖÖKOGEMUS

2008 - …	Tallinna Tehnikaülikool, Geenitehnoloogia instituut, teadur
2006 - 2008	Tallinna Tehnikaülikool, Geenitehnoloogia instituut, spetsialist
2005 - 2006	Tallinna Tehnikaülikool, Geenitehnoloogia instituut, inseneer
2000 - 2000	AS Tallinna Vesi (Järvevana tee 3, Tallinn, 10132; reg. kood: 10257326), kemoanalüüsi laborant

LIST OF PUBLICATIONS

- **Smirnova, J.,** Muhhina, J., Tõugu, V., Palumaa, P. "Redox and Metal Ion Binding Properties of Human Insulin-like Growth Factor 1 Determined by Electrospray Ionization Mass Spectrometry" (2012) Biochemistry; 51(29):5851-9

- Noormägi, A., Gavrilova, J., **Smirnova, J.**, Tõugu, V., Palumaa, P. "Zn(II) ions co-secreted with insulin suppress inherent amyloidogenic properties of monomeric insulin" (2010) Biochem J.; 430(3):511-8

- **Smirnova, J.,** Zhukova, L., Witkiewicz-Kucharczyk, A., Kopera, E., Oledzki, J., Wyslouch-Cieszynska, A., Palumaa, P., Hartwig, A., Bal, W. **"**Reaction of the XPA zinc finger with S-nitrosoglutathione" (2008) Chem Res Toxicol.; 21(2):386-92

- **Smirnova, J.,** Zhukova, L., Witkiewicz-Kucharczyk, A., Kopera, E., Oledzki, J., Wyslouch-Cieszynska, A., Palumaa, P., Hartwig, A., Bal, W. "Quantitative electrospray ionization mass spectrometry of zinc finger oxidation: the reaction of XPA zinc finger with H(2)O(2)" (2007) Anal Biochem.; 369(2):226-31

- Massad, T., Jarvet, J., Tanner, R., Tomson, K., **Smirnova, J.**, Palumaa, P., Sugai, M., Kohno, T., Vanatalu, K., Damberg, P. "Maximum entropy reconstruction of joint phi, psi-distribution with a coil-library prior: the backbone conformation of the peptide hormone motilin in aqueous solution from phi and psi-dependent J-couplings" (2007) J Biomol NMR.; 38(2):107-23. Epub 2007 Apr 26

DISSERTATIONS DEFENDED AT
TALLINN UNIVERSITY OF TECHNOLOGY ON
NATURAL AND EXACT SCIENCES

1. **Olav Kongas**. Nonlinear Dynamics in Modeling Cardiac Arrhytmias. 1998.

2. **Kalju Vanatalu**. Optimization of Processes of Microbial Biosynthesis of Isotopically Labeled Biomolecules and Their Complexes. 1999.

3. **Ahto Buldas**. An Algebraic Approach to the Structure of Graphs. 1999.

4. **Monika Drews**. A Metabolic Study of Insect Cells in Batch and Continuous Culture: Application of Chemostat and Turbidostat to the Production of Recombinant Proteins. 1999.

5. **Eola Valdre**. Endothelial-Specific Regulation of Vessel Formation: Role of Receptor Tyrosine Kinases. 2000.

6. **Kalju Lott**. Doping and Defect Thermodynamic Equilibrium in ZnS. 2000.

7. **Reet Koljak**. Novel Fatty Acid Dioxygenases from the Corals *Plexaura homomalla* and *Gersemia fruticosa.* 2001.

8. **Anne Paju**. Asymmetric oxidation of Prochiral and Racemic Ketones by Using Sharpless Catalyst. 2001.

9. **Marko Vendelin**. Cardiac Mechanoenergetics *in silico*. 2001.

10. **Pearu Peterson**. Multi-Soliton Interactions and the Inverse Problem of Wave Crest. 2001.

11. **Anne Menert**. Microcalorimetry of Anaerobic Digestion. 2001.

12. **Toomas Tiivel**. The Role of the Mitochondrial Outer Membrane in *in vivo* Regulation of Respiration in Normal Heart and Skeletal Muscle Cell. 2002.

13. **Olle Hints**. Ordovician Scolecodonts of Estonia and Neighbouring Areas: Taxonomy, Distribution, Palaeoecology, and Application. 2002.

14. **Jaak Nõlvak**. Chitinozoan Biostratigrapy in the Ordovician of Baltoscandia. 2002.

15. **Liivi Kluge**. On Algebraic Structure of Pre-Operad. 2002.

16. **Jaanus Lass**. Biosignal Interpretation: Study of Cardiac Arrhytmias and Electromagnetic Field Effects on Human Nervous System. 2002.

17. **Janek Peterson**. Synthesis, Structural Characterization and Modification of PAMAM Dendrimers. 2002.

18. **Merike Vaher**. Room Temperature Ionic Liquids as Background Electrolyte Additives in Capillary Electrophoresis. 2002.

19. **Valdek Mikli**. Electron Microscopy and Image Analysis Study of Powdered Hardmetal Materials and Optoelectronic Thin Films. 2003.

20. **Mart Viljus**. The Microstructure and Properties of Fine-Grained Cermets. 2003.

21. **Signe Kask**. Identification and Characterization of Dairy-Related *Lactobacillus.* 2003

22. **Tiiu-Mai Laht**. Influence of Microstructure of the Curd on Enzymatic and Microbiological Processes in Swiss-Type Cheese. 2003.

23. **Anne Kuusksalu**. 2–5A Synthetase in the Marine Sponge *Geodia cydonium*. 2003.

24. **Sergei Bereznev**. Solar Cells Based on Polycristalline Copper-Indium Chalcogenides and Conductive Polymers. 2003.

25. **Kadri Kriis**. Asymmetric Synthesis of C_2-Symmetric Bimorpholines and Their Application as Chiral Ligands in the Transfer Hydrogenation of Aromatic Ketones. 2004.

26. **Jekaterina Reut**. Polypyrrole Coatings on Conducting and Insulating Substracts. 2004.

27. **Sven Nõmm**. Realization and Identification of Discrete-Time Nonlinear Systems. 2004.

28. **Olga Kijatkina**. Deposition of Copper Indium Disulphide Films by Chemical Spray Pyrolysis. 2004.

29. **Gert Tamberg**. On Sampling Operators Defined by Rogosinski, Hann and Blackman Windows. 2004.

30. **Monika Übner**. Interaction of Humic Substances with Metal Cations. 2004.

31. **Kaarel Adamberg**. Growth Characteristics of Non-Starter Lactic Acid Bacteria from Cheese. 2004.

32. **Imre Vallikivi**. Lipase-Catalysed Reactions of Prostaglandins. 2004.

33. **Merike Peld**. Substituted Apatites as Sorbents for Heavy Metals. 2005.

34. **Vitali Syritski**. Study of Synthesis and Redox Switching of Polypyrrole and Poly(3,4-ethylenedioxythiophene) by Using *in-situ* Techniques. 2004.

35. **Lee Põllumaa**. Evaluation of Ecotoxicological Effects Related to Oil Shale Industry. 2004.

36. **Riina Aav**. Synthesis of 9,11-Secosterols Intermediates. 2005.

37. **Andres Braunbrück**. Wave Interaction in Weakly Inhomogeneous Materials. 2005.

38. **Robert Kitt**. Generalised Scale-Invariance in Financial Time Series. 2005.

39. **Juss Pavelson**. Mesoscale Physical Processes and the Related Impact on the Summer Nutrient Fields and Phytoplankton Blooms in the Western Gulf of Finland. 2005.

40. **Olari Ilison**. Solitons and Solitary Waves in Media with Higher Order Dispersive and Nonlinear Effects. 2005.

41. **Maksim Säkki**. Intermittency and Long-Range Structurization of Heart Rate. 2005.

42. **Enli Kiipli**. Modelling Seawater Chemistry of the East Baltic Basin in the Late Ordovician–Early Silurian. 2005.

43. **Igor Golovtsov**. Modification of Conductive Properties and Processability of Polyparaphenylene, Polypyrrole and polyaniline. 2005.

44. **Katrin Laos**. Interaction Between Furcellaran and the Globular Proteins (Bovine Serum Albumin β-Lactoglobulin). 2005.

45. **Arvo Mere**. Structural and Electrical Properties of Spray Deposited Copper Indium Disulphide Films for Solar Cells. 2006.

46. **Sille Ehala**. Development and Application of Various On- and Off-Line Analytical Methods for the Analysis of Bioactive Compounds. 2006.

47. **Maria Kulp**. Capillary Electrophoretic Monitoring of Biochemical Reaction Kinetics. 2006.

48. **Anu Aaspõllu.** Proteinases from *Vipera lebetina* Snake Venom Affecting Hemostasis. 2006.

49. **Lyudmila Chekulayeva**. Photosensitized Inactivation of Tumor Cells by Porphyrins and Chlorins. 2006.

50. **Merle Uudsemaa**. Quantum-Chemical Modeling of Solvated First Row Transition Metal Ions. 2006.

51. **Tagli Pitsi**. Nutrition Situation of Pre-School Children in Estonia from 1995 to 2004. 2006.

52. **Angela Ivask**. Luminescent Recombinant Sensor Bacteria for the Analysis of Bioavailable Heavy Metals. 2006.

53. **Tiina Lõugas**. Study on Physico-Chemical Properties and Some Bioactive Compounds of Sea Buckthorn (*Hippophae rhamnoides* L.). 2006.

54. **Kaja Kasemets**. Effect of Changing Environmental Conditions on the Fermentative Growth of *Saccharomyces cerevisae* S288C: Auxo-accelerostat Study. 2006.

55. **Ildar Nisamedtinov**. Application of ^{13}C and Fluorescence Labeling in Metabolic Studies of *Saccharomyces* spp. 2006.

56. **Alar Leibak**. On Additive Generalisation of Voronoï's Theory of Perfect Forms over Algebraic Number Fields. 2006.

57. **Andri Jagomägi**. Photoluminescence of Chalcopyrite Tellurides. 2006.

58. **Tõnu Martma**. Application of Carbon Isotopes to the Study of the Ordovician and Silurian of the Baltic. 2006.

59. **Marit Kauk**. Chemical Composition of $CuInSe_2$ Monograin Powders for Solar Cell Application. 2006.

60. **Julia Kois**. Electrochemical Deposition of $CuInSe_2$ Thin Films for Photovoltaic Applications. 2006.

61. **Ilona Oja Açik**. Sol-Gel Deposition of Titanium Dioxide Films. 2007.

62. **Tiia Anmann**. Integrated and Organized Cellular Bioenergetic Systems in Heart and Brain. 2007.

63. **Katrin Trummal**. Purification, Characterization and Specificity Studies of Metalloproteinases from *Vipera lebetina* Snake Venom. 2007.

64. **Gennadi Lessin**. Biochemical Definition of Coastal Zone Using Numerical Modeling and Measurement Data. 2007.

65. **Enno Pais**. Inverse problems to determine non-homogeneous degenerate memory kernels in heat flow. 2007.

66. **Maria Borissova**. Capillary Electrophoresis on Alkylimidazolium Salts. 2007.

67. **Karin Valmsen**. Prostaglandin Synthesis in the Coral *Plexaura homomalla*: Control of Prostaglandin Stereochemistry at Carbon 15 by Cyclooxygenases. 2007.

68. **Kristjan Piirimäe**. Long-Term Changes of Nutrient Fluxes in the Drainage Basin of the Gulf of Finland – Application of the PolFlow Model. 2007.

69. **Tatjana Dedova**. Chemical Spray Pyrolysis Deposition of Zinc Sulfide Thin Films and Zinc Oxide Nanostructured Layers. 2007.

70. **Katrin Tomson**. Production of Labelled Recombinant Proteins in Fed-Batch Systems in *Escherichia coli*. 2007.

71. **Cecilia Sarmiento**. Suppressors of RNA Silencing in Plants. 2008.

72. **Vilja Mardla**. Inhibition of Platelet Aggregation with Combination of Antiplatelet Agents. 2008.

73. **Maie Bachmann**. Effect of Modulated Microwave Radiation on Human Resting Electroencephalographic Signal. 2008.

74. **Dan Hüvonen**. Terahertz Spectroscopy of Low-Dimensional Spin Systems. 2008.

75. **Ly Villo**. Stereoselective Chemoenzymatic Synthesis of Deoxy Sugar Esters Involving *Candida antarctica* Lipase B. 2008.

76. **Johan Anton**. Technology of Integrated Photoelasticity for Residual Stress Measurement in Glass Articles of Axisymmetric Shape. 2008.

77. **Olga Volobujeva**. SEM Study of Selenization of Different Thin Metallic Films. 2008.

78. **Artur Jõgi**. Synthesis of 4'-Substituted 2,3'-dideoxynucleoside Analogues. 2008.

79. **Mario Kadastik**. Doubly Charged Higgs Boson Decays and Implications on Neutrino Physics. 2008.

80. **Fernando Pérez-Caballero**. Carbon Aerogels from 5-Methylresorcinol-Formaldehyde Gels. 2008.

81. **Sirje Vaask**. The Comparability, Reproducibility and Validity of Estonian Food Consumption Surveys. 2008.

82. **Anna Menaker**. Electrosynthesized Conducting Polymers, Polypyrrole and Poly(3,4-ethylenedioxythiophene), for Molecular Imprinting. 2009.

83. **Lauri Ilison**. Solitons and Solitary Waves in Hierarchical Korteweg-de Vries Type Systems. 2009.

84. **Kaia Ernits**. Study of In_2S_3 and ZnS Thin Films Deposited by Ultrasonic Spray Pyrolysis and Chemical Deposition. 2009.

85. **Veljo Sinivee**. Portable Spectrometer for Ionizing Radiation "Gammamapper". 2009.

86. **Jüri Virkepu**. On Lagrange Formalism for Lie Theory and Operadic Harmonic Oscillator in Low Dimensions. 2009.

87. **Marko Piirsoo**. Deciphering Molecular Basis of Schwann Cell Development. 2009.

88. **Kati Helmja**. Determination of Phenolic Compounds and Their Antioxidative Capability in Plant Extracts. 2010.

89. **Merike Sõmera**. Sobemoviruses: Genomic Organization, Potential for Recombination and Necessity of P1 in Systemic Infection. 2010.

90. **Kristjan Laes**. Preparation and Impedance Spectroscopy of Hybrid Structures Based on $CuIn_3Se_5$ Photoabsorber. 2010.

91. **Kristin Lippur**. Asymmetric Synthesis of 2,2'-Bimorpholine and its 5,5'-Substituted Derivatives. 2010.

92. **Merike Luman**. Dialysis Dose and Nutrition Assessment by an Optical Method. 2010.

93. **Mihhail Berezovski**. Numerical Simulation of Wave Propagation in Heterogeneous and Microstructured Materials. 2010.

94. **Tamara Aid-Pavlidis**. Structure and Regulation of BDNF Gene. 2010.

95. **Olga Bragina**. The Role of Sonic Hedgehog Pathway in Neuro- and Tumorigenesis. 2010.

96. **Merle Randrüüt**. Wave Propagation in Microstructured Solids: Solitary and Periodic Waves. 2010.

97. **Marju Laars**. Asymmetric Organocatalytic Michael and Aldol Reactions Mediated by Cyclic Amines. 2010.

98. **Maarja Grossberg**. Optical Properties of Multinary Semiconductor Compounds for Photovoltaic Applications. 2010.

99. **Alla Maloverjan**. Vertebrate Homologues of Drosophila Fused Kinase and Their Role in Sonic Hedgehog Signalling Pathway. 2010.

100. **Priit Pruunsild**. Neuronal Activity-Dependent Transcription Factors and Regulation of Human *BDNF* Gene. 2010.

101. **Tatjana Knjazeva**. New Approaches in Capillary Electrophoresis for Separation and Study of Proteins. 2011.

102. **Atanas Katerski**. Chemical Composition of Sprayed Copper Indium Disulfide Films for Nanostructured Solar Cells. 2011.

103. **Kristi Timmo.** Formation of Properties of $CuInSe_2$ and $Cu_2ZnSn(S,Se)_4$ Monograin Powders Synthesized in Molten KI. 2011.

104. **Kert Tamm**. Wave Propagation and Interaction in Mindlin-Type Microstructured Solids: Numerical Simulation. 2011.

105. **Adrian Popp**. Ordovician Proetid Trilobites in Baltoscandia and Germany. 2011.

106. **Ove Pärn**. Sea Ice Deformation Events in the Gulf of Finland and This Impact on Shipping. 2011.

107. **Germo Väli**. Numerical Experiments on Matter Transport in the Baltic Sea. 2011.
108. **Andrus Seiman**. Point-of-Care Analyser Based on Capillary Electrophoresis. 2011.
109. **Olga Katargina**. Tick-Borne Pathogens Circulating in Estonia (Tick-Borne Encephalitis Virus, *Anaplasma phagocytophilum*, *Babesia* Species): Their Prevalence and Genetic Characterization. 2011.
110. **Ingrid Sumeri**. The Study of Probiotic Bacteria in Human Gastrointestinal Tract Simulator. 2011.
111. **Kairit Zovo**. Functional Characterization of Cellular Copper Proteome. 2011.
112. **Natalja Makarytsheva**. Analysis of Organic Species in Sediments and Soil by High Performance Separation Methods. 2011.
113. **Monika Mortimer**. Evaluation of the Biological Effects of Engineered Nanoparticles on Unicellular Pro- and Eukaryotic Organisms. 2011.
114. **Kersti Tepp**. Molecular System Bioenergetics of Cardiac Cells: Quantitative Analysis of Structure-Function Relationship. 2011.
115. **Anna-Liisa Peikolainen**. Organic Aerogels Based on 5-Methylresorcinol. 2011.
116. **Leeli Amon**. Palaeoecological Reconstruction of Late-Glacial Vegetation Dynamics in Eastern Baltic Area: A View Based on Plant Macrofossil Analysis. 2011.
117. **Tanel Peets**. Dispersion Analysis of Wave Motion in Microstructured Solids. 2011.
118. **Liina Kaupmees**. Selenization of Molybdenum as Contact Material in Solar Cells. 2011.
119. **Allan Olspert**. Properties of VPg and Coat Protein of Sobemoviruses. 2011.
120. **Kadri Koppel**. Food Category Appraisal Using Sensory Methods. 2011.
121. **Jelena Gorbatšova**. Development of Methods for CE Analysis of Plant Phenolics and Vitamins. 2011.
122. **Karin Viipsi**. Impact of EDTA and Humic Substances on the Removal of Cd and Zn from Aqueous Solutions by Apatite. 2012.
123. **David Schryer**. Metabolic Flux Analysis of Compartmentalized Systems Using Dynamic Isotopologue Modeling. 2012.
124. **Ardo Illaste**. Analysis of Molecular Movements in Cardiac Myocytes. 2012.
125. **Indrek Reile**. 3-Alkylcyclopentane-1,2-Diones in Asymmetric Oxidation and Alkylation Reactions. 2012.
126. **Tatjana Tamberg**. Some Classes of Finite 2-Groups and Their Endomorphism Semigroups. 2012.
127. **Taavi Liblik**. Variability of Thermohaline Structure in the Gulf of Finland in Summer. 2012.
128. **Priidik Lagemaa**. Operational Forecasting in Estonian Marine Waters. 2012.
129. **Andrei Errapart**. Photoelastic Tomography in Linear and Non-linear Approximation. 2012.
130. **Külliki Krabbi**. Biochemical Diagnosis of Classical Galactosemia and Mucopolysaccharidoses in Estonia. 2012.
131. **Kristel Kaseleht**. Identification of Aroma Compounds in Food using SPME-GC/MS and GC-Olfactometry. 2012.

132. **Kristel Kodar**. Immunoglobulin G Glycosylation Profiling in Patients with Gastric Cancer. 2012.
133. **Kai Rosin**. Solar Radiation and Wind as Agents of the Formation of the Radiation Regime in Water Bodies. 2012.
134. **Ann Tiiman**. Interactions of Alzheimer`s Amyloid-Beta Peptides with Zn(II) and Cu(II) Ions. 2012.
135. **Olga Gavrilova**. Application and Elaboration of Accounting Approaches for Sustainable Development. 2012.
136. **Olesja Bondarenko**. Development of Bacterial Biosensors and Human Stem Cell-Based *In Vitro* Assays for the Toxicological Profiling of Synthetic Nanoparticles. 2012.
137. **Katri Muska**. Study of Composition and Thermal Treatments of Quaternary Compounds for Monograin Layer Solar Cells. 2012.
138. **Ranno Nahku**. Validation of Critical Factors for the Quantitative Characterization of Bacterial Physiology in Accelerostat Cultures. 2012.
139. **Petri-Jaan Lahtvee**. Quantitative Omics-level Analysis of Growth Rate Dependent Energy Metabolism in *Lactococcus lactis*. 2012.
140. **Kerti Orumets**. Molecular Mechanisms Controlling Intracellular Glutathione Levels in Baker's Yeast *Saccharomyces cerevisiae* and its Random Mutagenized Gluthatione Over-Accumulating Isolate. 2012.
141. **Loreida Timberg**. Spice-Cured Sprats Ripening, Sensory Parameters Development, and Quality Indicators. 2012.
142. **Anna Mihhalevski**. Rye Sourdough Fermentation and Bread Stability. 2012.
143. **Liisa Arike**. Quantitative Proteomics of *Escherichia coli*: From Relative to Absolute Scale. 2012.
144. **Kairi Otto**. Deposition of In_2S_3 Thin Films by Chemical Spray Pyrolysis. 2012.
145. **Mari Sepp**. Functions of the Basic Helix-Loop-Helix Transcription Factor TCF4 in Health and Disease. 2012.
146. **Anna Suhhova**. Detection of the Effect of Weak Stressors on Human Resting Electroencephalographic Signal. 2012.
147. **Aram Kazarjan**. Development and Production of Extruded Food and Feed Products Containing Probiotic Microorganisms. 2012.
148. **Rivo Uiboupin**. Application of Remote Sensing Methods for the Investigation of Spatio-Temporal Variability of Sea Surface Temperature and Chlorophyll Fields in the Gulf of Finland. 2013.
149. **Tiina Kriščiunaite**. A Study of Milk Coagulability. 2013.
150. **Tuuli Levandi**. Comparative Study of Cereal Varieties by Analytical Separation Methods and Chemometrics. 2013.
151. **Natalja Kabanova**. Development of a Microcalorimetric Method for the Study of Fermentation Processes. 2013.